OTFT-based DNA Detection System

Qintao Zhang

Electrical Engineering and Computer Sciences
University of California at Berkeley

Technical Report No. UCB/EECS-2007-170
http://www.eecs.berkeley.edu/Pubs/TechRpts/2007/EECS-2007-170.html

December 20, 2007

OTFT-based DNA Detection System

by

Qintao Zhang

B ENG (Shandong University of Technology) 1996
M ENG (Zhejiang University) 1999

A dissertation submitted in partial fulfillment of the

requirements for the degree of

Doctor of Philosophy
in

Engineering-Electrical Engineering and Computer Sciences

in the

Graduate Division

of the

University of California, Berkeley

Committee in charge:

Professor Vivek Subramanian, Chair
Professor Chenming Hu
Professor Song Li

Fall 2007

OTFT-based DNA Detection System

By

Qintao Zhang

The dissertation of Qintao Zhang is approved:

Chair Date

Date

Date

University of California, Berkeley
Fall 2007

Abstract

OTFT-based DNA Detection System

by

Qintao Zhang

Doctor of Philosophy in Engineering-Electrical Engineering and Computer Sciences

University of California, Berkeley

Professor Vivek Subramanian, Chair

This thesis describes an ultra-low-cost, disposable, portable and fast DNA hybridization detection system integrating Organic Thin Film Transistor (OTFT) based DNA sensors with microfluidic systems. OTFTs have attracted significant attention in recent decades for use in low-cost Radio Frequency Identification (RFID) tags and driver circuits for flexible displays, but their biological applications is still very rare. The capability of OTFTs on DNA detection was studied in this thesis. Because of their electrical-readability, OTFT based gene analysis toolkits greatly solve problems faced by current DNA detection systems, including expensive instruments and slow processing due to their fluorescence-based detection nature.

To implement this concept, DNA molecules were immobilized directly on the exposed channels of bottom-gated organic transistors. By carefully characterizing transistors, the doping mechanism caused by immobilized DNA was studied. Importantly, unhybridized and hybridized DNA molecules show substantial difference in the resultant threshold

voltage shift due to their different net doping and immobilization efficiencies. Thus, this method clearly enables direct electrical detection of hybridization through measuring OTFT saturation current. To dramatically speed up the analysis process, the pulse-enhanced DNA hybridization method was used to achieve hybridization in less than a millisecond. The net result of the research on OTFT DNA sensor is an overall analysis time of <40 minutes, compared with >24hrs using conventional techniques.

As a further step, a microfluidic system on OTFTs was built to automatically deliver DNA to detection sites. By carefully studying controllability of etching rate of the Polyvinyl Alcohol (PVA) film, a water-soluble polymer, a SU-8-based microfluidic system was patterned photolithographically on OTFTs as the first time. The process was proven not to change the morphology of pentacene film, and because the etchant is DI water, the process-induced performance shift is acceptable for following successful DNA detection. Even importantly, the integration of microfluidic system with OTFT DNA sensor dramatically drops data variance, thus enabling on-chip hybridization detection. Combing OTFT-based DNA sensors with microfluidic systems, the overall results of the research will enable the deployment of gene chip techniques for disposable field-deployable diagnosis toolkits, facilitating personalized medicine research and early-stage disease diagnosis.

Professor Vivek Subramanian
Dissertation Committee Chair

Table of Content

Chapter 0: Introduction ----------1
Chapter 1: Traditional DNA microarray technology ----------5
1.1 Early-stage disease diagnosis and personalized medicine ----------5
1.2 Genomic information facilitates personalized medicines / early-stage diagnosis ----------7
1.3 High-throughput DNA detection: DNA microarray technology ----------11
1.3.1 Current DNA microarray system ----------11
1.3.2 DNA base pairing principle ----------13
1.3.3 Fluorescence-based DNA microarray technology ----------15
1.4 A survey of reported DNA Sensors ----------16
1.4.1 DNA hybridization detection by monitoring physical shifts ------17
1.4.2 Electrochemical DNA sensors ---------- 19
1.5 Ideal DNA microarray chips for clinical applications ----------22
1.6 Conclusion: ----------24
Chapter 2: Organic Thin Film Transistor (OTFT) based sensors ----------26
2.1 Structures of OTFTs ---------- 28
2.1.1 Organic transistors fabricated by modern lithography methods ---- 28
2.1.2 Printability of organic electronics ----------31
2.2 Carrier transport in organic semiconductors and possible sensing mechanisms ----------39
2.3 OTFT-based biosensors ----------47
2.4 The feasibility of OTFT-based DNA sensors ---------- 49
2.5 DNA hydrophobic interaction immobilization ----------51
2.6 Control of evaporated pentacene morphology ----------55
2.7 Conclusion ----------60
Chapter 3: Statistical data Analysis and design of experiment ----------62
3.1 Continuous probability distributions ----------62
3.1.1 Normal distribution ---------- 63
3.1.1.1 Properties of a normal distribution ----------64
3.1.1.2 Evaluation of data normality ----------65
3.1.2 Chi-square distribution ----------66
3.1.3 t-distribution ----------67
3.1.3 F-distribution ----------68
3.2 Hypothesis test ----------69
3.2.1 t-test ----------71
3.2.2 Sample size calculation ---------- 72
3.2.3 F-test ---------- 74
3.3 Analysis of Variance (ANOVA) ---------- 74
3.4 Design of Experiments (DOE) ---------- 76
3.4.1 Screening experiments design ----------78
3.4.2 Response surface experiment design ----------80
3.5 Linear regression ----------82
3.6 Conclusion ----------84
Chapter 4: OTFT-based DNA sensors - Detection of off-chip hybridized DNA segments

----------85
4.1 Experiments ----------86
4.1.1 Sensor Operation ----------86
4.1.2 DNA Immobilization ----------88
4.2 cDNA Microarray with Organic Thin Film Transistors ----------91
4.2.1 Effect of buffer solution on OTFT performance ----------93
4.2.2 Doping effect of DNA molecules on OTFTs ----------94
4.2.3 Off-chip hybridization detection ----------99
4.2.4 DNA expression level detection ----------101
4.3 Oligonucleotide array application of OTFTs ----------104
4.3.1 Pulse-enhanced DNA on-chip hybridization ----------106
4.4. Response Optimization ----------108
4.4.1 Optimization of transistor performance ----------109
4.4.2 Optimization of sensor response ----------110
4.5 Variance shrinkage by optimizing evaporation process ----------113
4.6 Conclusion ----------115
Chapter 5: Integrating DNA sensors with Microfluidic channels
- Detecting on-chip hybridization ----------117
5.1 Current methods to make microfluidic channels on OTFTs ----------117
5.2 PVA as a photoresist ----------119
5.3 99% hydrolyzed PVA-based microfluidic system ----------121
5.4 Microfluidic integration with OTFTs ----------126
5.5 On-chip hybridization using OTFTs integrated with microfluidic channels ----
----------127
5.6 Conclusion ----------129
Chapter 6: Conclusions and Future Work ----------130

6.1 Optimization of DNA immobilization using fluorescence experiments -----131
6.2 New organic materials for covalent bonding DNA immobilization ---------133
6.3 Organic Transistor configuration optimization ----------134
6.4 Memory-like DNA microarray setup for automatic reading ----------135
6.5 Moving from evaporated organic materials to printed organic materials ---135
6.6 Conclusion ----------136

ACKNOWLEDGMENTS

This work has been supported by Semiconductor Research Corporation and National Science Foundation

Chapter 0:

Introduction

Early-stage disease diagnosis and personalized medicine has attracted more and more attention from researchers in research settings and the pharmaceutical industry in recent years because of the great medical promises of predicting diseases and correspondingly curing successfully. The success of these deeply relies on understanding and analysis of genetic information. As one of most powerful tools for gene investigation, DNA microarray technology has seen significant increase in use after its invention approximately twenty years ago. Unfortunately, the fluorescence signal based detection used in traditional DNA microarrays necessitates complex and delicate laser scanners and specialized software, thus making wide accessibility impossible; this is the most important merit required by personalized medicine. Hence, researchers around the world are focused on developing fluorescence-free or label-free gene investigation methods. One of the most successful methods takes advantages of silicon technology because of the possibility of integration with powerful integrated circuits. Unfortunately, the complexity and high-cost of integrated circuit fabrication has resulted in the costs being rather high and thus also not widely-accessible. Therefore, research on an ultra-low-cost and sensitive gene analysis tool is mandatory.

In this dissertation, an Organic Thin Film Transistors (OTFT)-based gene analysis system is studied, integrating OTFT-based DNA sensors with microfluidic systems. OTFTs

have already been broadly studied for use in low-cost Radio Frequency Identification (RFID) tags and driver circuits for flexible Liquid Crystal Displays (LCD). This has been driven by their potential low cost of manufacturing when fabricated using printing technology. Biological sensing applications of OTFTs are still rare because of their instability under air and water. Fortunately, instability is not a big concern for DNA sensing because of the disposable nature of the DNA sensor, establishing a perfect biological application direction. For the first time, herein, DNA segments were immobilized on exposed organic semiconductor surfaces of bottom-gated organic transistors. The immobilized DNA segments were found to dope transistors, resulting in threshold voltage shift. Importantly, OTFTs can unambiguously differentiate between single and double strand DNA by reading the resultant saturation current shift. To speed up the measurement, a single electric pulse was added between the source and drain of the transistors, causing pulse-enhanced hybridization of single-stranded DNA segments in less than 1ms. Thus, for the first time, OTFTs were proven to potentially detect hybridization in less than 40 minutes, including all the necessary steps, namely immobilization, hybridization and signal detection. As a final step to realize integrated DNA microarrays, microfluidic systems were integrated into OTFT DNA sensors to automatically deliver DNA solution to the detection sites. The patterned microfluidic channels are able to reduce variance of measured data, thus allow on-chip hybridization detection. Thus, through the technologies developed herein, we propose a pathway to realizing an ultra-low-cost, fast and widely-accessible gene analysis toolkit, facilitating early-stage disease diagnosis and personalized medicine.

The content of this dissertation is arranged and described as follows:

In chapter one, the basics of early-stage disease diagnosis and personalized medicine are discussed. The operation of conventional DNA microarrays is introduced and the disadvantages of the current system are pointed out. Based on an understanding of the current system, disadvantages of these systems with respect to widespread low-cost deployed are discussed, motivating the work.

In chapter two, the operation of OTFTs are first discussed and their applications are briefly reviewed. Specifically, the biosensing applications of OTFTs are investigated. The feasibility of using OTFTs for DNA detection is discussed. As the most important step in DNA detection, the DNA immobilization methods used for pentacene are discussed and optimized by controlling morphology of evaporated pentacene films.

In chapter three, data analysis and experiment design methods used in this work are introduced. As a powerful tool, statistic analysis of data and statistical design of experiments are necessary for DNA experiments because of the large variance typically seen in such experiments. Major data analysis methods, namely t-test, f-test, ANOVA and linear regression, and experiment design methods, namely screening experiment and surface response experiment, are introduced and the use of these techniques in this dissertation are discussed.

In Chapter four, experiments to test use of OTFTs in the detection of DNA hybridization are discussed. Two types of DNA segments, Lambda DNA and oligonucleotide DNA, representing two types of DNA microarray, cDNA microarrays and oligonucleotide microarrays, are discussed. Sensor preparation, operation of DNA detection, principle and optimization of DNA sensitivity are introduced and investigated in this chapter to demonstrate applicability of OTFT on off-chip hybridization detection.

In chapter five, as a further step after successfully making OTFT-based DNA sensors, microfluidic channels are integrated. The resultant channels not only are able to deliver DNA solutions but also shrink the measure variance, thus improving reliability of on-chip hybridization detection.

In the last chapter, chapter 6, some concluding remarks are provided. Possible future research directions are pointed out to finally make self-supported and automatically-readable DNA analysis systems, targeting ultra-low-cost, disposable, label-free, plastic compatible and fast DNA analysis.

Chapter 1

Trandidtional DNA microarray technology

Both early-stage disease diagnosis and personalized medicine show significant promise of improving life quality dramatically by predicting occurrence of diseases and then allowing rapid and effective curing of the same. The success of these techniques depends on the availability of fast, ultra low-cost and widely-accessible gene analysis tools. In this work, for the first time, the applicability of Organic Thin Film Transistors (OTFTs) for detecting DNA hybridization was investigated because of their ultra-low-cost manufacturing and potentially high sensitivity. The direct result of the research will enable disposable and field-deployable handheld DNA detection applications accessible by all level hospitals and even patients at home. Particularly, in this chapter, fundamentals of early-stage diagnosis and personalized medicines are discussed first, and then as a further step, traditional DNA hybridization detection methods, DNA microarrays, are introduced. Finally, currently available DNA sensors are discussed to illustrate their inability to realize low-cost DNA detection, motivating this work.

1.1 Early-stage disease diagnosis and personalized medicine

Thanks to the deep understanding of genes, we are experiencing a new era of medicine design and disease diagnosis, namely personalized medicine and early-stage disease diagnosis [1]. Different from current medicine design, personalized medicine designs a

medicine according to the specific conditions occurring within a specific person. Current medicine design depends on statistic models. As a result, a FDA-approved medicine has only 40% to 60% possibility of affecting a targeted disease [1]. Therefore, doctors are trained to prescribe 'average' types and dosage of drugs to patients and develop the "optimal" dosage regimen for a patient largely via a trial and error process. This approach often leads to adverse drug reactions (ADR) that cause 2.2 million serious injuries and 100,600 deaths (plus the incalculable number of patients that do not respond at all) every year in the U.S. alone, according to the National Human Genome Research Institute. Such a trial and error approach is unacceptable especially for life-threatening illnesses, such as cancers. Getting it right the first time is critical for drugs that have potentially serious side effects, and thus, personalized medicine holds significant medical promise. Using personalized medicines, it is promised to get the right dose of the right drug to the right patient at the right time. Personalized medicine will enable doctors and patients to make informed choices about treatments, providing a treatment type and dose that will deliver maximum therapeutic benefit, with the minimum amount of toxicity.

Early-stage disease diagnosis also shows paramount importance. The discovery of a disease is often reported by observed illness in a patient, caused by the strong accumulated effects of the disease. Numerous life-threatening illnesses, such as pancreatic cancer, do not manifest detectable symptoms till they are well established and difficult or impossible to cure. Therefore, as these diseases are diagnosed, they often are in a very late-stage and can kill patients in less than one year. Fortunately, many of these

life-threaten diseases are curable in their early-stage. Therefore, to fully cure these diseases or even prevent them, diagnosing diseases in their earliest stage is the key.

1.2 Genomic information facilitates personalized medicines / early-stage diagnosis

Both successfully designed personalized medicines and early-stage disease diagnosis require precise and fast detection of disease predictors and full understanding of how and for whom a drug works. Without a doubt, genetic information encoded by genes provides the most powerful tool to complete these two missions because of gene-mutation-induced disease mechanisms (fig 1.1). Upon determining correlations between gene mutations and diseases, we are able to successfully predict diseases through detection of the corresponding gene mutations. Furthermore, this aids in developing an understanding of drug effects, for example, by monitoring efficiency of a drug blocking expression of mutated genes. This enables the design of highly effective personalized medicines.

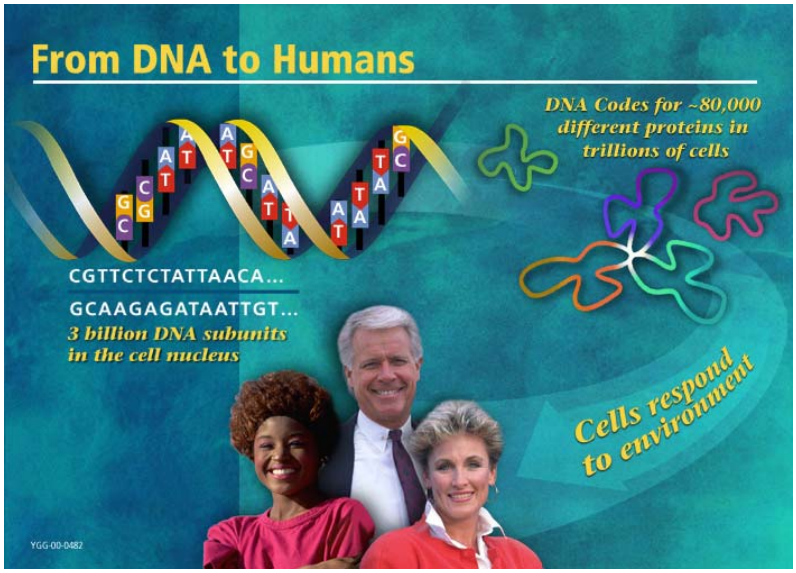

Figure 1.1: From DNA to humans (U.S. Department of Energy Human Genome Program)

Biologically, the genomic information of humans is encoded by a long-chain polymer called Deoxyribonucleic Acid (often abbreviated as DNA) [2]. 46 DNA molecules on 46 chromosomes are made of large numbers of small units, called nucleotides, with a backbone made of five-carbon sugars and phosphate atoms joined by ester bonds (Figure 1.2). Attached to each sugar is one of four types of molecules called bases - adenine (abbreviated A), cytosine (C), guanine (G) and thymine (T). It is the sequence of these four bases along the backbone that encodes full genetic information, instructing the development and functioning of all living organisms. A sequence of DNA nucleotides containing the information that specifies the amino acid sequence of a single polypeptide chain is known as a gene, which specifies the sequence of the amino acids within proteins. Proteins, as the most importantly organic molecules in living beings, form the building blocks of cells and tissues, catalyze biochemical reactions vital to metabolism, and recognize and react to invasive cells. Therefore, proteins are the chief actors in active cells, and understanding and detecting gene-guided protein construction is crucial for disease diagnosis and personalized medicine.

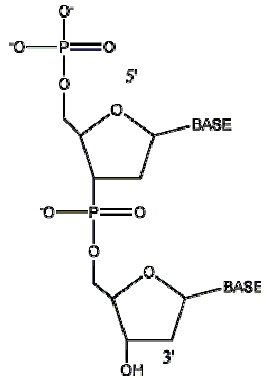

Figure 1.2: Molecular structure of a single-stranded DNA with two bases. Sugars and phosphate atoms form backbones, on which bases are attached to encode genetic information.

The process of gene guided protein construction is called gene expression. Functional genes are first read by copying into a related nucleic acid RNA, called messenger RNA, in a process called transcription. The transferred mRNA molecules go out of the cells, and guide protein construction in a process called translation. Because the onset of diseases is really caused by expressed disordered-genes, it is possible to detect those diseases in their earliest stage by monitoring the appearance of the corresponding mRNA. Also importantly, the efficacy of medicines can be investigated by monitoring gene expression blockage induced by medicines, such that the medicine can be fine tuned to treat diseases correctly and effectively, leading to personalized medicines. Therefore, central to early-stage disease diagnosis and personalized medicine, we have to find correlations between genes and diseases, and design corresponding fast detection tools to detect the disease-related genes.

Numerous efforts have been made to investigate correlations between diseases and genes. One of the most important milestones was completed four years ago by the Human Genome Project. Taking more than 13 years and with contributions of researchers from more than 10 countries, the Human Genome Project successfully unveiled a rough genome map covering the whole human gene sequence. With this knowledge of the genome map, theoretically we are able to find disease-related genes among sequences by simply comparing genes between health people and people with the disease.

Unfortunately, this comparison process is not trivial because of the gigantic amount of genetic information in the human body. Generally, people have 50,000 to 100,000 genes

[2], composed of more than 3 billion bases. In order to compare two persons' genes, the sequence of all those 3 billion bases has to be read very precisely. Even worse, gene disorders are commonly not the only reason inducing diseases; lots of other factors, such as environmental pollution, toxic foods, infections, and so on, also play very important roles. Therefore, to find a correlation between a disease and genes, multiple comparisons are necessary. Thus, a high throughput DNA sequencer is crucial to fast gene discovery for early-stage disease diagnosis and personalized medicine.

To date, more than 4000 genetic disorders have been found with more being discovered every day [3]. Using knowledge of those disorders, the genetic disease diagnosis method currently used in hospitals is Polymerase Chain Reaction (PCR). This is used to specifically replicate a disease-related gene through a commercially available primer. Electrophoresis is used for detecting the appearance of those replicated genes by reading the variation in movement speed of the same, driven by a voltage across a microfluidic channel. The method is basically a gene-by-gene procedure, making multi-gene mutation induced disease diagnosis extremely time-consuming and thus causing diagnosis delay. In reality, most diseases are correlated with more than 100 genes. For example, breast cancer has already been correlated with more than 250 genes and this number is likely to continue growing in the future. Therefore, in order to increase the diagnosis speed, a method that can investigate multiple genes in parallel has to be used; DNA microarray is such a technique.

1.3 High-throughput DNA detection: DNA microarray technology

A DNA microarray (also commonly known as gene or genome chip, DNA chip, or gene array) is a revolutionary technology that changed DNA research from a gene-by-gene method to a massively parallel experimental procedure. This high throughput measurement results in better and faster understanding of the implications of variations in DNA on disease, etc. One of the most important goals of current DNA microarrays is to improve the gene detection density in order to allow the study of the whole human genome (all genes in the human body) in one experiment. The highest density in a state of the art commercial DNA microarray chip is produced by Affymetrix: 500,000 measurement points on a 1.2cm×1.2 cm glass chip.

1.3.1 Current DNA microarray system

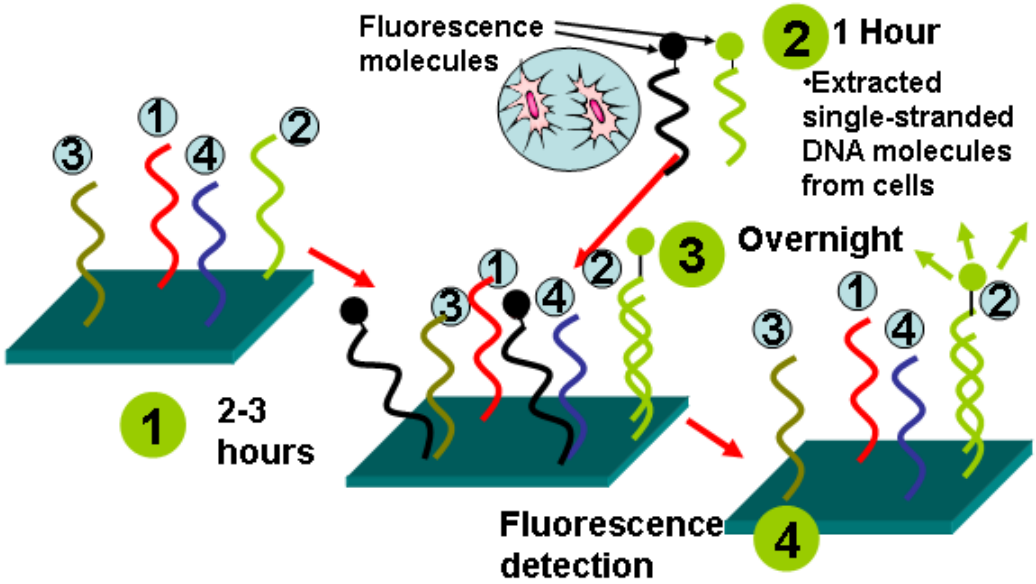

Figure 1.3: Scheme of a fluorescence-based DNA microarray analysis. Four crucial steps are included in a DNA microarray analysis: DNA immobilization or on-chip

syntheses, DNA extraction, purification and replication, Hybridization and rinse, and fluorescence detection using laser scanner.

The DNA microarray was first reported by researchers at Stanford University [4]. After more than sixteen years of development, DNA microarray technology has shown three main types of applications: 1) Discovery of new genes and their functions, 2) Comparative studies between different genes and 3) Drug development and toxicology studies. The next expected application of DNA microarray is in the clinical area, especially in early-stage disease diagnosis and personalized medications, as discussed in this dissertation. In January 2007, the first clinical application of a gene chip, namely a breast cancer diagnosis chip, was approved by the FDA. More successful products are expected in the near future because of the huge demand from patients.

DNA microarray assays rely on a technically simple idea. By converting each less-than-10μm-diameter point on a chip, typically made of glass, into a measurement point of gene sequences, DNA microarray chips can measure more than 100,000 genes in one test on a chip that is typically less than 4cm^2 in size. Research on DNA microarray is now focused on DNA Genotyping and Proteomic/Metabolomic analysis so as to understand the linkage between gene variations and diseases, drug discovery and so on. Four crucial steps are involved in a typical DNA microarray analysis (fig 1.3): single-stranded DNA (also called probe DNA) immobilization (Agilent method) or on-chip syntheses (Affymetrix method), target DNA extraction, purification and replication, and finally DNA hybridization and fluorescence signal detection. DNA hybridization is the most important step and often the most time-consuming step. Through hybridization, a DNA microarray analysis investigates similarities between probe DNA and target DNA

sequences, or in other words, sequences target DNA segments if the sequences of probe DNA segments are known previously.

1.3.2 DNA base pairing principle

The DNA base pairing principle is the fundamental principle making DNA microarray assays possible. It is well known that DNA molecules naturally structure as a double helix at room-temperature. The bonding between two single-stranded molecules is formed by hydrogen bonding between bases (figure 1.4). As discussed previously, only four kinds of bases exist in DNA molecules. Only two combinations between bases are allowed: A to T and G to C. A to T are bonded by two hydrogen bonds, while G to C by three hydrogen bonds. This specific match rule is called the DNA base pairing principle. With the principle, in a double stranded DNA molecule, if we know sequence on one strand, correspondingly, we can determine the sequence on the other strand. Two single-stranded DNA molecules that can be bonded perfectly together are called complementary DNA molecules.

The process required to form double-stranded DNA (dsDNA) molecules by combining complementary single-stranded nucleic acids is called hybridization, the most critical step in DNA microarray assays. Because of the hydrogen bonding nature of the base paring principle, nucleotides bind to their complements at low temperature, so two perfectly complementary strands will readily bind to each other. Because of the temperature heating and cooling steps involved in the whole process, hybridization is often called

annealing by many DNA synthesis companies. Depending on the number of hydrogen bonds (in turn related to the length of the DNA molecules), at certain high temperature, generally above 50^{o}C, a dsDNA molecule can be separated into two ssDNA molecule by breaking the hydrogen bonds. This temperature is called the melting point. Due to the different molecular geometries of the nucleotides, a single inconsistency between the two strands makes binding between them more energetically unfavorable, and thus dramatically drops the hybridization rate. Measuring the effects of base incompatibility by quantifying the hybridization rate can provide information about the similarity in base sequence between the two strands being annealed. Also importantly, reading hybridization rate is the essential method used to evaluate expression rate of a gene.

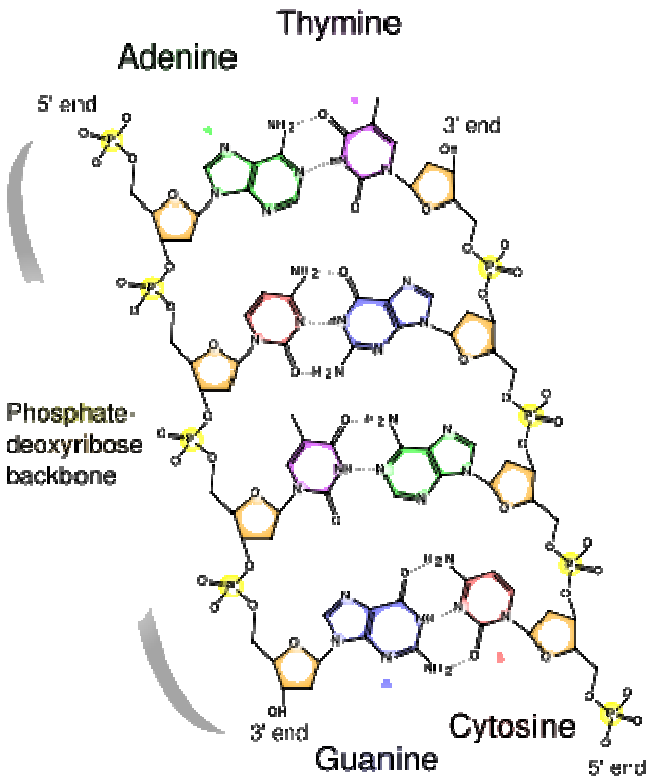

Figure 1.4: DNA base paring principle. Two combinations between four kinds of bases exist: A to T and G to C. A to T are bonded by two hydrogen bonds, while G to C by three hydrogen bonds

1.3.3 Fluorescence-based DNA microarray technology

Using the hybridization technique, a DNA microarray can be designed to test the similarity between known sequences, normally related to certain diseases, and unknown sequences, normally from cells. Toward this purpose, the first step in all kinds of DNA microarray systems is to mount known sequence DNA molecules, called probe DNA. Two types of methods are currently used, immobilization and on-chip syntheses. Most of companies except “Affymetrix”, such as Agilent, Illumina and so on, use immobilization methods: DNA molecules are extracted from cells and immobilized by covalent bonds. Affymetrix, on the other hand, synthesizes oligonucleotides on chip using the same photolithography methods used in modern silicon industry. This on-chip synthesis results in a higher density in the completed DNA microarray compared to systems formed using immobilization methods, because of the high resolution brought by the lithography technology. In both techniques, the mounted DNA molecules must be very stable to survive the following rinse steps.

Unknown DNA sequences, called target DNA, are extracted from cells to be studied and go through several purification and replication steps to separate large enough quantities of pure DNA molecules for the following hybridization with probe sequences. The hybridization step usually takes more than 12 hours in a current DNA microarray system in order to provide a long enough time for target sequences to find their complementary strands. The hybridized DNA microarray chip is rinsed to remove floating unhybridized target sequence DNA molecules. The ultimate consequence of this procedure is that the

dsDNA or hybridized DNA only exists in locations in which probe and target DNA show enough similarity. As shown in figure 1.3, only area 4 has dsDNA molecules, while other places remain as ssDNA. Thus the remaining task of a DNA microarray analysis is to determine where the dsDNA molecules are located.

Current commercially-available DNA microarray systems all use fluorescence signals to detect the location of dsDNA molecules. Fluorescence molecules are attached to the target DNA segments, which will uniquely bring the fluorescence signals onto dsDNA sites. By scanning the whole gene chip area with a laser scanner, the dsDNA can be easily found by monitoring fluorescent spots. Unfortunately, this step is time-consuming and must use expensive instruments. The fluorescent-bead attaching step, called labeling, requires more than one hour of processing time and requires a delicate and clearly not portable laser scanner system, and correspondingly complicated and expensive image processing software. Thus, fluorescence-based DNA microarray systems are not suitable for widely-accessible disease diagnosis and personalized medicine applications. Their use is typically limited to research settings. In order to bring DNA microarray technology to personal usage, various types of DNA sensors are being developed to realize label-free DNA detection for a low-cost, disposable, hand-held and fast DNA detection system.

1.4 A survey of reported DNA Sensors

The primary goal of DNA sensor research is to realize a sensor that can differentiate ssDNA from dsDNA without using fluorescence signals. Because of the physical and

electrical shifts involved in the change from ssDNA to dsDNA, most DNA sensors fall into two categories. First, because dsDNA is heavier than ssDNA, (ideally, if two complementary DNA molecules have same length, dsDNA is two times heavier than ssDNA),they can be differentiated physically, using sensors such as Surface Plasmon Resonance (SPR) sensors [5], Surface Acoustic Wave (SAW) sensors [6] and Quartz Crystal Microbalance (QCM) sensors [7]. The second category of DNA sensors detects the location of dsDNA electrically. Because of the phosphate groups on DNA molecule backbones, DNA molecules have negative charges, with one charge existing per base. Thus, the difference between ssDNA and dsDNA can also be distinguished by reading the charge concentration difference, using electrochemical sensors such as Ion-sensitive Field Effective Transistors (ISFET) [8, 9], and various sensors based on carbon nanotubes [10, 11], semiconductor nanowires [12], gold nanoparticles [13] and conductive polymers [14]. In the following section, several DNA sensors in these two categories are reviewed.

1.4.1 DNA hybridization detection by monitoring physical shifts

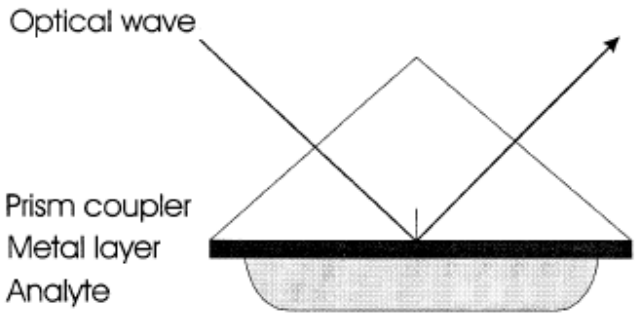

Figure 1.5: Scheme of a Surface Plasma Resonance Sensor [5]. A sensitive thin metal film is deposited typically on a glass prism. An incoming optical wave excites the resonance of surface plasmons, whose frequency can be changed by DNA-DNA bonding-induced mass shift.

One of the best DNA sensors for measuring physical shifts caused by hybridization is the Surface Plasmon Resonance (SRP) sensor because of its ultra high sensitivity and stability. SPR is a very well known technique for real-time biomolecular interaction detection [5]. Taking advantage of the sensitivity of the surface resonance frequency of a thin metal layer, such as a 10nm-gold layer, to the interface condition, the sensor is broadly used for molecular bonding monitoring, such as DNA-DNA bonding and antigen-antibody bonding.

Surface plasmon resonance is a charge-density oscillation, existing at the interface of two media with dielectric constants of opposite signs, for instance, a metal and a dielectric and propagating parallel along the interface. Since the wave is at the boundary of the metal and the external medium (air or water for example), these oscillations are very sensitive to any change at this boundary, such as the adsorption of molecules to the metal surface and the bonding of additional layers to the existing biomolecular layer. Because the shift from ssDNA to dsDNA actually changes the molecule mass on the thin film surface, this can be differentiated by reading the oscillation frequency.

The detection of SPR sensors is done by a laser scan, exciting the resonance by a visible/infrared light beam (figure 1.5). The incoming beam has to be matched to the plasmon. In the case of p-polarized light, this is possible by passing the light through a block of glass to increase the wave number (and the impulse), and achieve the resonance at a given wavelength and angle. S-polarized light cannot excite surface plasmons. By scanning the laser along the surface, the minimum reflection density point is detected,

corresponding to the resonance frequency of the current film condition. The bonding of complementary ssDNA to the ssDNA molecules on the sensor surface changes this minimum point depending on the bonding concentration.

The high sensitivity of this response to bonding/adsorption concentration results in a sensor with very high sensitivity. Generally, the sensitivity of the sensor can be as high as 1pg/mm^2. Unfortunately, this optical-based detection also makes integration extremely hard. In order to realize multi-detection points with SPR, multiple laser sources and/or scanning mechanics are required. These complexities make the detection instrument expensive and unsuitable for low-cost applications, such as DNA microarray. Other mass-shift-based DNA sensors also face the same challenges. Thus, techniques such as SAW and QCM are normally used to monitor the dynamics of DNA bonding but not for in-array detection.

1.4.2 Electrochemical DNA sensors

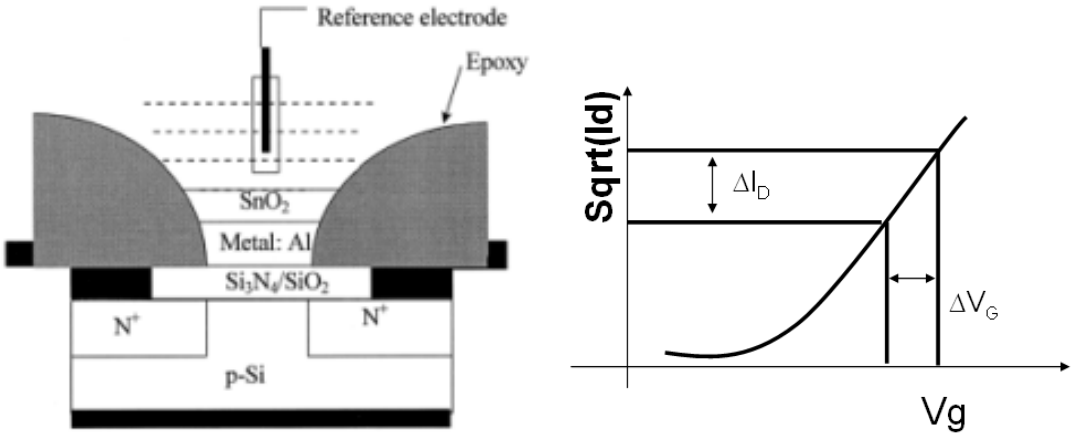

Figure 1.6: Scheme of an Ion-sensitive Field Effective Transistor and a typical transfer curve of an ISFET. DNA-DNA bonding on the sensitive film shifts negative charges on the transistor gate, correspondingly shifting the measured saturation current.

An alternative method with higher potential to reach a high integration level is to use electrically-readable DNA sensors, avoiding optical detection instruments. Because DNA molecules naturally have negative charges on their backbones, hybridization essentially doubles the concentration of the charges and correspondingly changes the performance of devices. A good example of an electrically-readable DNA sensor is the Ion Sensitive Field Effect transistors (ISFET) sensor [8]. ISFET sensors detect hybridization by monitoring the shift of the negative charge concentration on the gate. This is accomplished by reading the resultant current shift between the source and drain (fig. 1.6). The accumulated negative charges on the gate of an ISFET positively shift the threshold voltage and correspondingly shift measured saturation current [9].

ISFETs have similar structures to the transistors used for integrated circuits. Photolithography steps are used to pattern the source and drain, the current between which is controlled by the third electrode, the gate. Unlike fully-packaged conventional transistors, ISFET sensors typically require an open structure with a floating reference electrode (fig. 1.6). The floating electrode performs a similar function to the gate electrode of conventional transistors, superimposing the gate voltage through the electrolyte with the potential of the gate with DNA molecules on the top.

The floating gate in the setup detrimentally impacts the ability to integrate ISFETs, and also makes the fabrication of these devices much more complex than conventional transistors because of the required gate-last processing sequence. Transistors are first fabricated using relatively conventional processing, and then the gate area is opened

lithographically and coated with a sensitive layer. Moreover, because the floating gate directly contacts the ion-rich electrolyte, any disturbance in the electrolyte such as ion concentration shifts influence the performance of the ISFET transistors, causing instability of the sensors. These disadvantages of ISFET-based DNA sensors together make them unsuitable for disposable DNA detection applications.

Beside ISFET sensors, there has been substantial research into the application of nanostructures in DNA electrochemical sensing. Both nanotubes [11] and nanowires [12] have been used for high sensitivity DNA sensing because of their large surface/volume ratio. Central to the problems faced by nanotube and nanowire based biosensors are the alignment of pre-synthesized nano materials, unfortunately, making integration with silicon-based circuits hard. One promising way to make integration better is to use nanotube/wire networks, avoiding alignment requirements. Also enabled by advances in nanomaterials, gold nanoparticles [13] have shown clear promise in DNA hybridization detection. There are several other types of DNA sensors, such as conducting polymer-based [14], magnetic beads based [15] and capacitance-based DNA sensors [16], whose usage are also limited by their complicated measurement strategy. The overall situation is therefore that none of the currently available DNA sensors are suitable for disposable and widely-accessible applications.

1.5 Ideal DNA microarray chips for clinical applications

The main purpose of current commercially-available DNA microarray systems, produced by Affymetrix, Agilent, Iluumina, etc, is to detect the whole genome of humans on one chip. Thus, improving the resolution of measurement points is the major development path pursued by these companies. Over the past fifteen years, Affymetrix has pushed the limits of DNA sensing resolution. Currently, they fabricate 500,000 spots on a $1.2cm \times 1.2cm$ chip. By using photolithography technology, leveraged from the modern IC industry, specific bases, A/T/G/C, are selectively and locally grown layer-by-layer on specific spots on a chip. Thus each layer of the chip requires four masks. The high resolution of photolithography technology drops the diameter of every spot to less than $5\mu m$, but it unfortunately also makes the fabrication extremely complicated, limiting the length of oligonucleotide to typically less than 25 bases with 100 masks. This short length is not suitable for disease diagnosis because genes corresponding to diseases are normally longer than 1000 bases. Agilent technologies, on the other hand, use inkjet printers to selectively deposit cDNA. These are therefore better than Affymetrix technology for disease diagnosis because they investigate DNA expression. However, the use of fluorescence-based detection limits application to disease diagnosis for economic and complexity reasons.

More importantly, such a high resolution system is over-designed for disease diagnosis because most known diseases are only related to less than 300 genes. For example, the most researched genetic disease, breast cancer, is related to around 250 genes [17]. Thus,

a low-density DNA microarray is already good enough for disease diagnosis or personalized medicine development. The key point for a successful DNA microarray clinical application, therefore, is to overcome high cost and complicated operation.

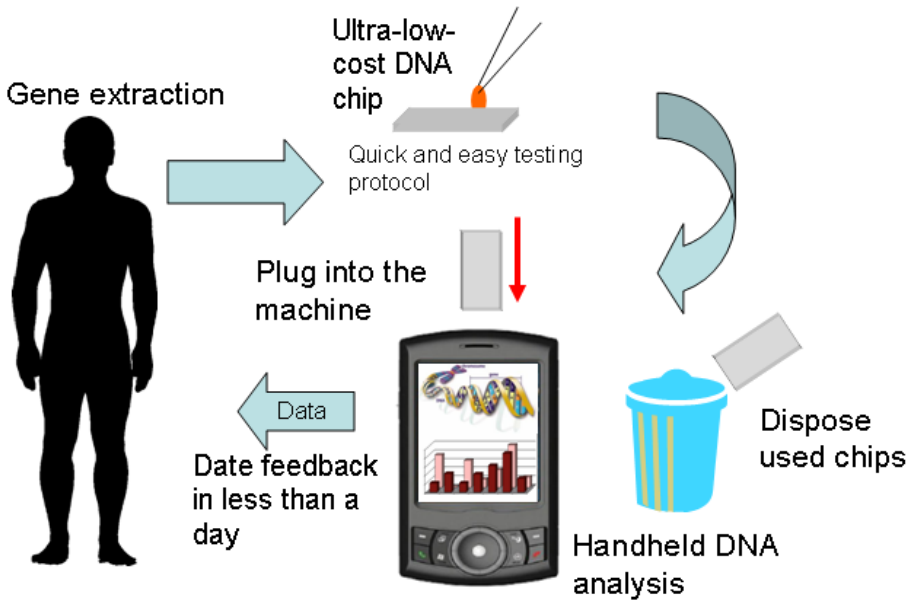

Figure 1.7: Scheme of an ideal DNA chip clinical application. A disposable DNA sensor is used to detect diseases and effects of drugs for personalized medicine quickly, simply and effectively.

Ideally, a DNA microarray chip for clinical applications should be ultra-low cost, i.e., less than $1 per chip plus less than $100 for the detection instrument. The system should enable a quick and easy testing protocol, definitely less than 1 day analysis time, and low-density (fig. 1.7). With such a DNA microarray chip, it will be possible to realize real field-deployable applications accessible by people throughout the world, even in developing countries. This ideal DNA microarray chip will eventually make DNA detection in hospitals and in the field as easy as urine testing or blood testing, thus dramatically improving life quality through customized, accurate healthcare. To

accomplish this mission, an electrically-readable DNA sensor with ultra-low manufacturing and easy operation has to be developed.

1.6 Conclusion:

DNA microarray technology is an important tool for early-stage disease diagnosis and personalized medicine. Unfortunately, the complexity of measurements and required expensive instrumentation make it impractical for daily usage. DNA sensors are very promising for this application but none of the current DNA sensors are suitable for disposable and field-deployable applications because of their low integration level, expensive manufacturing and complex operation. Thus an ultra-low-cost DNA sensor with high sensitivity is necessary and urgent. In this dissertation, we report on our Organic Thin Film Transistors (OTFT) based DNA sensor, which should be manufacturable at extremely low cost while enabling complete detection in less than 40 minutes.

Reference:

1. Personalized Medicine: the emerging Pharmacogenomics Revolution, Pricewaterhouse Coopers LLP. 2005
2. Vander A. et al., Human physiology: the mechanism of body function, Eight Edition, McGraw-Hill, 2001
3. http://en.wikipedia.org/wiki/Genetic_diseases
4. Michael J. Heller, DNA Microarray Technology, Devices, Systems and Applications, Annu. Rev. Biomed. Eng. Vol. 4, pp.129, 2002
5. J. Homola, *et al*, Surface plasmon resonance sensors: review, Sensor and actuator B Vol. 54, pp 3, 1999,
6. Gronewold, M.A T., et al, Discrimination of Single Mutations in Cancer-Related Gene Fragments with a Surface Acoustic Wave Sensor, Anal. Chem. Vol. 78, pp 4865, 2006

7. Caruso F. et al, Quartz Crystal Microbalance Study of DNA Immobilization and Hybridization for Nucleic Acid Sensor Development, Anal. Chem. Vol 69, pp 2043, 1997
8. Ir. P. Bergveld Em, ISFET, Theory and Practice, IEEE Sensor Conference, Toronto, October, 2003
9. Bandiera L. et al, A fully electronic sensor for the measurement of cDNA hybridization kinetics, Biosensors and Bioelectronics, Vol. 22, pp 2108, 2007
10. Wang J., Carbon-nanotube Based Electrochemical Biosensors: A review, Electroanalysis, Vol. 17, pp 7, 2005
11. Tang X.W. et al, Carbon Nanotube DNA Sensor and Sensing Mechanism, Nano letters, Vol. 6, pp 1632, 2006
12. Hahm J.I. et al, Direct Ultrasensitive Electrical Detection of DNA and DNA Sequence Variations Using Nanowire Nanosensors, Vol. 4, pp 51, 2004
13. Luo X.L. et al, Application of nanoparticle in electrochemical sensors and biosensors, Electroanalysis, Vol. 18, pp 319, 2006
14. Cosnier, S., Recent Advances in biological sensors based on electrogenerated polymers: A review, Analytical Letters, Vol. 40, pp 1260, 2007
15. Drummond T.G., et al, Electrochemical DNA sensors, Nature Biotechnology, Vol. 21, pp 1192, 2003
16. Venuto D.D. et al, Design and Characterization of novel read-out systems for a capacitive DNA sensor, Microelectronics Journal, Vol. 37, pp 1610, 2006
17. Lacroix, M. *et al*, A low density DNA microarray for analysis of markers in breast cancer, the international journal of biological markers, Vol. 17, no. 1, pp. 5, 2002

Chapter 2:

Organic Thin Film Transistor (OTFT) based sensors

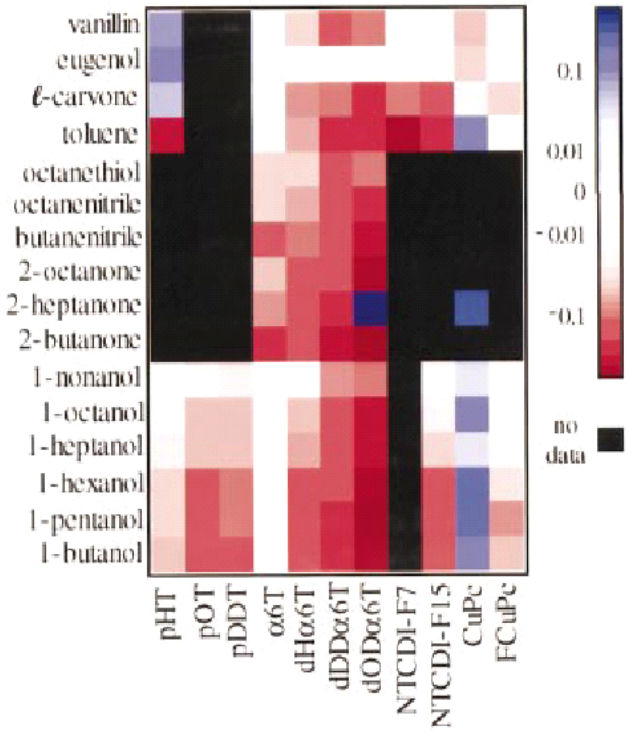

Figure 2.1 Gas sensing of organic thin film transistors demonstrated by Dr. B. Crone et al. Color Map illustrating the effect of 16 analytes on 11 sensor materials. Black indicates that data are not available and white indicates negligible response. Positive changes in sensor current are shown in shades of blue while decreases are shown in shades of red.

In recent decades, Organic Thin Film Transistor (OTFT) based sensors have received attention from researchers around the world because of their ultra-low-cost manufacturing (enabled by the printability of all the necessary materials) and potentially high chemical and biological sensitivity (achieved by their potentially easily tunable chemical structures). In recent years, OTFTs have already shown broad sensitivity to

many different odors, such as vanillin, butanol and so on [1], and been used for food quality control [2]. More importantly, using printing technologies, including inkjet printing, screening printing, gravure printing, etc., different organic semiconductor materials with different sensor sensitivity and selectivity can be selectively printed on a cheap substrate [3,4], avoiding the high costs associated with traditional semiconductor manufacturing techniques, thus enabling ultra-low-cost electronic nose systems (e-nose). This ultra-low-cost e-nose system is expected to cost less than $1 when implemented with OTFTs compared to costs of >$1000 for existing conventional systems. This will certainly enable disposable applications of gas / fluid sensors in the food industry and environmental monitoring applications.

For the same reason, Organic thin-film transistors (OTFTs) also offer a great deal of promise for applications in chemical and biological sensing [5]. For a broad range of bio/chemical sensing applications, there is a clear demand for portable and disposable sensors. The printability and electrical-readability of OTFTs makes them the best fit for this purpose. Importantly, both molecular structure and morphology of organic semiconductors can be carefully adjusted to enhance sensory sensitivity and selectivity; for example, the chemical structure of organic semiconductors can be changed to form covalent bonding with measured analytes, thus improving sensitivity and selectivity. In comparison to chemiresistors, amperometric and potentiometric sensors, the detection limits and sensitivity of organic transistor-based biosensors also benefit from the signal amplification that is inherent in transistor structures.

In this chapter, the operation and processing of OTFTs is reviewed first to demonstrate the potential for ultra-low-cost manufacturing. OTFT-based biosensors are also discussed to validate the applicability of OTFTs to the detection of biological molecules and ions. In the last part of the chapter, control of morphology is investigated to optimized DNA immobilization. The overall discussion and experiments in this chapter prove that the OTFT is a great candidate of DNA hybridization detection, making disposable disease diagnosis chips possible.

2.1 Structures of OTFTs

2.1.1 Organic transistors fabricated by modern lithography methods

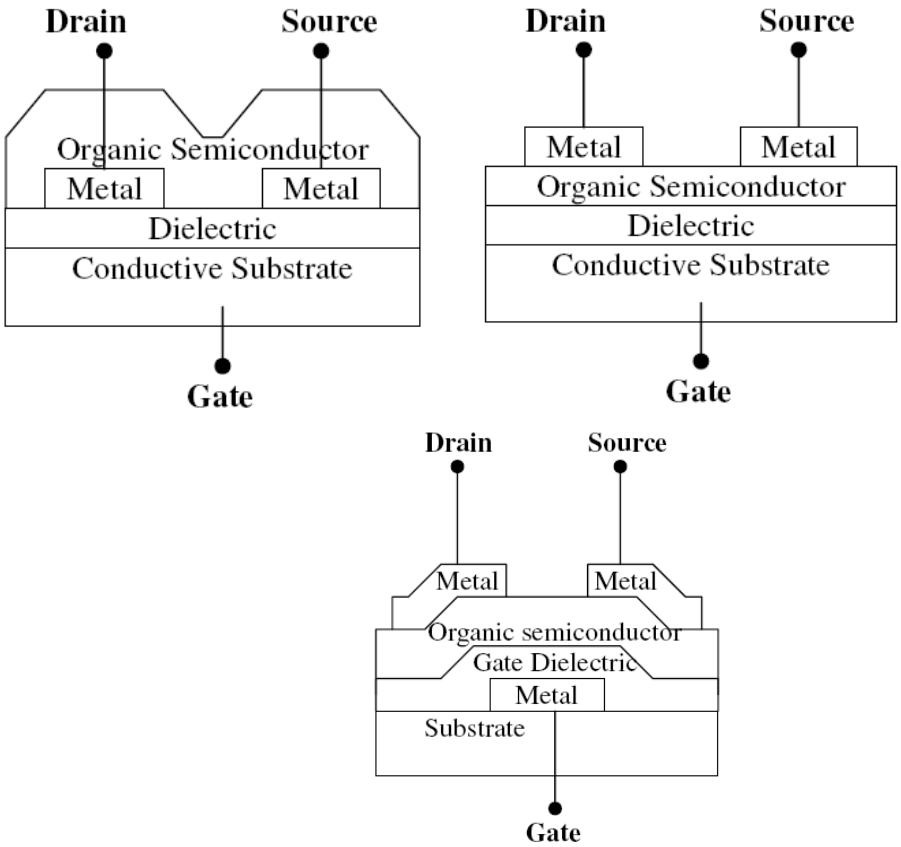

Figure 2.2: Typical test structure of OTFTs a) Bottom-gated bottom contact OTFT, b) bottom-gated top contact OTFT and c) Top contact OTFT with patterned bottom gate

To test performance of organic electronics, three bottom-gated structures are commonly used (figure 2.2). These are bottom-gated bottom contact OTFT, bottom-gated top contact OTFT and top contact OTFT with patterned bottom gate. Those structures are typically built using microfabrication techniques similar to those used in the conventional semiconductor industry, including lithography, thin film deposition and so on. In these applications, organic semiconductors are normally deposited by evaporation, spin-coating and printing. Because there is usually no body contact, OTFTs are actually three-terminal field-effect transistors in which charge conduction between two terminals, the source and the drain, is controlled by modulating the electrical potential of the gate.

In bottom-contact bottom-gated devices, a highly conductive substrate, such as a heavily-doped silicon wafer, acts as a common gate for all devices fabricated on the same (Figure 2.2a). This substrate is then insulated with a gate dielectric layer such as thermally-grown silicon dioxide. On this insulated substrate, a metal layer is deposited and patterned lithographically to form source and drain contact electrodes. Finally, the organic semiconductor is deposited on top of the structure. Conduction between the source and the drain occurs through an ultra-thin current channel formed in the organic semiconductor film close to silicon dioxide layer.

The bottom-contact substrate-gated structure is commonly used in the field of organic electronics to characterize new materials due to the ease of fabrication. In this dissertation, for convenience, all transistor measurements are done using this structure. The entire structure except for the active layer can be built and patterned using standard

photolithography and microfabrication techniques, which, while not compatible with low-cost manufacturing, are mature and readily available to many research laboratories. The microfabricated structures can then serve as ready-made structures, on top of which various organic semiconductors can be deposited. Unfortunately, this process sequence also brings with it a disadvantage: since the organic semiconductor is deposited on two different materials simultaneously (i.e., the gate dielectric and the source/drain contacts), the organization and crystallinity of the organic thin film is disrupted by the nonuniformity of the substrate. The differences in surface energy and surface roughness between the electrodes and the dielectric cause the organic film to adapt different microstructures in the two regions, resulting in regions of disorder at the source/drain contacts. As a result, bottom-contact structures typically suffer from larger source and drain contact barriers and contact resistance.

To reduce the contact resistance, a variation on this structure is the substrate-gated top-contact TFT (Figure 2.2b), in which the organic semiconductor is deposited directly onto a uniform dielectric layer such as an oxidized silicon wafer. The formation of the organic film on a uniform substrate is advantageous for obtaining well-ordered films. Source and drain electrodes are then deposited on top of the organic semiconductor typically through a shadow mask, avoiding possible damage caused by chemicals used in photolithography steps. Though this structure typical shows much smaller contact resistant than the bottom-contact structure, its broad application is limited by the low alignment resolution inherent in the use of the shadow mask method.

Though useful for materials characterization, substrate-gated devices are impractical for organic electronics applications. First of all, the use of silicon substrates and microfabrication techniques is not compatible with the low-cost, reel-to-reel manufacturing goal of organic electronics. More importantly, the construction of OTFT-based circuits requires that devices be individually gated to enable realization of any circuits. Thus, transistors with a patterned gate are required. The patterned back-gate structure (Figure 2.2c) also places the gate and dielectric below the active layer, but the use of an insulating substrate and individually patterned gates allows devices to be independently controlled. Different from other two structures, because of the metal-gate-first structure, a polymer dielectric is used instead of Silicon Dioxide. This has to be spin coated or printed instead of being thermally grown. These structures have been successfully fabricated on a number of substrates including silicon, glass, and plastic.

2.1.2 Printability of Organic electronics

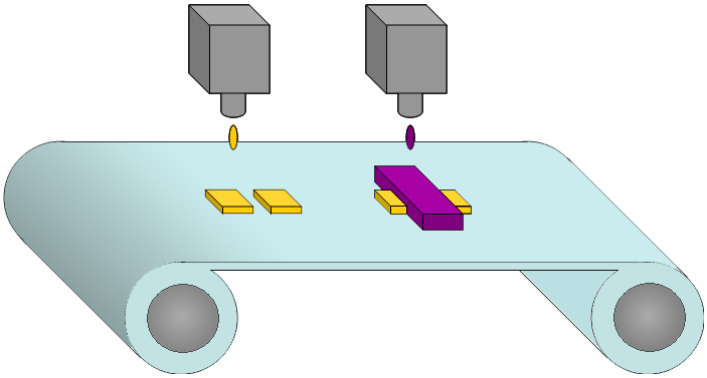

Figure 2.3: A demonstration of reel-to-reel fabrication system for organic electronics

The potential printability of organic electronics is the driving paradigm for organic transistor research. Unlike state-of-the-art silicon fabrication technologies, the printability

of organic electronics enables the pursuit of reel-to-reel fabrication strategies (fig. 2.3) [6]. An ideal reel-to-reel fabrication process continuously prints functional materials layer-by-layer, including metal, dielectric and semiconductor materials, thus realizing designed circuit functions. This technology will significantly drop the fabrication cost of circuits because of its ease of implementation, and low-cost of fabrication tools in comparison to expensive and complex tools used in current silicon technology. While it is unlikely that any technology will ever compete with silicon-based electronics at a cost-per-transistor level, reel-to-reel fabricated electronics can surely beat them at a cost-per-area level. Therefore, instead of constant function applications, printed electronics is suitable for constant area applications, such as DNA microarrays.

Of the many printing techniques available, inkjet-printing technology has been mostly researched because of its high printing flexibility and well-understood printing physics. While inkjet doesn't offer throughput as high as other printing methods, such as gravure and screen printing, the versatility of design is unparalleled. As a research tool, inkjet printing allows users to design customized patterns simply with CAD software (fig. 2.4). Inkjet systems also generally have many adjustable parameters which can be used to control printing quality, namely shape, smoothness, and continuity of printed patterns. Those parameters include ink viscosity, substrate surface energy and temperature, the working distance from the head to the substrate, the speed of the ejected drop, the volume of the drop, and the drop-to-drop distance on printed lines. Because of the fairly good control of printing quality achievable using inkjet in a research environment, most current all-printed transistors are injected [3,4]. The biggest disadvantage of inkjet printing

technique is probably the slow printing process and lack of high-speed manufacturability knowhow. Although multi-head printing can solve this problem to a certain extent, the development of high-speed printing techniques with good manufacturability is still mandatory.

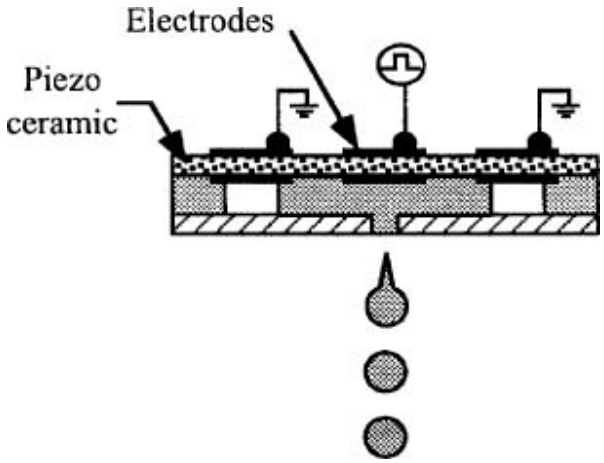

Figure 2.4: A typical Piezo-inkjet printer

Screen and gravures printing technologies [6] have been studied to improve printing speed. Screen-printing is attractive because of its printing flexibility that is largely due to the simplicity of the process and the ability to print ink films from submicron to hundreds of microns thick. This technology has already been used in the electronic industry for years to build interconnects during assembly of printed circuit boards (PCB). A screen, serving as a mask and typically made by polyester and stainless steel, is pre-patterned by chemical etch and is held slightly above the substrate, which is known as the off contact gap (fig. 2.5). To print the image, a blade is brought down forcing the screen into contact with the substrate. The passage of the blade pushes the ink through the screen onto the substrate. Though screen printing has a high throughput and is more cost effective than inkjet printing, most published works cite line pitch limits at 75μm [7]. This greatly limits applications of screening printing on high performance electronics. Thus a higher

resolution printing solution with high printing speed has to be pursued. While higher resolution screen printing has been demonstrated in research, virtually all demonstrations of screen printing have necessitated the use of high-viscosity inks, which is a significant challenge for organic electronics. In general, it is difficult to realize such high viscosity electronic inks without using binder additives; these binders degrade film properties and are therefore high undesirable in printed electronics applications.

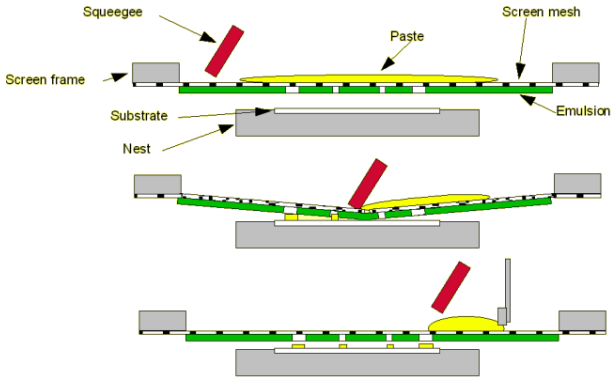

Figure 2.5: A typical screen printing process

Gravure, on the other hand, is expected to enable higher pitches. The basic gravure system is composed of an engraved metal image carrier, a sharp blade called a doctor blade and a rubber-covered impression roll (fig. 2.6). The engraved image carrier is wetted with ink and the doctor blade wipes the ink from the cylinder surface leaving only ink in the recessed image. The ink is then transferred to the substrate by pressing the substrate against the cylinder with an impression roll. With this process, larger area materials, such as several-meter wide plastic rolls, can be printed at a very high speed, typically over several meters per minute. This technique has been used to print large volume magazines, folding cartons, flexible packaging and so on for decades. For use in electronics printing, the gravure technique is difficult to optimize to ensure pattern

continuity and smoothness of the roll to provide absolutely no residue on non-patterned area. Gravure printing also tends to need higher viscosity inks than inkjet printing, though the viscosity requirements are much more achievable than those required by screen printing.

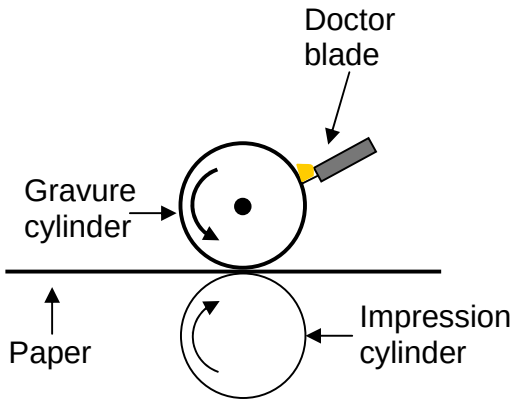

Figure 2.6: A simple gravure printing process

Clearly, different printing technologies are advantageous for different applications. Thus a reasonable future printing process will combine several printing technologies for different materials, layers or other requirements. For example, the gate layer may be printed with gravure printers because of its high resolution, while the semiconductor layer can be inkjet printed because it doesn't require as high resolution as gate or source/drain but does require precise thickness control for performance optimization.

Using above printing technologies, fully-printed organic electronics have already been reported by many laboratories [3] [4]. Three types of materials were printed to fabricate functional devices, namely conductive, dielectric and semiconductive materials. As for conductive materials, both conductive polymers and metallic nanoparticles have been

studied to make gate and source/drain materials [7]. Compared to conductive polymers, the metallic nanoparticle technique is capable of producing printed conductors with conductivities greater than three orders of magnitude better than printed polymers, which enables the creation of higher performance interconnections and passive components. Initial work has been reported using gold nanoparticles [8]. In this process, these nanoparticles are produced with particle diameters as low as 5nm with standard deviation of 2 nm. To prevent agglomeration, the nanoparticles are encapsulated with alkanethiol molecules, whose length changes the annealing temperature of those nanoparticles. An important consequence is that the gold nanoparticles show significantly low melting temperatures, typically less than 150ºC, while bulk gold is known to melt above 1000ºC. By printing encapsulated gold nanoparticles in solution with toluene, and then heating the substrate to 150ºC, conductive gold lines can be created on plastic substrates. After further optimization, this process was able to produce conductivities as high as 312,000 S/cm (70% bulk gold) [9]. Other nanoparticle materials have also been developed, including silver and copper, to complement the gold nanoparticle work, and to provide metals of varying workfunction to the realm of printed electronics [10].

Soluble dielectrics for printed devices have also been investigated. The most successful printable dielectric material, in terms of device mobility, is polyvinylphenol (PVP) dielectrics [11]. In this work, PVP was spin-cast and used as a gate dielectric in a non-printed OTFT process. The high mobilities achieved ($1cm^2/Vs$) and high breakdown strength caused this dielectric to become the standard polymer dielectric for printed OTFTs. The main disadvantage of solution processed polymer gate dielectrics is non-

scalable thickness of such films, typically >100nm. Thin gate dielectric layers for high capacitance coupling between the gate and the channel are especially important for high performance printed circuits to drop the power consumption. Thus research on soluble high-k dielectric materials is imperative. Currently these materials are typically made by a polymer film filled with high-k nanoparticles [12]. This method unfortunately drops the mobility significantly because of the rougher surface than spin-coated PVP films. A more promising method is to use self aligned monolayer (SAM) dielectrics, but the application of this method is greatly limited by easily-formed pinholes in the film because the growth of monolayers is very sensitive to surface contaminations. As a consequence, in the near future, PVP as a gate dielectric material will still dominate in printed electronics..

Materials for the organic semiconductors have also improved with time. Both polymer semiconductors and small molecule semiconductors have been widely studied. Polythiophene, as the mostly studied polymer semiconductor material, attracted significant attention in the early stages of organic electronics research because of its solubility in chemicals, like chloroform. By carefully choosing dielectric layers and optimizing annealing process, the highest reported mobility of spin-coated P3HT-based transistors is as high as $0.1 cm^2/VS$ [13]. The biggest disadvantage of P3HT is the low air stability. Generally, P3HT in the air works as resistor instead of semiconductor, because of oxygen doping effects.

In this aspect, pentacene became more attractive because it is the most air-stable organic semiconductor materials with the highest reported mobility, $>1 cm^2/V\text{-}s$. Such results

have been achieved using evaporated pentacene, since pentacene has very low solubility in most solvents. Importantly, several methods have been studied to transform the chemical structure of the material to be soluble in chemicals, like toluene. Such transformations produce soluble precursors that are printable and convert to insoluble pentacene upon subsequent heating. One of the higher performance pentacene precursors was reported by IBM [14]. In this process, the bulky side group was effectively removed through a post-deposition anneal processes at temperatures less than 200ºC. This process initially demonstrated saturation mobilities of 0.13 cm^2/Vs and on/off ratios of 2×10^7 for a spin-cast deposition. As this precursor material was integrated into a printed OTFT [15], mobilities of 0.02 cm^2/Vs and on/off ratios of 10^5 were achieved. Further optimization of the inkjet deposition process produced mobilities as high as 0.3 cm2/Vs [16]. As a result, printed OTFTs have begun to demonstrate performance only slightly less than vacuum-deposited OTFTs. As this new method for solution-based deposition of organic molecules matures, it is not inconceivable that printed organic semiconductors may have mobilities on par with their vacuum processed counterparts. Combined with common polymer dielectrics and metallic nanocrystal contacts, high-performance fully-printed OTFTs for RFID are a realistic endeavor, and may enable a fully printed RFID tag in the near future.

Though all work in this dissertation is done using lithographically-fabricated organic transistors, the process steps have been chosen to be implementable in printed process flows. It is reasonably believed that printed organic transistors have undoubted potential to detect biological molecules and ions because of their similar performance when compared to evaporated counterparts.

2.2 Carrier transport in Organic semiconductors and possible sensing mechanisms

Organic molecules which can be characterized as semiconducting are highly conjugated in nature, meaning a regular alternation of single and double bonds in the material, accompanied by delocalization of the out-of-plane pi electrons over the same. For example, a pentacene molecule is formed by five fused benzene rings that have a hexagonal structure with six alternated single and double bonds inside. Each carbon atom in a benzene ring is connected to only three other atoms: two carbons and one hydrogen atoms (fig. 2.7 left). Each carbon is therefore sp^2-hybridized, as in an ethylene molecule. Two sp^2 orbitals of each carbon atom overlap with similar orbitals of adjacent carbon atoms to form the σ bonds of the hexagonal ring. The third sp^2 orbital of each carbon overlaps with a hydrogen 1s orbital to form a C-H σ bond. Perpendicular to the plane of these three σ bonds at each carbon is a p orbital containing one electron, the fourth valence electron. The p orbitals on all six carbon atoms can overlap laterally to form a π orbital that create a ring or cloud of electrons above and below the plane of the ring (fig. 2.7b). Hence, while the electrons participating in σ-bonds are considered stationary, along a conjugated path π- electrons are delocalized and free to move. These free electrons make pentacene semiconductive.

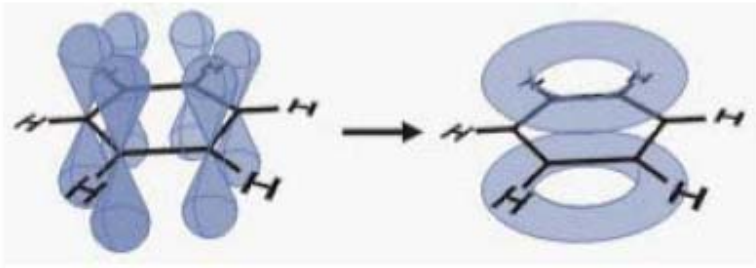

Figure 2.7: Benzene ring with π-orbitals highlighted (left), and effective electron ring (right).

Based on above understanding, two major classes of organic semiconductors designed and used in many laboratories are low molecular weight materials, like pentacene, and polymer, like polythiophene. Both of them clearly show alternating single and double bonds, meaning a conjugated π-electron system (fig. 2.8). The five fused benzene rings of a pentacene (fig. 2.8a) molecule not only provide a big and continuous π orbital cloud, but also the rigidity of the structure results in strong crystalline packing in thin films. This has been found to result in strong pi overlap between adjacent molecules, thus facilitating efficient hopping of carriers, resulting in the highest thin film mobility seen in organic semiconductor thin films, around $1cm^2/V\text{-}s$. But this clean structure without any side functional groups also makes it insoluble in any kinds of organic chemicals. Polythiophene, on the other hand, (fig. 2.8b) is readily soluble in chloroform. The added side chains help the solubility and alignment of polymers to form bigger crystalline. Therefore, small molecules are usually deposited from the gas phase by sublimation or evaporation, while conjugated polymers can only be processed from solution, such as by spin-coating or printing techniques as discussed above.

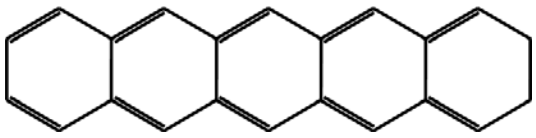

(a)

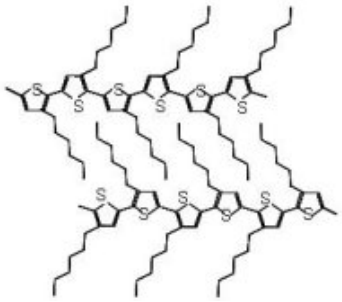

(b)

Figure 2.8: Two widely-used organic semiconductor materials showing rotated double and single carbon bonds a) Pentacene, b) polythiophene

Analogous to band theory used in inorganic semiconductor, organic semiconductors also exhibits electronic structures that are in some ways analogous to the bands seen in inorganic semiconducting crystals. Because π-bonds are much weaker than σ-bonds, the lowest excited state of a conjugated system involves the transition of an electron from a bonding (π orbital) to an antibonding (π*)-orbital. The delocalization of electrons across many π-orbitals results in a splitting of molecular orbital energy levels to form a spread of energy levels comparable to the energy bands in inorganic materials. The gap between the highest occupied molecular orbital (HOMO) energy band, corresponding to the valence band edge in inorganic system, and the lowest unoccupied molecular orbit (LUMO) energy band, corresponding to the conduction band edge in inorganic system, provides the equivalent of an energy bandgap (E_g) in organic molecules. However, the energy bands in organic materials arise from the interactions of a handful of molecules, rather than a large crystalline lattice of atoms, and the resulting band is narrower and contains a lower density of states than the energy bands in inorganic semiconductors such as silicon. As a result, this low density of states make organic semiconductor materials degenerate, thus the injected carriers greatly change the material conductivity (this will be discussed in Chapter 4). It is important to note that materials with overlapping HOMO and LUMO bands or very small E_g can be doped and used as conductors, while materials with larger E_g (typically in the range of 2-3 eV) are used as semiconductors. As an example, the bandgap of pentacene molecules is around 2.8eV. E_g is affected by the nature of π-bonding within the system, the immediate environment of the molecule, and its conjugation length. In a film, molecules exhibit a random distribution of defects, molecular orientations, and grain structure. This results in conjugated segments with

variable lengths, as well as heterogeneities in the immediate environments of different conjugated segments. Therefore, organic semiconductors exhibit density-of-states profiles with gradual band edges, typically shown as a Gaussian or exponential distribution, in contrast to the sharp band edges typically seen in the more perfectly ordered crystalline inorganic semiconductors (fig. 2.9)

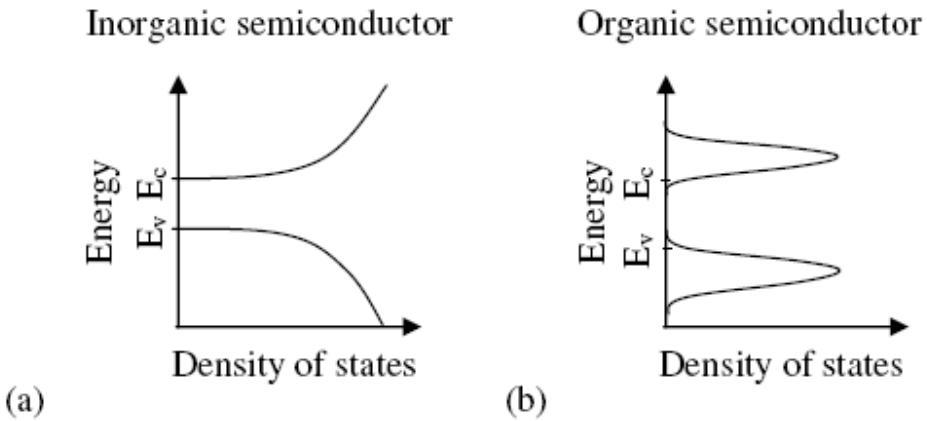

Figure 2.9: Typical band density of states vs. energy of single crystal inorganic semiconductor (a) and organic semiconductors (b)

It is clear that a significant part of the gradual band edge falls into the bandgap (fig 2.9b), illustrating large number of localized energy states, thus forming traps. Therefore, vastly different from the conduction physics of single crystal silicon transistors, carriers in organic semiconductors don't exhibit band-based transport but rather hopping between localized states. Those localized states are from chemical impurities, structure defects and self-trapping events and develop donor-like traps close to the LUMO level and acceptor-like traps close to HOMO level. In silicon, all atoms are bonded covalently and a uniform energy band is formed through the whole wafer, thus the charge transport occurs in delocalized states, and is limited by scattering of the carriers. On the other hand, the organic semiconductor molecules are weakly forced together by van de wals bonds, such

that the no continuous energy bands exists and charge transport occurs by hopping of charges between localized states. A main difference between the delocalized and localized transport is that, in the former, the transport is limited by scattering, while, in the latter, it is phonon assisted. Accordingly, the charge mobility decrease with temperature and electrical field in silicon devices, the reverse being true in most organic materials.

Two models borrowed from amorphous silicon transistor transportation are used to explain temperature and field-dependent mobility in OTFTs: Multiple trapping and release (MTR) model [8] and Variable Range Hopping (VRH) model [9]. Compared to the VRH model, the MTR model has been found to be more suitable for polycrystalline organic semiconductor materials, such as the pentacene used in this dissertation, while, on the other hand, VRH model works well in poorly ordered organic semiconductor materials, commonly seen in OLEDs. Because of the large density of traps localized in the band gap, the MTR model dictates that carriers are commonly and repeatedly trapped in these localized states. Thermal energy causes periodic release of these carriers to extended (i.e., more band-like) states. The carriers are then free to move until they are trapped again, and the process repeats. As the model is used, the following assumptions are usually made: First, the carriers arriving at the trap are instantaneously trapped with a probability close to one. Second, the release of trapped carriers is controlled by a thermally activated process. The MTR model explains this mechanism and correctly predicts the thermal and gate voltage dependence of field mobility [17, 18].

It is important to note that the field-effect mobility of OTFTs increases strongly with increasing (negative) applied gate bias. This behavior is commonly observed in all OTFTs, regardless of active material or processing conditions. A number of explanations have been offered to explain this phenomenon. An early explanation for this effect invoked the Poole-Frenkel mechanism, in which the columbic potential near the localized levels is modified by the applied field, increasing the tunneling rate between those sites. For cases in which significant conduction is assumed occur through the tunneling of trapped charges between localized states, then, the mobility at high fields (>10^5V/cm) is expected to depend exponentially on applied field: $\mu(F) = \mu(0)\exp\left(\frac{q}{kT}\beta\sqrt{F}\right)$,[19]

A more accurate explanation uses MTR model, predicting a power-law relationship of the form: $\mu_{FET} = K(V_{SG}\text{-}V_T)^{\alpha}$, where α is expected to fall between 0 and 1 [19]. Because organic TFTs operate in the accumulation mode, which means that as the gate bias is increased (i.e. more negative), the Fermi level gradually approaches the nearest delocalized band edge. In pentacene-based transistors, the Fermi level moves to HOMO level. At low gate bias, most of induced charges fill traps, thus the mobility is low. With an increase of the gate voltage, the Fermi level approaches the HOMO level and most traps are filled, increasing free carrier concentration and thus increasing mobility. This model has been used successfully to fit experimental pentacene OTFT I-V curves.

The MTR model can also successfully explain temperature-dependent mobility [19]. As the Fermi level moves closer to the valence band, deep traps become filled, and the remaining shallower traps are more easily thermally activated. Thus, reports of relatively

temperature independent behavior could simply be an indication of a shallow, narrow trap distribution above the valence band.

Organic semiconductor materials used in transistors are typically polycrystalline. The crystalline size depends strongly on deposition conditions and methods. Normally, printed organic semiconductor materials have smaller crystalline size than evaporated films, thus producing devices with lower mobility due to the scattering between crystals. The band tail in organic semiconductors (fig. 2.9) and the frequent presence of energy states within the band gap due to impurities and defects result in a high density of traps within the band gap, making it difficult to invert. Therefore, similar to amorphous silicon-based TFTs, OTFTs run in accumulation mode. For a p-type organic semiconductor (the major carriers are holes), a negative voltage applied to the gate electrode accumulates positive charge carriers within the active layer near the dielectric interface. When enough charge carriers have been accumulated, the conductivity of the accumulated layer increases dramatically, providing a conductive channel running through a thin layer in the organic semiconductor material between the source and drain. The current-voltage (I-V) characteristics of a representative substrate gated, bottom contact, pentacene-based OTFT are given in Figure 2.10

To a first approximation, OTFT transfer curves are similar to those seen in their inorganic counterparts [20]. All critical properties are discernable, including cutoff, subthreshold, linear, and saturation regimes of operation (fig. 2.10). In addition, drain current scales as expected with device width, length, and gate dielectric thickness. Because of this, OTFTs

are characterized with many of the same metrics as inorganic FETs: field-effect mobility (μ_{FET}), threshold voltage (V_T), on-off current ratio (I_{on}/I_{off}), transconductance (g_m), output resistance (Ro), contact resistance on source and drain (R_S and R_D). However, standard square-law MOSFET equations do not provide a good quantitative fit for OTFT behaviors. Because OTFTs often suffer from significant non-idealities at contacts, addressing contact resistance and contact injection barriers, using standard MOSFET theory for Schottky contacts improves the accuracy of these models, but not completely. In particular, several aspects of OTFT behavior cannot be explained by direct adaptation of bulk silicon MOSFET theory including gate-bias-dependent mobility and thermally activated transport as discussed above.

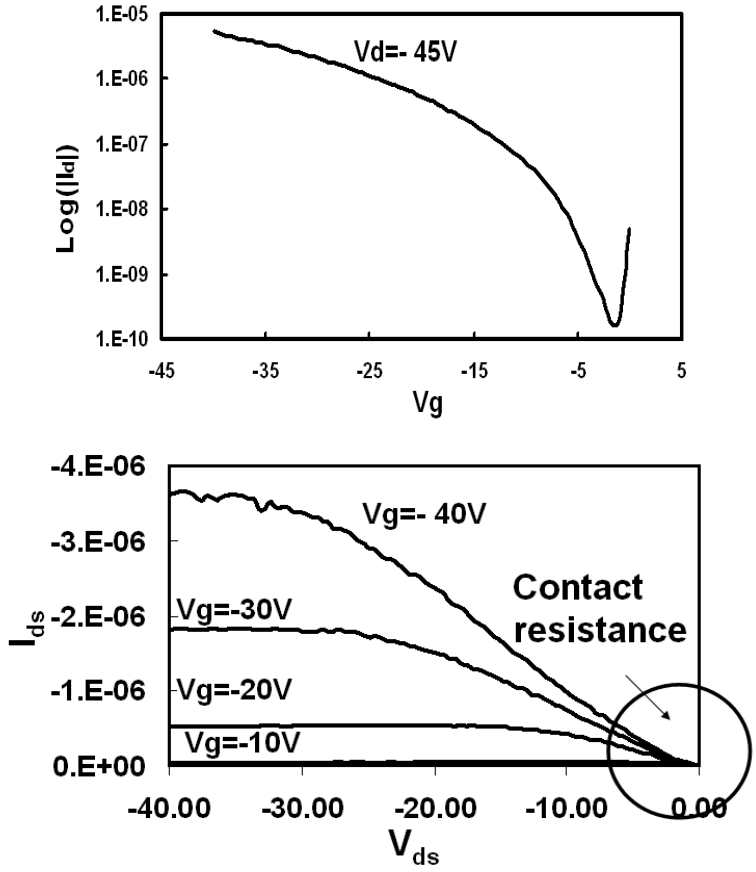

Figure 2.10, typical characteristic curves of pentacene-based OTFTs. (a) Log(Id)-Vg curve and (b) Id-Vd curve. The device in the curves is a substrate-gated, bottom contact

OTFT with W/L of 1100μm/ 110μm and HMDS-coated 1000Å SiO_2. As expected, the contact resistance is clearly shown in the Id-Vd curve and the tail of the Id-Vg curve in the low Vg region is possibly caused by gate leakage.

2.3 OTFT-based Biosensors

Because of the instability of organic semiconductors in both air and water [21], the usage of organic semiconductor materials directly as a biosensitive layer is still rare. The first successful demonstration of OTFTs bioapplication is in ion concentration monitoring [22]. A substrate-gated top-contact OTFT was used with various organic semiconductor materials: Pentacene, PTPTP, CuPc, DHα6T, α6T, etc. (fig. 2.11). A fluorochemical-coated layer was applied to cover the source/drain area of the 1.6*mm* wide and 5*mm* long transistor channel. The hydrophobicity of the coating material successfully prevents the source/drain area from being damaged by water (Note that these regions are more sensitive to water-induced degradation because of the high electrical field drop across the same). With this structure, the performance shift of OTFTs exposed to water, lactic acid, and glucose were measured as a function of time. Although the experiments were limited to ion detection, the experiment does unveil two necessary components required for a successful bioapplication of OTFTs: the biosensitivity and integrated microfluidic channels. In this dissertation, we will discuss both parts to make a DNA microarray system on pentacene-based OTFTs.

Though there have been previous reports claiming the demonstration of OTFT-based biosensors, they are in fact ISFET structures, in which the sensitive layer is coated on the gate and the organic semiconductor materials replace the silicon substrate [23]. This

structure does drop the price of the devices because of the usage of cheap substrate, but unfortunately is also disadvantageous compared to silicon-based ISFETs because of the lower sensitivity resulting from the slower turn-on characters. Thus, this structure won't be discussed in this thesis.

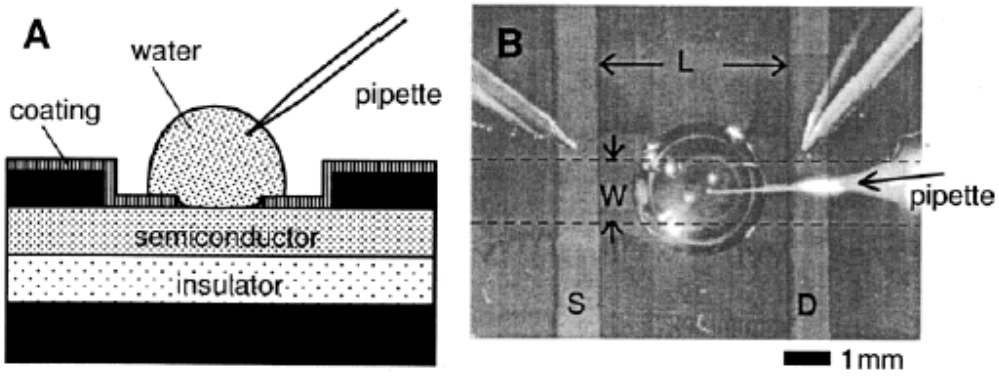

Figure 2.11, Schematic and experimental setup of Dr. Someya research: the application of OTFTs as ion sensors [23]

2.4 The feasibility of OTFT-based DNA sensors

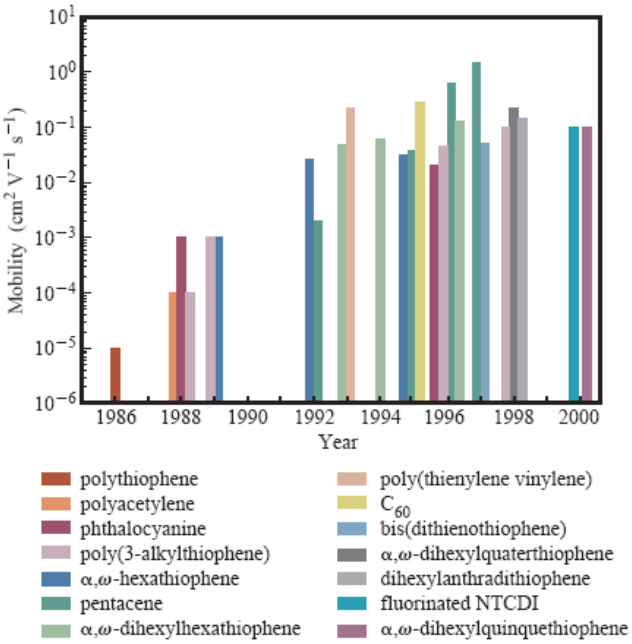

Figure 2.12, list of available organic semiconductor materials and their mobility [25]

Commercialization of OTFT products, such as ultra-low-cost RFID tags and backplanes for flexible display applications has been very slow. Progress has suffered due to the instability and low performance of organic materials. It is well known that the chemically sensitive carbon backbones of organic materials interacts readily with both oxygen and water vapor [21], causing both immediate and gradual shifts in electrical characteristics. Even if degradation by air or water can be satisfactorily addressed by encapsulating whole structures, shifts during operation due to bias stress effects will still be a serious concern [24]. Even when used in inert environments, the simple act of operating an OTFT causes shifts in the device characteristics. This type of drift, known as bias stress and mainly caused by deep traps in semiconductor bulk materials, can be reduced through careful choice of fabrication methods, materials, and operating conditions, but cannot be completely avoided.

Low performance, particularly low mobility, is another metric that has retarded the commercial viability of OTFTs. Numerous different organic semiconductor materials have been researched by laboratories around the world over the past twenty years [25]. With their efforts, mobility of materials have been improved significantly from less than 10^{-5}cm^2/V·s to over 1 cm^2/V·s (fig. 2.12). In recent years, pentacene has become the most-researched material because of its air-stability and high performance. OTFTs with thermally-evaporated pentacene have achieved mobility over 1 cm^2/V·s and the devices formed with printed pentacene variants have achieved mobilities greater than 0.3 cm^2/V·s [26]. This mobility is already good enough for some initial applications, but is still below the needs of most major OTFT target applications.

Fortunately, these factors are not big concerns for DNA sensory applications. For example, bias stress is not a serious concern because of the disposability requirement of DNA chips. In practice, although conventional silicon-based DNA chips are typically very expensive, from $200 to $10,000, they aren't reused because of the actual bonding occurring between detected sequences and immobilized sequences. Although, technically, the bonds can be separated by heating the chip to a certain high temperature, this processing also simultaneously brings intolerable variance for data analysis, making reusable DNA sensors impractical. As a result, this one-time-use nature of DNA chips doesn't require endurance of sensor operation but does require high stability and high sensitivity.

To date, Pentacene is the most stable organic semiconductor material. Though organic semiconductors are very sensitive to air or water, the degraded performance is mostly recovered by storage of OTFTs in nitrogen or vacuum because of nonpermanent chemical reactions between air/water with pentacene molecules. To demonstrate the recoverability of pentacene-based OTFTs, transistors with a 100nm thick SiO_2 layer followed by patterned gold source/drain electrodes forming channel width/ length of $1.1mm/110\mu m$ channels were fabricated following manufacturing methods discussed previously. A $10nm$ pentacene film was evaporated as the last step. The fabricated transistors was soaked in DI water for 22 hours and followed by storing in nitrogen for overnight. Four transistors were measured before and after soaking process. Representative transfer curves clearly concluded that the overnight storage of the transistor in nitrogen only increases the leakage current to less than ten times higher than original value with almost no change of saturation current (figure 2.13). The recoverability of OTFTs certainly

suggests the nonpermanent effects of water on pentacene and thus it is safe to deploy immobilization and hybridization for hours on OTFTs without worrying about the loss of performance.

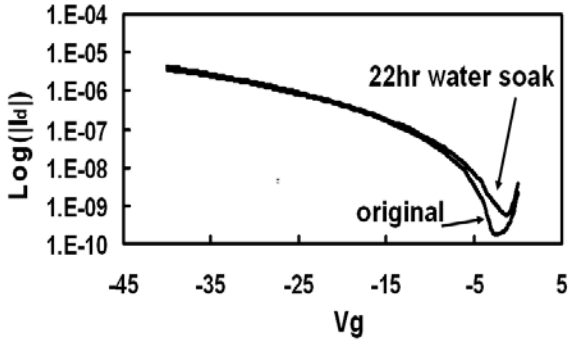

Figure 2.13: the recoverable performance of pentacene-based OTFTs soaked in DI water for over 22hr. The overnight storage in nitrogen recovers the performance of the transistor with almost no saturation current shift and less than ten times off-current increase.

Even better, the use of organic semiconductor materials directly as the sensitive layer for DNA molecules potentially offer high sensitivity, because the molecules are able to change several characteristics of the active organic semiconductor film simultaneously, including mobility, threshold voltage, and crystalline structure, all of which result in a strong saturation current shift. This electrical-readout of the transistor structure also readily makes high integration level, enabling portable applications. Thus these advantages of OTFT-based DNA sensors unambiguously outperform their counterparts, including ISFET, chemiresistors as well as amperometric and potentiometric sensors.

2.5 DNA hydrophobic interaction immobilization

Because of the high performance and good air-stability of pentacene, the applicability of pentacene in detecting DNA hybridization was tested. As discussed in Chapter 1, two

critical steps are involved in all DNA sensors: DNA immobilization and on-chip hybridization. These two steps, as will be proved in this dissertation, can be readily implemented on pentacene-OTFTs. Actually, the hydrophobicity of a DNA-doped pentacene film makes it an excellent testbench for DNA detection.

The first step to implement DNA detection for all kinds of DNA sensors is always the immobilization of the probe DNA molecules onto sensitive layers. Two types of immobilization methods are typically used: immobilizing covalently by chemically modifying both DNA molecules and sensor surfaces [27] and immobilizing physically by taking advantages of hydrophobic interactions between ssDNA molecules and crevices on the hydrophobic substrate surface [28]. The most common method currently used in most DNA sensors is the first one because of its strong, and thus stable, and controllably directional immobilization. Commonly, amino groups are added to one end of the DNA molecules. Correspondingly, Aldehyde supports or epoxide activated supports are added to the sensor surface to develop covalent bonds with aminated single-stranded DNA molecules.

Clearly, the covalent bonding method requires specific chemical function groups on the sensitivity surface, thus making the procedure complex. In this dissertation, a physical immobilization method is used because it is faster and easier than immobilization based on chemical reactions. Unfortunately, the physical method also brings non-directional immobilization and drop hybridization rate significantly [29], therefore the covalent

bonding-based DNA immobilization methods using different organic semiconductor materials are suggested as topics for investigation in future work.

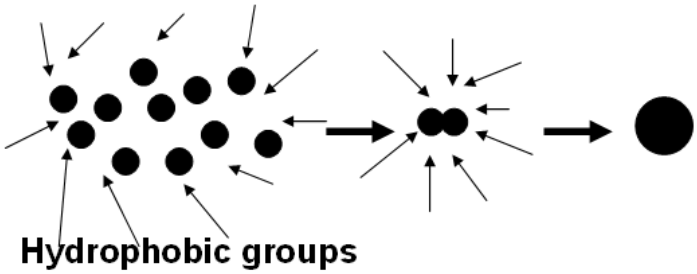

(a)

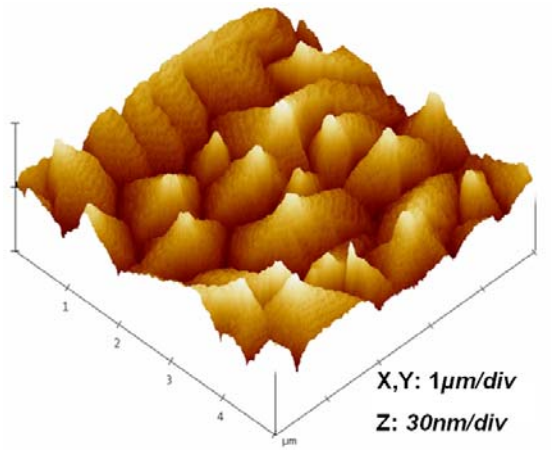

(b)

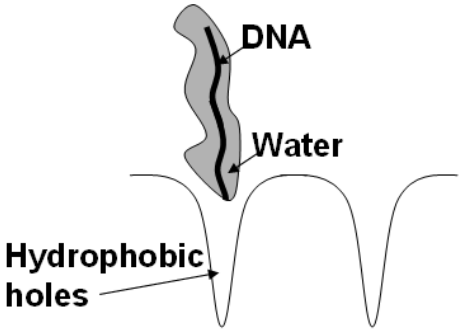

(c)

Figure 2.14: Scheme of hydrophobic interactions and feasibility of DNA immobilization on a pentacene film using hydrophobic interactions. a) Hydrophobic interactions occur as hydrophobic groups are dipped into hydrophilic liquid, b) A typical AFM picture of an evaporated pentacene film, showing controllable roughness and hydrophobic surface, c) Scheme of DNA immobilization caused by hydrophobic interactions between DNA molecules and hydrophobic pentacene film.

It is reasonable to consider the physical adsorption of DNA molecules on a pentacene film because it is well known that surfaces of evaporated pentacene film are hydrophobic and rough (Fig 2.14 b), and bases of DNA molecules are also hydrophobic. The

immobilization proceeds in a manner similar to that seen during the dropping of oil (non-polar molecules) into water (polar solution). In this analogy, small oil droplets turn to each other, assembling together to form big drops instead of remaining as the small droplets (fig 2.14a). Similarly, when DNA and pentacene are introduced into an aqueous environment, the hydrophobic parts of both DNA molecules and pentacene film attract each other (fig 2.14c). This attraction assures hydrophobic interactions between DNA molecules and pentacene films, pushing DNA segments into hydrophobic holes (i.e. crevices or crystalline boundaries) on the pentacene film, thus forming immobilization of the DNA molecules on the sensor surface through physical adsorption. The hydrophobic interaction immobilization was a very common method in the early stage of DNA microarray development [28], and is still broadly used in the current protein immobilization. Although this physical method loses immobilization directionality, it is stable enough for the DNA sensing tested in this dissertation

.

A typical hydrophobic interaction based immobilization process can be detailed with four continuous steps: namely 1) Transport of the DNA segments to the membrane surface by diffusion; 2) Alignment of hydrophobic domains on the DNA segments and the membrane; 3) Penetration of hydrophobic regions on the segments into hydrophobic regions in the membrane; 4) Elimination of layers of hydration surrounding these regions on both the membrane and DNA segments. Through those four steps, DNA segments are secured in the crystal boundaries of the pentacene film. Therefore, depth and density of crystal boundaries define the efficiency of the immobilization. Optimizing these two factors is then the main purpose of the pentacene morphology control. Besides these two,

concentration of DNA solution also influences the immobilization through changing DNA concentration gradient between solution and the pentacene film. Of course, the hydrophobicity of the film is significantly important, but because only the pentacene system is considered in this dissertation, this factor won't be discussed.

2.6 Control of evaporated pentacene morphology

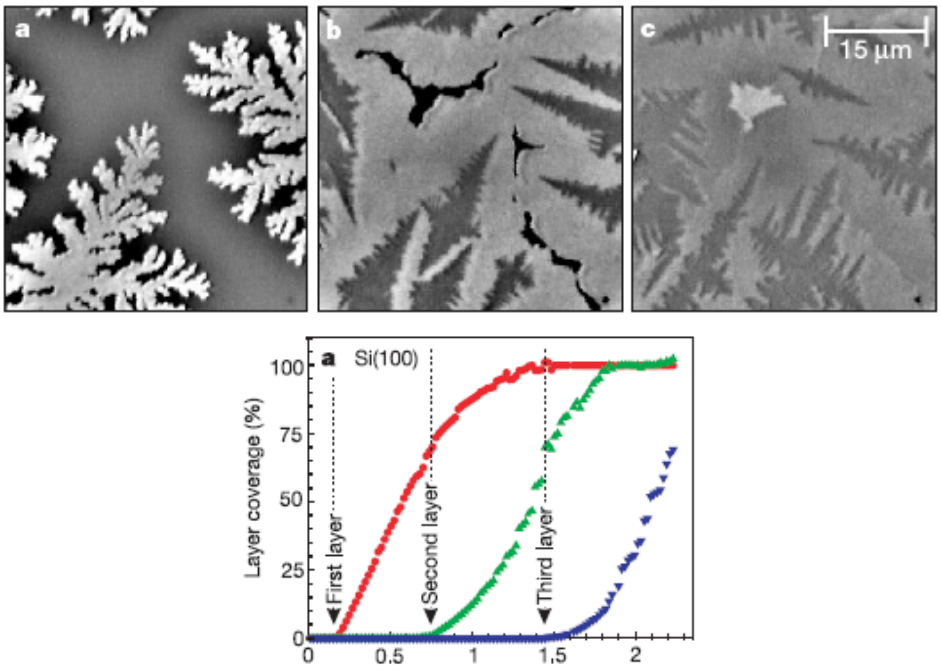

Figure 2.15, the layer-by-layer growth of pentacene on bare silicon surface [20]

Based on the understanding of hydrophobic interaction immobilization, it is important to control the shape and density of crevices in pentacene films in order to make immobilization efficient. The pentacene film deposited on the silicon dioxide surface is actually grown by a layer by layer process [30], in which each layer is around 1.5nm thick (fig. 2.15). The pentacene nucleation is aggregated first on the SiO_2 surface, extending all over the surface to form the first layer. As the first layer almost covers 60%

of the surface (the percentage depends on the deposition conditions, substrate temperature and surface treatments), the second layer starts to grow. Similarly, as the second layer covers 60% of the first layer, the third layer starts to grow. By repeating cycles of deposition, the pentacene film finally reaches the designed thickness and the layer-by-layer growth naturally builds islands on the surface (figure 2.15).

Table 2.1 Experiment table for roughness control

	Pattern	Deposition Thickness	Deposition Rate	Deposition Temperature	Surface Treatment
1	----	100	2	30	Bare
2	--+ +	100	2	70	HMDS
3	-+-+	100	10	30	HMDS
4	-+ +-	100	10	70	Bare
5	+--+	300	2	30	HMDS
6	+-+-	300	2	70	Bare
7	+ +--	300	10	30	Bare
8	+ + + +	300	10	70	HMDS

To investigate factors that may influence deposited pentacene morphology, a statistically-designed screening experiment was done. The experiment tested 16 wafers with 8 combinations of experimental conditions including all four factors mentioned above (table 2.1). The designed experiment investigates not only the four main factors effects, but also some crossing factors effects. The details of experiments design will be discussed in the following chapter. Root Mean Square (RMS) value was measured for each evaporated pentacene film using an Atomic Force Microscope (AFM) analysis to represent corresponding roughness level. Based on measured results, it is clear that the thicker film, the film deposited at higher rate, the film deposited under lower substrate temperature or the film deposited on the bare silicon dioxide surface results in a rougher surface (fig. 2.16).

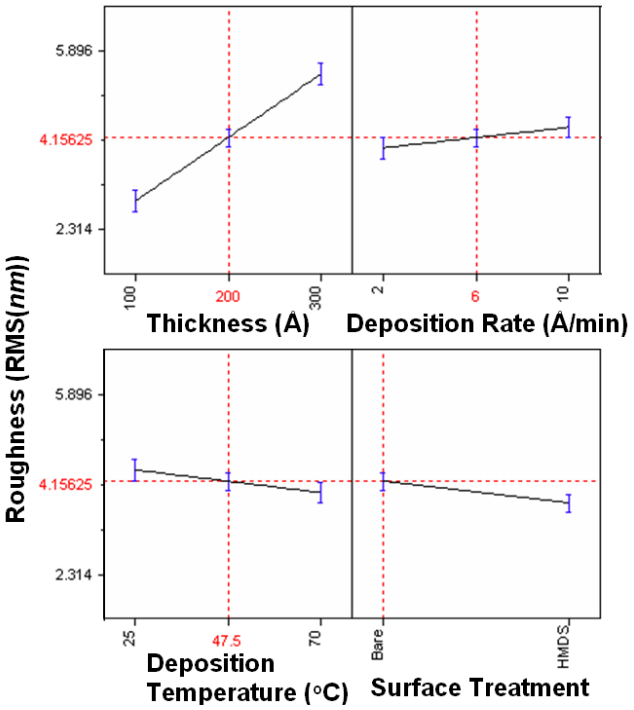

Figure 2.16: Surface roughness control of pentacene film using deposition thickness, rate, substrate temperature and surface treatment

A proposed pentacene deposition procedure helps understanding of conclusions given by above experiments (fig. 2.13). Analogous to a Chemical Vapor Deposition (CVD) deposition, the whole deposition can be divided into three continuous steps: gas-phase transport, adsorption (or nucleation) and extension (fig. 2.17). As the evaporation starts, pentacene molecules transport from the source to the substrate surface; the rate of the transport is solely decided the heating power of the source if the vacuum level is constant. Some of the molecules close to the substrate surface are absorbed, forming initial nuclei. Upon nucleation, these nuclei extend along the surface horizontally, forming crystalline domains. The edges of adjacent abutting crystals form crystalline grain boundaries, impacting electric performance of transistors as discussed previously. Thus the density of nuclei, which is decided by the substrate surface condition, and the ratio of pentacene flux over extension, F/D, defines crystalline size and surface roughness.

Using the proposed pentacene deposition model, deposition rate is expected to change final surface roughness. Because the low evaporation rate due to low heating power results in small pentacene flux and thus generates small ratio of F/D, the crystalline size of the resultant pentacene film is big, producing a smooth surface. Similarly, the high substrate temperature minimizes the surface roughness by increasing the extension rate, thus again generating small F/D ratio. Aside from the F/D ratio effect of the top factors, the hydrophobic surface coating, HMDS, changes the surface morphology of the film by decreases density of nuclei. It is well known that a HMDS monolayer can passivate broken bonds on a SiO_2 layer and develop uniform surface energy, thus reducing density of nuclei [30]. The deposition thickness effect on surface roughness has nothing to do with the deposition dynamic, but simply that a thicker film can provides more molecule layers, giving deeper crevices.

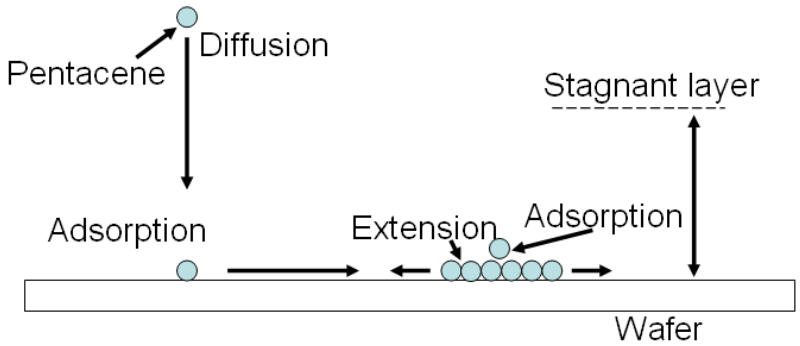

Figure 2.17: Scheme of Pentacene deposition, explaining roughness control strategy

As an example, two substrate temperatures, 27°C and 70°C, were used during evaporation of the pentacene films, resulting in the deposition of films of clearly different roughness: low temperature gives rougher surfaces (rms (root mean square) roughness = 5.493 nm versus rms roughness = 4.448 nm) because it allows faster adsorption of pentacene on the

SiO_2 surface, as expected, forming pentacene islands on the surface faster than high temperature evaporation (fig. 2.18).

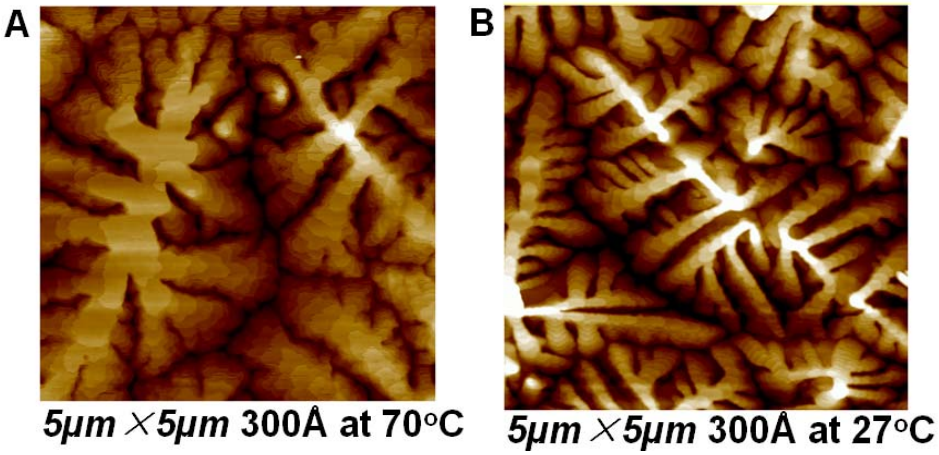

Figure 2.18: A typical roughness control using different substrate temperature

Based on the controllable morphology of pentacene film, the immobilization of DNA molecules can be optimized. Because the hydrophobic character of DNA molecules is actually due to the bases on the side, long chain DNA segments can be more easily immobilized than short chain DNA segments. As two types of DNA segments are used in the dissertation, Lambda DNA molecules clearly show easier immobilization than oligonucleotides do. Similarly, double-stranded DNA segments also are immobilized less effectively than single-stranded DNA segments because they enclose the hydrophobic bases on the inside of the hybridized pair. This immobilization difference directly enables off-chip hybridization detection discussed in the dissertation. For all types of DNA used in this work, pentacene with a rougher surface has been found to make immobilization easy and stable.

2.7 Conclusion

The low performance and instability of organic semiconductors has slowed the commercialization of organic electronics but fortunately bring a unique chance for disposable DNA sensors. Because of the hydrophobicity and controllable roughness of pentacene thin films, it is possible to immobilize DNA molecules on the pentacene surface. This is easily accomplished by exposing the pentacene layer directly to DNA molecules, thus leading to high DNA sensitivity. This OTFT-based DNA sensor potentially is able to realize disposable, portable, high sensitivity and high selectivity DNA detection for early-stage disease diagnosis and personalized medications.

Reference:

1. Crone B. *et al*, Electronic sensing of vapors with organic transistors, Appl. Phys Lett., vol 78, pp. 2229, 2001
2. Liao F., et al, Organic TFTs as gas sensors for electronic nose applications, Sensors and Actuators B, Vol. 107, pp 849, 2005
3. Molesa, S.E. *et al*, A high-performance all-inkjetted organic transistor technology, IEEE International Electron Device Meeting Technical Digest, pp 783, 2004
4. Kawase T., *et al*, All-polymer thin film transistors fabricated by high-resolution ink-jet printing, IEEE International Electron Device Meeting Technical Digest, pp 623-626, 2000
5. Mabeck J.T., *et al*, Chemical and biological sensors based on organic thin film transistors, Anal. Bioanal. Chem., Vol 384, pp 343, 2006
6. Gamota, D. *et al*, Printed organic and molecular electronics, Kluwer Academic Publishers, 2004 ISBN: 1 4020 7707 6
7. Bao Z. Materials and fabrication needs for low-cost organic transistor circuits, Advanced Materials, Vol 12, pp227, 2000
8. Huang D. et al, Plastic-compatible low-resistance printable gold nanoparticle conductors for flexible electronics", Journal of the electrochemical society, Vol. 150, pp. 412, 2003
9. Redinger, D., *et al*, An Ink-Jet Depositied Passive Component Process for RFID *IEEE Trans. Elec. Dev.,* vol. 51, pp. 1978, 2004.
10. Volkman, S., *et al*, Ink-jetted silver/copper conductors for printed RFID applications, *Proc. Mat. Res. Soc. Spring Meeting*, vol. 814, Paper I7.8, 2004.

11. Drury, C.J., *et al*, Low-cost all polymer integrated circuits, Applied Physics Letter, Vol. 73, pp. 108, 1998
12. Chen, F.C., *et al*, Organic thin-film transistors with nanocomposite dielectric gate insulator, Applied Physics Letters, Vol. 85, pp 3295, 2004
13. Park J. *et al*, a polymer gate dielectric for high mobility polymer thin film transistors and solvent effects, Applied Physics Letters, Vol. 85, pp. 3283, 2004
14. Afzali, A., *et al*, High-performance, solution processed organic thin film transistors from a novel pentacene precursor, J. Amer. Chem. Soc., vol. 123, pp. 8812, 2002
15. Volkman S. *et al*, Inkjetted organic transistors using a novel pentacene precursor, Proceedings of the Materials Research Society Spring 2003 meeting, Volume 769, H11.7, 2003
16. Subramanian, V., Printed organic transistors for ultra-low-cost RFID applications, IEEE Trans. Comp. Pack. Tech., vol. 28, pp.742, 2005
17. Horowitz G., *et al*, Temperature and gate voltage dependence of hole mobility in polycrystalline oligothiophene thin film transistors, Journal of Applied Physics, Vol. 87, pp 4456, 2000
18. Brown A.R., et al, A universal relation between conductivity and field effect mobility in doped amorphous organic semiconductors, Synthetic Metals, Vol. 68, pp 65, 1994
19. Horowitz G., Organic Field Effect Transistor, Advance Materials, Vol 10, pp 365, 1998
20. R. F. Pierret, Semiconductor Device Fundamentals, Addison Wesley, 1996
21. Ye R.B., et al, Effects of O_2 and H_2O on electrical characteristics of pentacene thin film transistors, Thin Solid Films, Vol, 464-465, pp 437, 2004
22. Takao S., et al, Integration and Response of Organic electronics with Aqueous Microfluidics, Langmuir, Vol 18, pp 5299, 2002
23. Bartic C. et al, Organic thin film transistors as transducers for (bio)analytical applications, Anal Bioanal Chem, Vol 384, pp 354, 2006
24. Lee J., et al, Effect of active layer thickness on bias stress effect in pentacene thin-film transistors, Appl. Phys. Lett., Vol, 88, pp 233513, 2006
25. Dimltrakopoulos C.D., et al, Organic thin film transistors: A review of recent advances, IBM J. RES. & DEV. Vol. 45, pp 11, 2001
26. Molesa S.E., et al , Low-voltage inkjetted organic transistors for printed RFID and display applications, IEEE International Electron Device Meeting Technical Digest 2005
27. Lobert P.E. et al, Immobilization of DNA on CMOS compatible materials, Sensors and Actuators B, Vol. 92, pp 90, 2003
28. Gillespie D. et al, A quantitative assay for DNA-RNA hybrids with DNA immobilized on a membrane, Journal of molecular biology, Vol. 12, pp 829, 1965
29. Dugas, V., et al, Immobilization of single-stranded DNA fragments to solid surfaces and their repeatable specific hybridization: Covalent binding or adsorption? Sensors and Actuators B, Vol. 101. pp 112, 2004
30. Meyer zu Heringdorf FJ, et al, Growth dynamics of pentacene thin films, Nature, 421, pp 517, 2001

Chapter 3

Statistical data Analysis and design of experiment

Statistical data analysis and experiment design are necessary for a successful DNA microarray analysis because of the large variance typically seen in such experiments and large amount of data used for analysis [1]. The use of statistic analysis, including t-test, f-test, Analysis of Variance (ANOVA), etc, is helpful to effectively extract “true” information from data affected by substantial variance. Based on the understanding of statistics, it is also helpful to design experiments statistically, to maximize the amount of "information" that can be obtained for a given amount of experimental effort. In this chapter, qualitative explanations of models and calculations used for the research discussed in this thesis are introduced for the requisite statistical analysis.

3.1 Continuous probability distributions

A probability distribution is a mathematical model that relates the value of a random variable with its probability of occurrence. There are two types of probability distributions: discrete and continuous. Discrete distributions are used to describe random variables that can only take on certain specific values, such as two faces of a coin as it falls on the floor. On the other hand, when the random variable can have any value on a continuous scale (such as measured transistor saturation current), the probability distribution is continuous. A discrete distribution typically follows binomial, Poisson or

Pascal probability distribution, while continuous distributions follow normal, chi-square or F-distribution. In this chapter, only continuous probability distributions will be discussed because all parameters used to evaluate DNA sensitivity of OTFTs, including saturation current, threshold voltage and mobility, are continuous.

3.1.1 Normal distribution

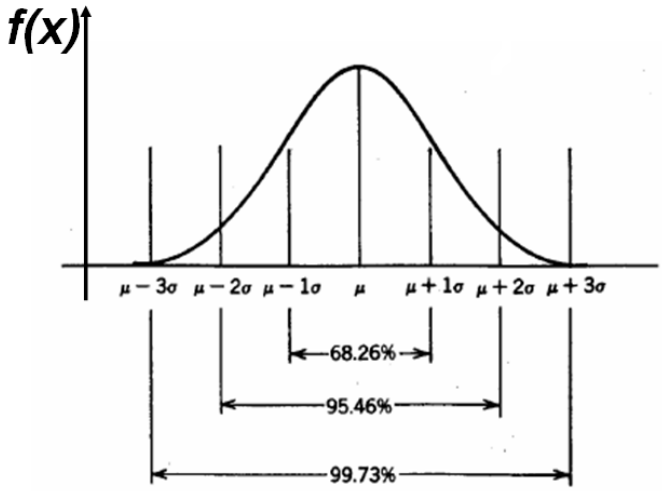

Figure 3.1: A schematic explanation of a normal distribution with labeled mean and variance

Without a doubt, the normal distribution is the most important and also the most well-known continuous probability distribution in applied statistics [2, 3]. Most physical phenomena, such as noise involved in experiments, can be approximated well as a normal distribution. More broadly, according to the Central Limit Theorem, the sum of the variables that has a finite variance is normally distributed. This theorem applies to most scientific experiments because their variances are not infinite unless the experiments are totally out of control. Therefore, all statistic analysis methods and statistically designed experiments discussed in this dissertation are based on the assumption that data used for analysis is independent and identical normal distributed.

3.1.1.1 Properties of a normal distribution

A normal distribution is expressed as $N(\mu,\sigma^2)$ and its necessary metrics can be graphically interpreted clearly (fig. 3.1). As shown in the graph, the normal distribution shows a symmetric bell shape. In the curve, the center of x-axis is called mean (represented as μ), the parameter used to evaluate the spread of the curve is called variance (represented as σ), and the y-value of the curve is the probability density function (equation 3-1). Apparently, the shape of the curve is defined by both μ and σ. The area under the curve in a certain x-axis range represents the probability of x-value falling into that region. This area is calculated by integrating y through the range of x. Several useful numbers worthy of remembering is that 68.26% of the area under a normal curve lies in the interval $\mu\pm\sigma$; 95.46% of the area lies in the interval $\mu\pm2\sigma$; and 99.73% of the area lies in the interval $\mu\pm3\sigma$. Those numbers are particularly helpful to estimate a confidential interval of a number's occurrence.

$$f(x)=\frac{1}{\sigma\sqrt{2\pi}}e^{-\frac{1}{2}\left(\frac{x-\mu}{\sigma}\right)^2} \quad \text{3-1}$$

Statistic analysis is a method to estimate whole information with limited sample data. It is important to note that the definition of a normal distribution, both mean and variance are terminologies of true value of the whole data and are hidden values that we can't know exactly. Because only limited data points are sampled, average and standard deviation are used as the best estimators of mean and variance respectively and can be calculated easily from the measurements. Importantly, by increasing the measurement numbers to infinite, the "average" can infinitely approximate "mean" but can't equal it. This infinite

approximation is explained by the additivity of variance and mean. If an "add" action is done by $y=a_1x_1+ a_2x_2+\ldots+ a_nx_n$, the corresponding mean and variance of the sum are $\mu_y=a_1\mu_1+ a_2\mu_2+\ldots+ a_n\mu_n$ and $\sigma_y^2= a_1^2\sigma_1^2+ a_2^2\sigma_2^2+\ldots+ a_n^2\sigma_n^2$. Thus, the mean and variance of an average can be calculated as $\mu_y=1/n(\mu_1+ \mu_2+\ldots+ \mu_n)$ and $\sigma_y^2= 1/n^2(\sigma_1^2+ \sigma_2^2+\ldots+ \sigma_n^2)$ If all x value are sampled from the same set of experiments, then all data have same μ and σ, and the mean and variance are simplified as $\overline{\mu}_n = \mu$ and $\overline{\sigma}_n = \frac{\sigma}{\sqrt{n}}$. Clearly, large number of replications of an experiment always increases estimation accuracy of its mean, but unfortunately also increase experiment complexity. As a consequence, an optimum replication number is necessary, which is the concept of sample size that will be discussed in following paragraphs.

3.1.1.2 Evaluation of data normality

The normality of collected data can be evaluated mathematically. One of the most visualizable methods for the evaluation is the Normal Quantile Plot (figure 3.2 a) [4]. The plot compares calculated quantiles for each measured data set and predicted quantiles based on ideal normal distribution. Thus the data samples from a normal distribution will form a diagonal line in the plot in which the two side curves are the confidential interval of the evaluation. For example, the data in figure 3.2a is normal distributed because the data points follow a diagonal line very well. More quantitatively, the evaluation can also be done by a hypothesis test (the concept will be discussed in details in section 3.2): The Shapiro-Wilk W test (Figure 3.3 b). This test tests a null hypothesis that samples are from a normal distributed data set. The hypothesis is rejected if the probability less than W is

much smaller than 5%, meaning that the distribution can not be treated as normally distributed. Using Shapiro-Wilk W test, the same set of data was reanalyzed. Clearly, because the probability is actually very close to 1 instead of smaller than 5%, the hypothesis that the data is normally distributed should be accepted.(fig. 3.3b), showing the same conclusion as the graphic method does.

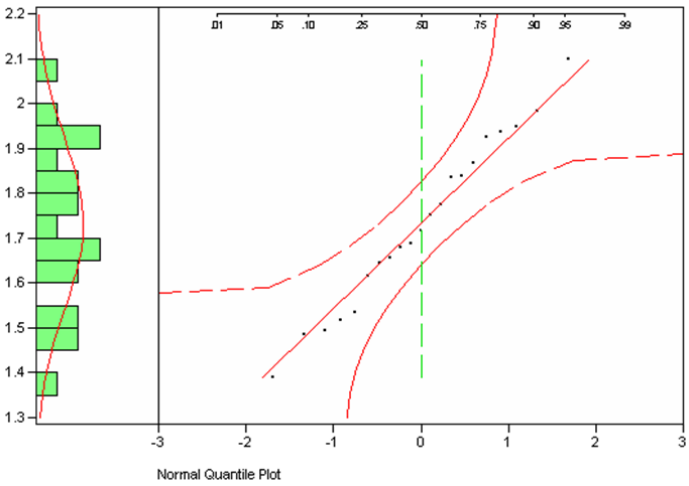

(a)

Goodness-of-Fit Test

Shapiro-Wilk W Test

W	Prob<W
0.980628	0.9186

(b)

Figure 3.2: Methods to test normality of collect data. a) Left, A histogram of a twenty-point data, a) Right, the evaluation of normal distribution using normal quantile plot, b) quantitative test of the normality using Shapiro-Wilk W test

3.1.2 Chi-square distribution

An important sampling distribution that originates from the normal distribution is the chi-square (χ^2) distribution. If x1 , x2 ,..., xn are normally distributed random variables with mean zero and variance one (also called standard normal distribution, represented as N(0,1)), then the random variable:$x1^2$+ $x2^2$+…+ xn^2 follows chi-square distribution with

degree of freedom of n (fig. 3.3). The Chi-square distribution is used to estimate variances of normal distributed data, because $(n-1)S^2/\sigma^2$ follows chi-square distribution.

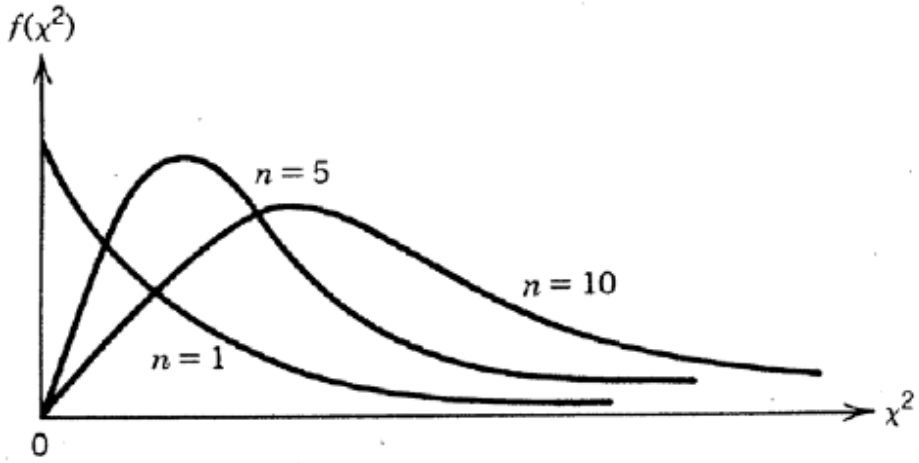

Figure 3.3, Examples of chi-square distributions with different n

3.1.3 t-distribution

The *t* distribution is another useful sampling distribution based on the normal distribution. If x and χ_k^2 are standard normal and chi-square random variables, then the random variable $t_k = \frac{x}{\sqrt{\chi^2/k}}$ is distributed as t-distribution with degree of freedom of k. More particularly, for a random sample of size n collected from a $N(\mu, \sigma^2)$ distribution with a sample average $\bar{x}$ and a sample standard deviation of S^2, it can be shown that $\frac{\bar{x}-\mu}{S/\sqrt{n}}$ follows a t-distribution. A t-distribution has similar shape to a normal distribution. Actually, as the sample size approaches infinity, the shape of a t-distribution reaches a normal distribution (figure 3.4). Unlike a normal distribution, in a t-distribution, the

"variance" in the curve is actually the standard deviation instead of the "true" variance in a normal distribution. The most important application of t-distribution is to do a t-test, testing means of a distribution in cases where the sample size is small.

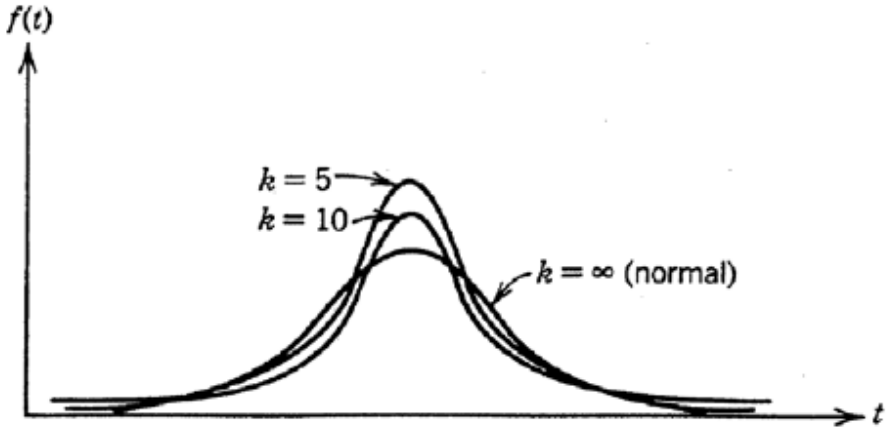

Figure 3.4: A group of t-distribution. As k reach infinity, a t-distribution approaches a normal distribution

3.1.3 F-distribution

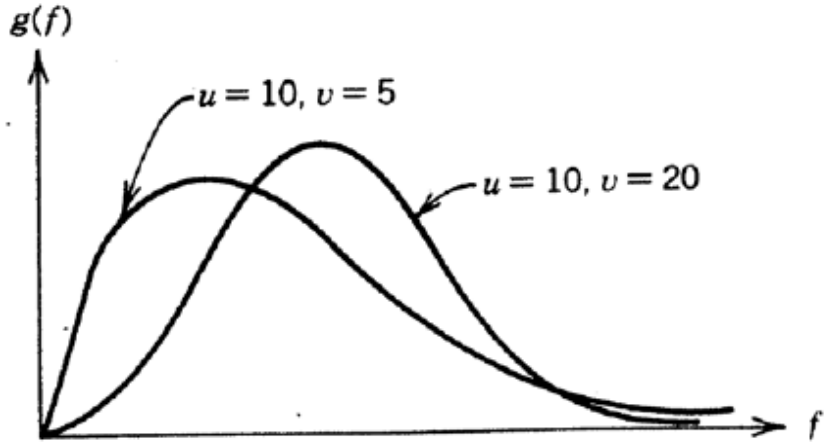

Figure 3.5: Several examples of F-distribution

The last sampling distribution to be considered that is based on the chi-square distribution is the *F* distribution. If χ_u and χ_v are chi-square random variables with *u* and *v* degrees of

freedom, then the ratio: $F_{u,v} \equiv \frac{\chi_u^2 / u}{\chi_v^2 / v}$ follows F-distribution. The F distribution can thus be used to make inferences in comparing the variances of two normal distributions because $\frac{S_1^2 / \sigma_1^2}{S_2^2 / \sigma_2^2}$ follows the F-distribution. More broadly, F-distribution is the fundamental principle supporting Analysis of Variance (ANOVA), which will be discussed in detail in section 3.3.

3.2 Hypothesis test

The hypothesis test is broadly used in the experimental results analysis for testing equality of means or variances of two populations. In general, a hypothesis test is performed by evaluating two pre-assumed hypotheses, according to some criterions, in which the hypotheses are expressed in the following manner:

H_0: X1=X2 ---- null hypothesis

H_1: X2≠X2 alternative hypothesis

Here X1 and X2 represent factors for the test, such as mean or variance. Two types of errors may result when performing such a test. If the null hypothesis is rejected when it is actually true, then a *Type I error* has occurred. On the other hand, if the null hypothesis is accepted when it is actually false, this is called a *Type II error*. The probabilities for each of these errors are denoted as:

α = P(type I error) = P(reject H_0 | H_0 is true)

β = P(type II error) = P(accept H_0 | H_0 is false)

The values of α and β broadly accepted in research and industry are 5% and 10% respectively. If α is<5% for a hypothesis test, H_0 can be safely rejected because we only have less than 5% possibility to wrongly say the H_0 is wrong. As for β, normally it is not used directly, instead 1-β is used to indicate the "power" used in sample size calculation discussed in following chapters. After collecting the data, the actual procedure of an evaluation is to first assume that H_0 is true and thus the pre-assumed distribution applies. Then, the appropriate test statistic is calculated, followed by placing the statistic against its assumed distribution and reading corresponding probability. Depending on whether the probability value is larger or smaller than 5%, a decision to accept or reject H_0 can be made. A hypothesis test is the fundamental statistic to test responses of OTFTs to DNA segments and ANOVA analysis used for design of experiments in the dissertation and will be discussed in details in the following paragraphs.

As an example, a hypothesis test is used to test if the mean of a population is μ0 with known variance σ. As an assumption constantly used in the dissertation, the data set is sampled from an independent, identical normal distribution. To test the mean of the population, a null hypothesis is set first as μ=μ0. By assuming the hypothesis correct, the distribution of the population is known as $N(\mu 0, \sigma^2)$. Considering additivity of statistics of samples from normally distributed data, the average of the distribution follows $N(\mu 0, \sigma^2/n)$, here n is the sample size. After the predicted distribution is known, the average, which is the estimator of the distribution mean, is calculated as μ1. By placing the calculated statistic, μ1, back to the assumed distribution $N(\mu 0, \sigma^2/n)$, we can calculate the probability of μ>μ1. Depending on distance between μ1 and μ0, if it is bigger than

$2 \times \sigma / \sqrt{n}$,which means μ1 is two time bigger than the variance of average of the population, the hypothesis is safely rejected because the probability of type I error is smaller than 5% as introduced in section 3.1.1.1. Same procedures can be applied on more complex tests, such as t-test and F-test which will be discussed in details as follows.

3.2.1 t-test

One of the most important hypothesis tests used in this dissertation is a t-test. The t-test is any statistical hypothesis test in which the test statistic has a Student's t distribution if the null hypothesis is true [3]. The main purpose of the t-test is to test the equality of means of two populations when the experiment's sample size is small such that the variance is unknown. Because in reality variance is always unknown unless an infinite sample is measured, t-test is the most powerful tool to test means. In practice, as long as the sample size is larger than 10, the t-test is accurate enough to replace the test using normal distribution.

In analogous to the test of mean of a population discussed above, a t-test also starts from assuming the null hypothesis true, meaning equal means between two populations. Depending on the equality of standard deviations of two populations, the variance of H0 distribution can be $S\sqrt{\frac{1}{n1}+\frac{1}{n2}}$ for equal standard deviation and $\sqrt{\frac{S1^2}{n1}+\frac{S2^2}{n2}}$ for unequal standard deviation. The statistic, or the distance between averages of two

distributions in terms of numbers of H0 variance, is calculated as $\bar{X}1-\bar{X}2 \Big/ S\sqrt{\frac{1}{n1}+\frac{1}{n2}}$ or $\bar{X}1-\bar{X}2 \Big/ \sqrt{\frac{S1^2}{n1}+\frac{S2^2}{n2}}$. If the statistic is larger than 2, the H0 hypothesis is rejected otherwise, it is accepted.

3.2.2 Sample size calculation

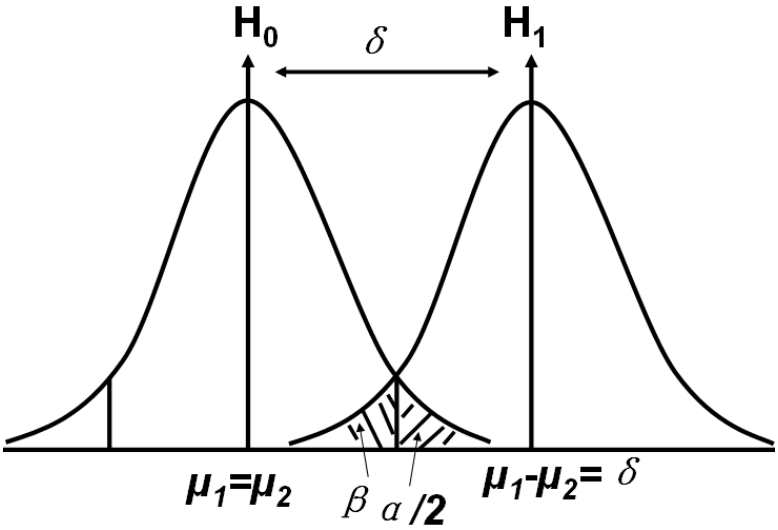

Figure 3.6: Graphic explanation of sample size calculation.

The understanding of t-test leads to an important concept: sample size. In practice, we often have to know the minimum replications for each experiment needed to tell a certain difference between means of measured data, as more replications give more accurate estimation. For example, as the most important t-test in this dissertation, the estimated different between OTFT responses to ssDNA and dsDNA with 95% confidential interval (95% probability that the measured data falls into this region) is (0.57386, 0.80179) and the mean of it is 0.69. In order to tell if this response difference of OTFTs to ssDNA and

dsDNA molecules is significant, considering a calculated global standard deviation, 0.04, at least 4 transistors for each type of DNA segments need to be measured. This predicted number will greatly save measurement time without compromising accuracy. The theory of sample size calculation is detailed as follows.

The calculation of sample size uses the concept of statistical power of a test: power=1-β, showing the probability that correctly rejects a false null hypothesis. Experimentally, a broadly accepted number of power is 90%, meaning β=10% as mentioned above. Given that the expected difference is 0.69 with a standard deviation of 0.04, two distributions representing means of responses of OTFTs to dsDNA and ssDNA segments are $X1 \sim N(\mu 1, \frac{0.04^2}{n})$ and $X2 \sim N(\mu 2, \frac{0.04^2}{n})$, in which $\mu 1$ and $\mu 2$ are means of responses and n is the sample size that we are calculating. Thus that null hypotheses is H_0: μ1=μ2 and the alternative hypothesis is μ1-μ2=0.69. Correspondingly, the distributions of those hypothesis can be written as H_0: $\overline{X}1 - \overline{X}2 \sim N(0, \frac{2 \times 0.04^2}{n})$ and H_1: $\overline{X}1 - \overline{X}2 \sim N(0.69, \frac{2 \times 0.04^2}{n})$. The coefficient of "2" in both variance expressions is due to additivity of the normal distributions. Then, as we can reject H0 with 95% confidential interval, we have to simultaneously be exactly at the point that we can't reject H1 because we have to conclude that μ1≠μ2 and μ1-μ2=0.69 simultaneously. In other words, if 5% limit is set on H_0, the upper 2.5% limit on H_0 exactly corresponds to the lower 10% limit of H_1 (fig. 3.6), meaning that as we correctly reject the assumption of equal means, the correct approval of mean difference of 0.69 is gotten automatically.

Because 2.5% and 10% corresponds to $1.986\,\overline{\sigma}_n$ and $1.28\,\overline{\sigma}_n$ respectively, an equation can then be written as follows to calculate n, the sample size.

$$0 + 1.986\sqrt{\frac{2\times 0.04^2}{n}} = 0.69 - 1.28\sqrt{\frac{2\times 0.04^2}{n}} \quad (3\text{-}2)$$

3.2.3 F-test

F-test is another important test used in this work and is the fundamental of the Analysis of Variance (ANOVA). An F-test is any statistical test in which the test statistic has an F-distribution if the null hypothesis is true [3]. The main purpose of the F-test is to test if the variances from two populations are different, because the ratio between the standard deviation square divided by the variance square follows an F-distribution (3-3).

$$\frac{S_1^2 / \sigma_1^2}{S_2^2 / \sigma_2^2} \sim F_{n_1-1,n_2-1} \quad (3\text{-}3)$$

3.3 Analysis of Variance (ANOVA)

Having understood the t-test and f-test, we are able to compare means or variances of two populations, but it is more common in experiments to compare multiple populations to see if one of them is significantly different from others and to correspondingly understand which recipe or treatment has more significant effects on the experiment. Analysis of Variance (ANOVA) is the best tool to do this type of analysis.

An ANOVA test is done by comparing the variance between treatments, S_T^2, and variance within treatment S_R^2. Here treatments refer to different recipes and so on. With

the hypothesis of same means between all results of treatments, meaning no difference between treatments, we can only have one variance, no matter how we calculate it, meaning that S_T^2/ S_R^2 is very close to 1. Thus a much bigger than 1 ratio of S_T^2/ S_R^2 suggests that the hypothesis is rejected or at least one mean of the populations is significantly different from others. Because S_T^2/ S_R^2 falls into a F-distribution, F-test is used to test probability of the ratio equaling one.

Table 3.1, An example data for ANOVA analysis

Recipe A	Recipe B	Recipe C	Recipe D
62	63	68	56
60	67	66	62
63	71	71	60
59	64	67	61
	65	68	63
	66	68	64
			63
			59

As an example, an ANOVA analysis is used to test recipes for yield improvement. The target of the analysis is to find out if all four recipes have same effects on yield. Statistically, the analysis goal is expressed to test if discrepancy caused by recipes is greater than variations within each group. The null hypothesis here is that all groups of data have the same spread and are normally distributed. To accomplish the analysis, standard deviations of between treatments and within treatments are calculated using following two equations: (here treatments refer to recipes used for test).

$$s_R^2 = \frac{S_R}{v_R} = \frac{\sum_{t=1}^{k}\sum_{i=1}^{n_t}(y_{ti} - \bar{y}_t)^2}{N-k}$$

$$s_T^2 = \frac{S_T}{v_T} = \frac{\sum_{t=1}^{k} n_t(\bar{y}_t - \bar{y})^2}{k-1}$$

In the equation of variance within treatments (top), $\bar{y}_t$ is the average in each treatment. S_R is calculated by adding standard deviations of all groups and $s_R^2=S_R/(N-k)$, in which N-k is the degree of freedom for variance within treatments calculation. As for the variance between treatments calculation equation (bottom), $\bar{y}$ is the global average. S_T is calculated as the sum of difference between treatment average and the global average. s_T^2 is then calculated as $S_T/(k-1)$, here k-1 is the degree of freedom for between treatments variance calculation. Results of ANOVA are typically summarized in a table (table 3.2). As a result, the F-ratio is calculated and a conclusion is drawn: at least one of recipes has significant effects on yield of the system because F ratio >>1

Table 3.2, ANOVA table for data in table 3.1 [2]

Source of Variation	Sum of Squares	Degrees of Freedom	Mean Square	F-Ratio
Between treatments	$S_T = 228$	$\nu_T = 3$	$s_T^2 = 76.0$	$s_T^2/s_R^2 = 13.6$
Within treatments	$S_R = 112$	$\nu_R = 20$	$s_R^2 = 5.6$	

3.4 Design of Experiments (DOE)

Design of experiments technique is a powerful tool to statistically design sufficient experiments maximizing the amount of "information" we can get from them. In reality, experiments usually include more than two parameters with more than two levels for each parameter. The normal way to do those experiments without thinking about DOE techniques is to test all combinations of parameters. The collected data is then processed using an experiment-by-experiment strategy to find effects of each parameter. This

method is called full factorial design in the DOE technique, and experiments actually include much more information than just the effects of each parameter, called main effects in DOE. For example, such a full factorial also allows determination of interactions between parameters, though this information is commonly lost because of the experiment-by-experiment approach typically used to analyze data. With DOE, we are able to design a set of experiments and analyze data in parallel and in a systemic way to extract all hidden information simultaneously. Because of the strength of DOE, in this dissertation, most experiments were designed statistically.

Table 3.3, design table for a two-level seven factors experiment design

Choose a Design

Number Of Runs	Block Size	Design Type	Resolution - what is estimable
8		Fractional Factorial	3 - Main Effects Only
12		Plackett-Burman	3 - Main Effects Only
16		Fractional Factorial	4 - Some 2-factor interactions
16	8	Fractional Factorial	4 - Some 2-factor interactions
16	4	Fractional Factorial	4 - Some 2-factor interactions
16	2	Fractional Factorial	4 - Some 2-factor interactions
32		Fractional Factorial	4 - Some 2-factor interactions
32	16	Fractional Factorial	4 - Some 2-factor interactions
32	8	Fractional Factorial	4 - Some 2-factor interactions
32	4	Fractional Factorial	4 - Some 2-factor interactions
32	2	Fractional Factorial	4 - Some 2-factor interactions
64		Fractional Factorial	5+ - All 2-factor interactions
64	32	Fractional Factorial	5+ - All 2-factor interactions
64	16	Fractional Factorial	5+ - All 2-factor interactions
64	8	Fractional Factorial	5+ - All 2-factor interactions
64	4	Fractional Factorial	4 - Some 2-factor interactions

Just as DOE techniques enable efficient mining of data from existing experiments, reversely, if we predefine the amount of information we want, using DOE, we are able to minimize the amount of experiments required to obtain the requisite measurements. The power of the DOE can clearly illustrated using an example. Supposedly, a set of experiments has to be designed to test effects of seven main factors only, which are all two-level parameters. It is well known that full factorial design follows a 2^n principle,

thus 7 factors require 128 experiments, which actually include all information of all possible crossing (i.e., interacting) factors. While using DOE techniques, considering that only effects of 7 main factors are needed, 8 experiments by minimum are actually already good enough (table 3.3). This power of shrinking experiment size is even clearer when dealing with more factors. In this work, I mainly used two experiment design techniques: screening experiments for finding important factors for measured results and response surface experiments for finding the optimum condition for measured results.

3.4.1 Screening experiments design

Screening experiments are always the first set of experiments used when initiating new studies, since these screen the significance of factors involved. As an example, OTFT fabrication factors were investigated using the DOE technique to maximum the saturation current of transistors, making high signal/noise ratio for sensors. The designed transistors have constant channel length and width, and constant SiO_2 thickness, such that the only process to be optimized is the evaporation. Four factors are involved in the evaporation: substrate temperature, deposition rate, deposition thickness and surface treatment on SiO_2 surface. Therefore, the screening experiment set is a two-level four-factor design to find which factors are important to maximum saturation current.

Using a full factorial design, a two-level and four- factor screening experiment design requires 2^4=64 experiments and correspondingly needs 64 wafers. Such a large amount of wafers makes experiments extremely time-consuming. To simply experiments, a

fractional factorial design is used here to shrink the experiment size to 8 wafers (table 3.4). This design loses some crossing factors but does include effects of all necessary main factors. Five transistors on each wafer were measured to provide enough replications for the estimation of real variance caused by experiments. All measurements were done under the nitrogen using an Agilent 4156.

Table 3.4: Screening experiment design for saturation current improvement

	Pattern	Deposition Thickness(Å)	Deposition Rate(Å/min)	Deposition Temperature(°C)	Surface Treatment
1	----	100	2	30	Bare
2	--++	100	2	70	HMDS
3	-+-+	100	10	30	HMDS
4	-++-	100	10	70	Bare
5	+--+	300	2	30	HMDS
6	+-+-	300	2	70	Bare
7	++--	300	10	30	Bare
8	++++	300	10	70	HMDS

The analysis of collected data mainly includes ANOVA and effect test (Figure 3.7). Instead of finding a different mean from a set of experiment data with only one factor, ANOVA used in the design of experiments is actually multi-factor ANOVA, called MANOVA, analyzing multi-factor effects on experiment results. By hypothesizing only one common mean in the all measurements, similar with ANOVA, the probability larger than F-ratio tells if we should reject or accept the hypothesis. In this case, it is clear that there are some significant factors among four factors we researched (figure 3.7) because of much smaller than 5% probability. The effect test, comparing the standard deviation caused by each factors to the residual, discovers that only two factors, thickness and surface treatment can actually change saturation current while other two factors won't change it statistically.

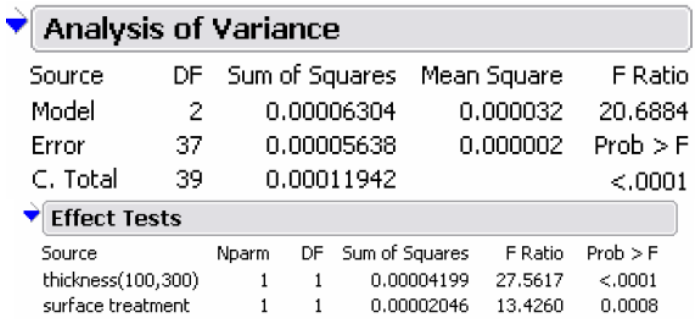

Analysis of Variance

Source	DF	Sum of Squares	Mean Square	F Ratio
Model	2	0.00006304	0.000032	20.6884
Error	37	0.00005638	0.000002	Prob > F
C. Total	39	0.00011942		<.0001

Effect Tests

Source	Nparm	DF	Sum of Squares	F Ratio	Prob > F
thickness(100,300)	1	1	0.00004199	27.5617	<.0001
surface treatment	1	1	0.00002046	13.4260	0.0008

Figure 3.7: Screening experiment results including ANOVA table and Effect test. The results clearly tell than a good model is found and deposition thickness and surface treatment are important for saturation current improvement

3.4.2 Response surface experiment design

As a further step after we know significant factors in an experiment, a response surface experiment is used to find out where the optimum point exactly is [3]. Different from the two-level factors used in screening experiments, response surface experiments use three-level continuous factors. Thus for a two-factor response surface experiment, it at least requires nine experiments. Because the middle point always is repeated to estimate variance involved, the design actually needs a total of ten experiments, corresponding to ten different experimental conditions (figure 3.9 a). The resultant experiment design covers the whole experiment space, such that the response surface can be estimated mathematically by analyzing measured data (figure 3.9 b). Because only three levels are used for each factor, the estimated relationship between factors and responses is limited to quadratic models by assuming that only one optimum point exists in the space. Thus, it is important to realize that such surfaces are not fitted to physically derived models, but do provide statistically valid ways of representing variation in measured parameters over the experimental space.

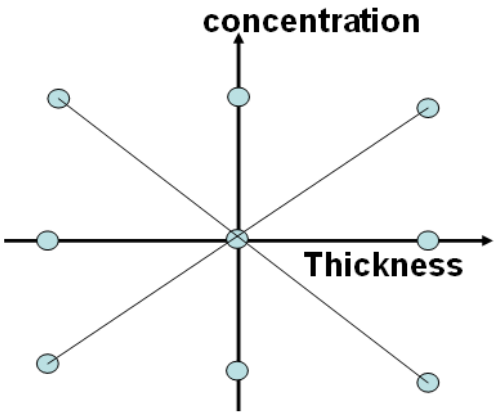

(a)

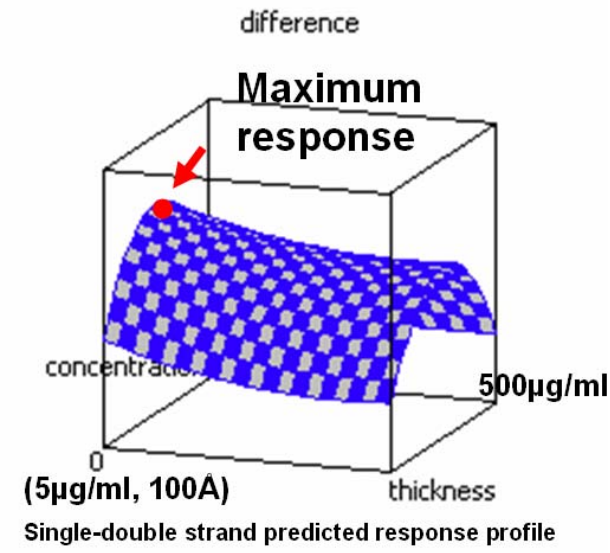

(b)

Figure 3.9: An example of surface response experiment design to find the optimum condition for the highest DNA response with OTFTs

As an example, the response of OTFTs to DNA molecules was optimized using a surface response experiment. Based on previous study results, it was already known that both thicknesses of the pentacene layer and concentration of the DNA solution change DNA response, thus a two-factor response surface experiment is necessary. Following the design rule discussed above, ten experiment conditions were tested. Specifically, the concentration of DNA solution varies from 5 *µg/ml* to 500 *µg/ml* with middle point at 250 *µg/ml*. Three pentacene thicknesses were used in the experiment from 100 Å to 300 Å

with the middle point at 200 Å. For each combination, four data point were measured. Again, similar as done in screening experiments, ANOVA and effect tests were done to evaluate practicability of models. One point worthy to note is that since all factors used in response surface experiments have been proved to have significant effects on experiment output, ANOVA and effect tests are only used to find out coefficients of the model. Because a two-parameter quadratic model is used, the resultant model can be drawn three-dimensionally (fig. 3.9 b), clearly finding the maximum response value. By this example, it is clear that instead of dramatically shrinking experiment size, response surface examples actually increase experiment complexity, thus experimental factors must be carefully selected.

3.5 Linear regression

Linear regression is an important tool to find the best-fit relationship between dependent output (Y) and independent input (X). The term "Linear" is obtained because all coefficients of extracted model are linear, instead that only linear curves are fitted to data. A proposed formula used for a linear regression is $Y=a_1+a_2\times X+a_3\times X^2+ a_5\times X^3+\ldots+ a_n\times X^n+\varepsilon$, in which terms with independent inputs are the final equation we are going to use and ε is the residue that model can't explain, typically called error. The final goal of a linear regression is then to minimize the error and ideally make the error normally distributed with mean of zero. The most popular method to solve linear regression problem is the Least-Squares Analysis by computing the standard deviation between real data and the data calculated with the proposed model. The quality of a proposed model is

also can be evaluated using ANOVA by comparing calculated data with the proposed model to errors remained by the model using F-test.

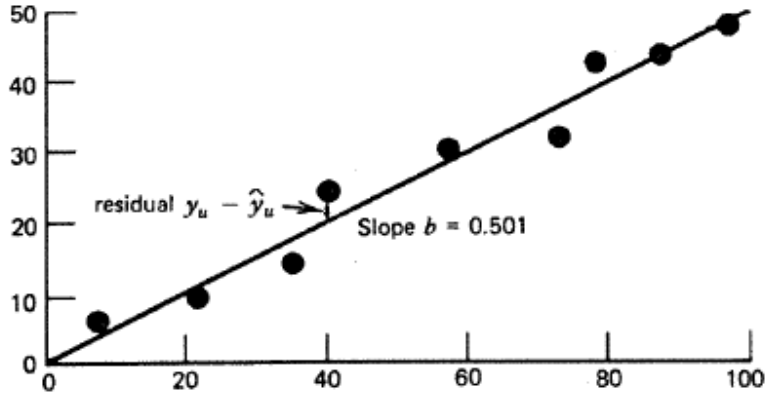

Figure 3.10: An example of linear regression to fit a line to a set of data[2]

As an example, a linear regression is used to fit a line through origin to a set of data. Although rather elementary, this example illustrates important aspects of the least square method. Clearly, the relationship between independent input x and dependent output y is $y_n = \beta x_n + \varepsilon_n$. The objective of this regression analysis is to find the value of b, the estimate of β, which minimizes the difference between the measured values of y and the predictions of equation: $S(\beta) = \sum_{i=1}^{n}(y_i - \beta x_i)^2$, in which y_i is measured data and βx_i is estimated y value. The curve represented by this equation is a parabola, so the goal is to find the value of β at the minimum of the parabola. Let b be the estimator of β at the minimum point. Using the rules of calculus, we can find b by simply taking the derivative of S with respect to β and setting the derivative equal to zero. The accuracy of the estimated value of b is evaluated by ANOVA analysis. The null hypothesis here is b=0, meaning that there are no relationship between y and x. Because F-ration>>1, the

hypothesis is rejected, suggesting a clear relationship between y and x and estimated b is accurate enough.

Table 3.5, ANOVA table for linear regression done with data in figure 3.10

Source of Variation	Sum of Squares	Degrees of Freedom	Mean Square	F-Ratio
Model	$S_M = 8836.64$	1	$s_M^2 = 8836.64$	$s_M^2/s_R^2 = 1094$
Residual	$S_R = 64.67$	8	$s_R^2 = 8.08$	
Total	$S_T = 8901.31$	9		

3.6 Conclusion

As a powerful tool for the experiments design and data analysis, the DOE and statistics were broadly used in this dissertation. Using these techniques, the fabrication and operations of OTFTs were researched and optimized to maximize OTFT response to DNA molecules. Based on these techniques, in the next chapter, organic transistors are successfully designed to differentiate dsDNA molecules from ssDNA unambiguously, enabling ultra-low-cost and fast DNA hybridization detection.

Reference:

1. Dudoit, S. et al, Multiple Hypothesis Testing in Microarray Experiments, Statistical Science, Vol. 18, pp 71, 2003
2. EE290H Lecture Notes, Taught by Professor Costas Spanos in Fall 2005
3. Jerrold H. Zar, Biostatistical Analysis, Fourth Edition, Prentice Hall, 1999
4. JMP reference book

Chapter 4

OTFT-based DNA sensors

- Detection of off-chip hybridized DNA segments

According to the length difference of immobilized DNA molecules, DNA microarrays have two levels of applications. On the function level, a cDNA microarray immobilizes longer-than-1k-base DNA molecules and investigates DNA expression, or gene-level functions. On the molecule level, an oligonucleotide microarray typically immobilizes less-than-25-bases DNA molecules and investigates single base mutations of DNA molecules. In this chapter, both applications were tested using our OTFT sensors.

As discussed in chapter two, both long-chain and short-chain DNA molecules are directly immobilized by physical adsorption on the exposed channels of substrate-gated bottom contact organic transistors. The immobilized DNA molecules have been found to dope organic semiconductors, causing a threshold voltage shift. Importantly, ssDNA and dsDNA molecules show substantial difference in the resultant threshold voltage shift due to their different net doping and immobilization efficiencies. This enables the direct electrical detection of hybridization through the measurement of TFT saturation current. To dramatically speed up the analysis process, we also make use of pulse-enhanced DNA hybridization [1] by using the TFT electrodes to generate an electrical field near the DNA, causing hybridization. Importantly, the sensor responds linearly to the hybridization rate,

the ratio of dsDNA in ssDNA, enabling the quantitative measurement of DNA expression, and also representing the great potential of single mismatch measurement for the oligonucleotide microarray. This linearity can be further improved by minimizing involved data variance by using a patterned response area on the top of source and drain. The net result of this work is an overall analysis time of less than 40 minutes, compared with more than 24hrs using conventional techniques. Combined with the electrical readout and low-cost processing, these techniques together will enable the deployment of DNA microarray techniques for disposable field-deployable diagnosis toolkits, used for early-stage disease diagnosis and personalized medicines.

4.1. Experiments

4.1.1 Sensor Operation

In all experiments, bottom-gated bottom contact transistors were used (fig. 4.1). A 4-inch heavily doped silicon wafer served as the shared gate for all transistors on the wafer. 100nm SiO_2 was grown by wet oxidization and followed by coating a thermal evaporated 100nm gold layer. Lithography and a lift-off processing were used to pattern the gold layer to form source and drain electrodes. In this work, transistors with a constant width/length ratio of $1.1mm/110\mu m$ were used to test DNA response. Before the organic material coating step, pre-patterned wafers were cleaned by sonicating in acetone and isopropanol alcohol for over 20 minutes each. The clean wafers were then coated with a HMDS monolayer to improve transistor performance and sensor stability. As the final

step, a pentacene layer, the organic semiconductor used in this work was evaporated at a substrate temperature of 70°C. The thickness and roughness of this layer was varied to optimize DNA response as discussed in chapter 2.

As discussed in chapter 2, pentacene is a p-type semiconductor and works in an accumulation mode. Id-Vg curves of the transistors were measured and device parameters, such as threshold voltage and mobility, were extracted from the resultant curves by assuming a square law principle of the saturation currents: $I_{dsat} = k\mu C_{ox}(V_g - V_t)^2$. Though this equation is known to have inaccuracies in OTFTs, the extracted parameters were found to be useful device metrics to analyze sensing response. For analyzing sensor response, a fixed bias-point measurement of saturation current was taken, since this parameter may easily be measured in an integrated sensor system. All measurements were done using an Agilent 4156 in nitrogen, and drain voltage and gate voltage were set to 45V and 40V respectively. Measurement in air is also reasonable and expected to have similar results because of air-stability of pentacene [2].

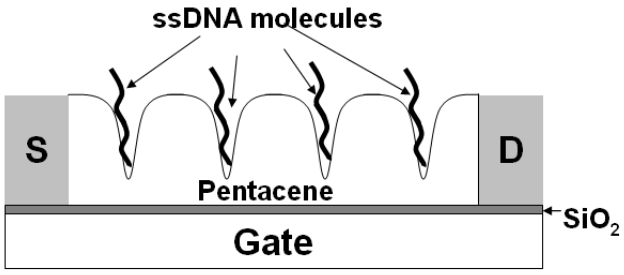

Figure 4.1: Bottom gated transistor (not to-scale). From the bottom to the top, layers are gate, 100 *nm* thick SiO_2 as the gate dielectric, patterned source and drain, and evaporated pentacene. Due to hydrophobic interactions, the DNA naturally immobilizes itself in grain boundaries and other troughs on the hydrophobic semiconductor surface.

4.1.2 DNA Immobilization

Two types of DNA molecules were tested with the pentacene TFTs. Lambda hind III DNA molecules with lengths ranging from 125 base pairs (bp) to 23,130 base pairs (bp) and oligonucleotide chains with lengths of 20 bases were tested, targeting two applications, namely complementary DNA microarrays (cDNA) and oligonucleotide microarrays. The as-purchased Lambda DNA were originally double stranded and corresponding ssDNA were obtained by heating dsDNA solution in boiling water for 5 minutes and storing on ice immediately. Designed oligonucleotides have three different sequences and two of them were designed to be complementary, so as to be able to form double-stranded oligonucleotides.

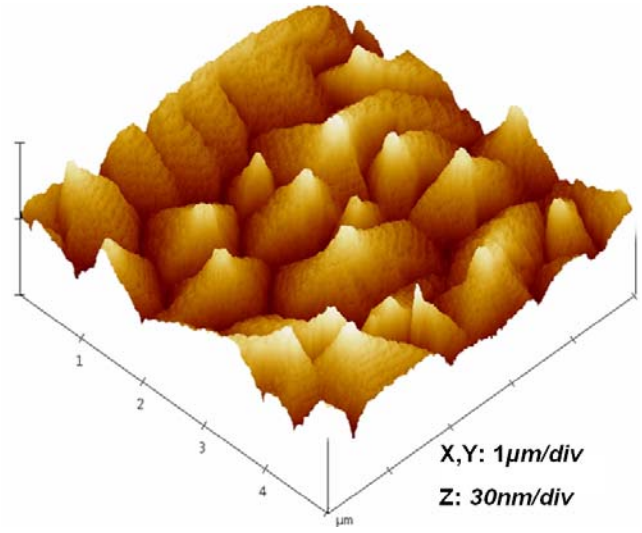

Figure 4.2: 3-D AFM picture of a 300Å evaporated pentacene film. The large roughness is exploited to maximize immobilization of DNA on the semiconductor surface

The first step in implementing DNA sensing is immobilization of the DNA molecules onto the sensory layers. As discussed in Chapter 2, we used a physical immobilization method because it is faster and easier than immobilization based on chemical reactions.

In this case, physical immobilization is driven by hydrophobic interactions between organic semiconductor films and DNA targets. It is well known that surfaces of evaporated pentacene film are hydrophobic and rough (fig. 4.2), and bases of DNA molecules are also hydrophobic. Both characteristics assure hydrophobic interactions between DNA molecules and pentacene films, causing immobilization of the DNA molecules on the sensor surface through physical adsorption. The immobilization can be optimized according to the sizes of DNA molecules by controlling morphology of pentacene films (chapter 2). Experimentally, the adsorption processing was performed by pipetting a drop of 1.5μl DNA-containing buffer onto each transistor channel followed by a 20 to 30 minutes air-dry. The air-dry time was strongly dependent on the ambient conditions and longer dry time was found to lead to better immobilization. The DNA-immobilized wafers were then rinsed under flowing de-ionized water for 1 minute and stored overnight in nitrogen. This overnight storage can be avoided by using a low-temperature annealing step, which will be calibrated in the future research.

Lambda DNA was used to test the immobilization efficiency on a pentacene film. Lambda DNA molecules are those extracted from lambda phage and are broadly used in molecular biological experiments as a standard electrophoresis ladder. A typical Lambda DNA solution normally contains molecules with several different lengths, for example the lambda DNA digest used in the experiments contains double-stranded DNA molecules with eight different lengths ranging from 125 bp to 23130 bp. The long chains of lambda DNA molecules secure stable immobilization. An air-dry process discussed above was used to immobilize DNA molecules. It's clear that single-stranded DNA

molecules form an immobilized network on the pentacene surfaces with both 100Å and 300Å thickness (fig. 4.3 a and c). More clearly on the 300Å-thick pentacene film, most of DNA molecules, as expected, were immobilized into the grain boundaries with certain amount of them on the surface. Importantly, ssDNA and dsDNA exhibits significantly different immobilization, as single-stranded DNA molecules were successfully immobilized, double-stranded DNA molecules form negligible immobilization. This difference assures electrically detectable difference between ssDNA and dsDNA molecules. Also importantly, the 300Å pentacene film shows higher immobilization efficiency than the 100Å pentacene film. This different immobilization will also significantly influence the electrical detection using OTFTs.

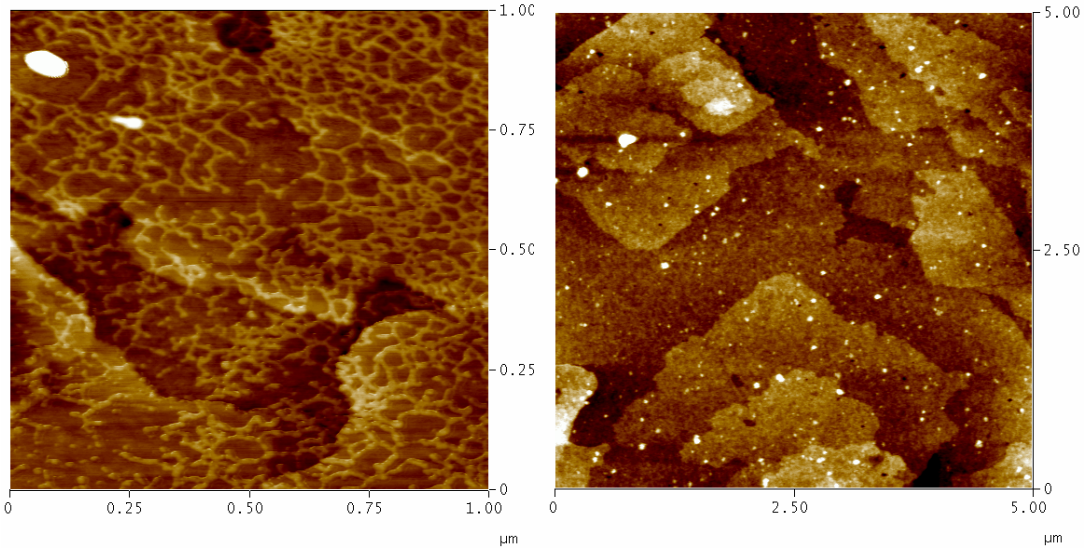

(a) (b)

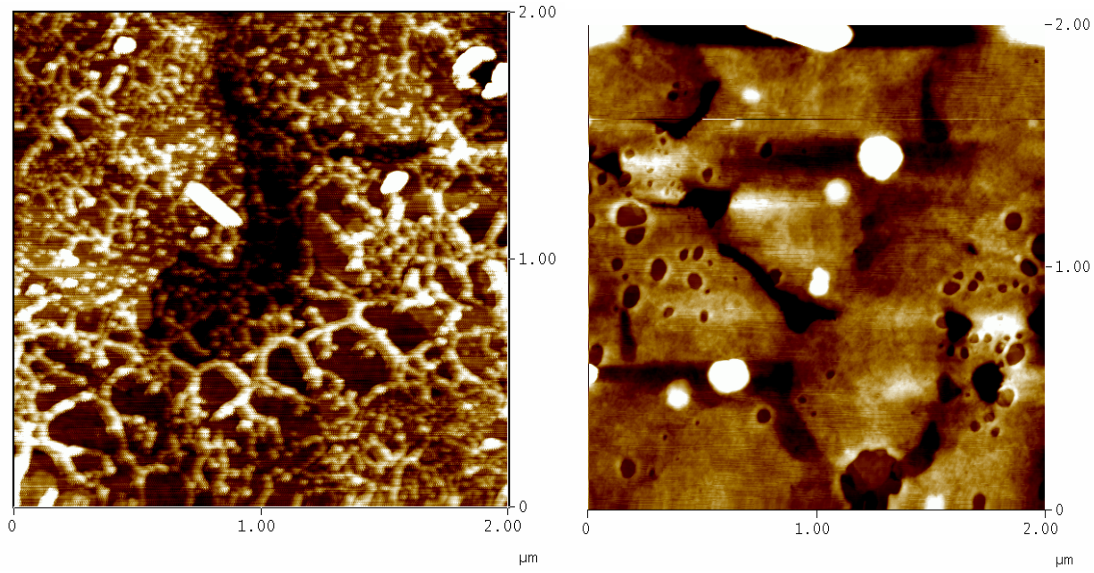

(c) (d)

Figure 4.3: Typical DNA immobilization examples a) 5*µg/ml* single stranded λDNA on a 100Å pentacene film b)5*µg/ml* double-stranded λDNA on a 100Å pentacene film c) 5*µg/ml* double-stranded λDNA on a 300Å pentacene film d) 5*µg/ml* single-stranded λDNA on a 300Å pentacene film

4.2. cDNA Microarray with Organic Thin Film Transistors

Currently, genetic diseases diagnosis chips on the market are all cDNA microarrays, also called gene expression chip. Gene expression is a fundamental process for a gene to represent its functions [3], for example, disease-related genes represent their functions in the human body by converting the genes inside cells to functional proteins outside cells (fig 4.4). The whole expression process includes two continuous steps, transcription and translation. Through the transcription process, genes inside of a cell are copied into messenger RNA that can transfer out of the cell. The transferred mRNA instructs construction of proteins that normally form sketches of muscles and cells. Therefore, the

mRNA is the core molecules which connect genes and diseases. Monitoring occurrence of mRNA thus becomes an important clue to predict the occurrence of diseases. One of the most effective tools to investigate mRNA is the cDNA microarray, immobilizing the complementary DNA of mRNA, called cDNA and testing the hybridization with unknown DNA segments from cells. Also, effects of drugs can be investigated using a cDNA microarray by watching efficiency of the drug in blocking the expression of the disease-related genes. Therefore, the understanding of blockage mechanisms will automatically enable personalized medicines.

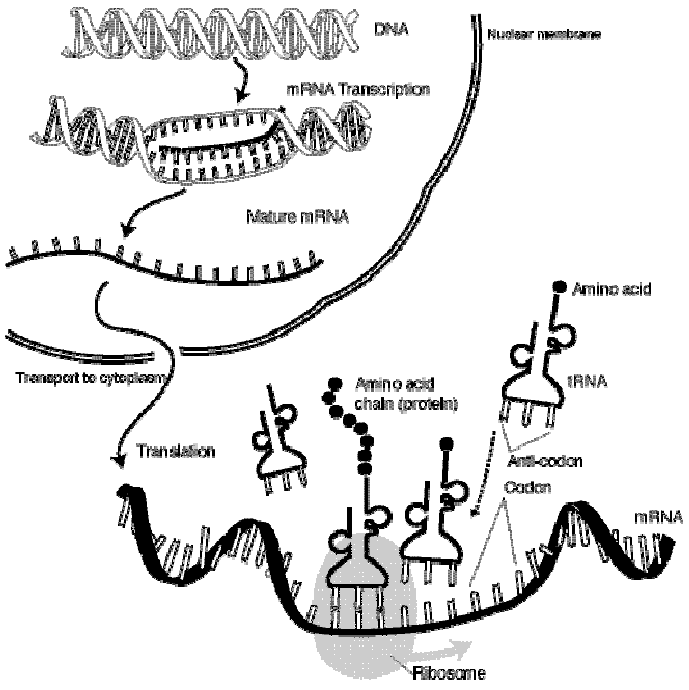

Figure 4.4: Scheme of DNA expression. The gene inside a cell is read by copying stretches of DNA into the related nucleic acid RNA, called messenger RNA, in a process called transcription. Furthermore, the mRNA molecule guides the construction of proteins outside the cell. This whole process, the conversion from DNA to functional proteins, is called DNA expression

Lambda DNA was used to simulate the cDNA microarray application because of its similar length to cDNA molecules. The DNA molecules were dissolved in specific buffer solutions to maintain their activity. Thus, to ensure an accurate baseline, the sensory response of pure buffer solutions was first ascertained. Following the same recipe as in the DNA experiments, the effect of the pure buffer solution on transistor performance was measured on different transistors on the same wafer used for the DNA experiments. The sensor response for DNA was extracted by deducting any resultant current change caused by the buffer solution from the DNA-containing buffer solution measurements and the mechanism of DNA sensitivity is discussed based on the characteristic curve shifts. Most importantly, response of both ssDNA and dsDNA were measured and compared using statistical calculations to test the overall ability of OTFTs for DNA hybridization detection.

4.2.1 Effect of buffer solution on OTFT performance

The buffer solution, 2×SSC (Sodium Chloride, Sodium Citrate) used here was expected to change performance of OTFTs in two different ways: water can swell pentacene film physically and improve film conductivity chemically [4], and ions in buffer solution can change conductivity of the semiconductor film. Fortunately, experimental results show a statistically negligible shift caused by the pure buffer solution (fig. 4.5). This negligible shift suggests that the swelling effect was recovered by nitrogen storage and ions diffused into organic materials were removed by de-ionized water rinse. Thus any expected DNA-containing buffer responses can be considered to be caused solely by the DNA molecules.

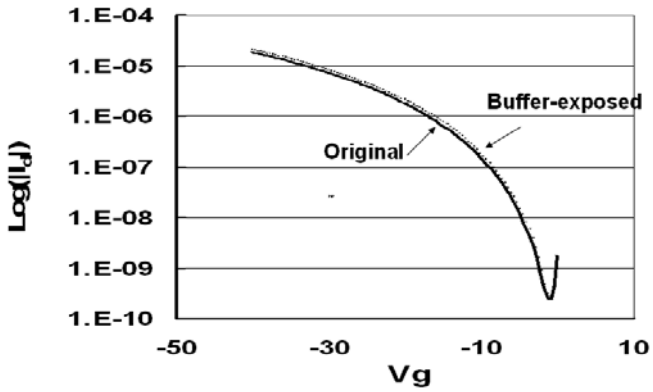

Figure 4.5: Transfer curves for a TFT DNA sensor (W/L=1*mm*/100μm) showing negligible impact of the buffer solution on the sensor response. Same recipes as DNA experiments were used.

4.2.2 Doping effect of DNA molecules on OTFTs

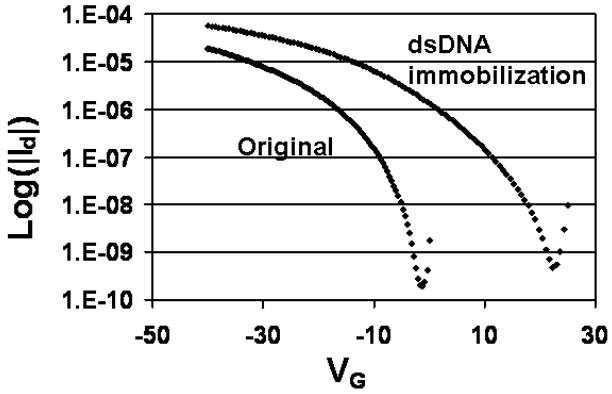

Figure 4.6: Transfer curves for a typical DNA-sensing organic TFT (W/L=1mm/100µm), showing strong positive threshold voltage shift on exposure to double-stranded DNA. This is caused by the electron-withdrawing nature of the phosphate groups within the DNA backbone. Drain voltages of both two curves were 45V.

As discussed previously, DNA molecules in solution have negatively charged groups on them because of phosphorus groups on their backbones [5]. The negative charges on DNA molecules are likely to change the electrical performance of the OTFTs, thus enabling the use of OTFTs as DNA sensors. OTFTs with a 100Å thick pentacene layer evaporated at 1 Å /min, were used to test response to 250$\mu g/ml$ dsDNA-containing buffer

solutions. Experimental results before and after DNA immobilization were compared statistically and a representative characteristic curve shift is shown in fig. 4.5. DNA molecules increase the OTFT saturation current by making threshold voltage more positive: threshold voltage is shifted from -12.5V to 6.6 V. The saturation mobility shift is very small and can be ignored. This threshold voltage shift is to be expected, since the phosphate groups on the DNA backbone are known to be able to attract electrons, causing an effective p-doping of the semiconductor. The parameter shifts, including the significant threshold voltage shift and the virtually negligible mobility shift together result in a saturation current shift. Hence the saturation current ratio of post-DNA-exposure transistors over original transistors was used to represent the sensor response for DNA.

Possible doping mechanisms of DNA molecules on pentacene were studied using Kelvin probe microscopy and Space Charge Limited Current (SCLC) techniques. Kelvin probe microscopy (KPM) technique has been broadly used to characterize electrical properties of metal, semiconductor and polymers thin films because of its high resolution and high sensitivity [6]. Recently, KPM technique has also been used for macromolecules investigation, such as DNA hybridization detection and antigen-antibody reaction detection [7]. Unlike workfunction mismatch induced surface potential seen in solid thin film study, the surface potential of macro biomolecules is caused by dipoles. DNA hybridization or antigen-antibody reactions have been proved to increase the amplitude of potential differences [9]. Surface potential of immobilized DNA molecules on a pentacene film has been measured (fig. 4.7). As expected, DNA molecules show negative

potential, which is likely caused by surrounding humidity or electron-withdrawing from the bottom pentacene layer. Therefore, it is highly possible that DNA molecules dope the pentacene film by extracting electrons, although this is not a direct evidence because DNA molecules always cover the pentacene film, blocking the direct measurement of the underlying pentacene film.

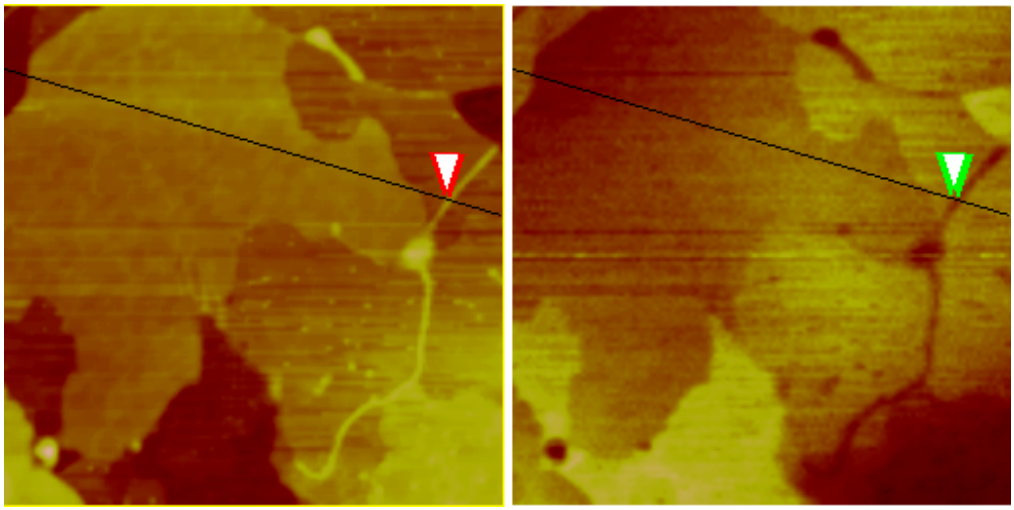

(a) (b)

(c)

Figure 4.7: Surface potential measurement of DNA molecules on a pentacene film. a) An Atomic Force Microscopy (AFM) image of a DNA molecule, the single bright thread is an immobilized DNA molecule. b) A surface potential image matching the same area of the AFM image on the left. It is clearly that the DNA molecule has negative potential,

which is possibly caused by surrounding humidity or electron-withdrawing from the bottom pentacene film. c) The cross section diagram along the line in a and b.

A space charge limited current (SCLC) measurement clarifies the doping mechanism in a more direct way. The SCLC technique is an important tool for mobility, carrier concentrations and trap distributions studies in insulator-like materials. It has been broadly used to study traps in amorphous silicon based transistors [6] and also been used to study pentacene [7]. A SCLC setup measures two-terminal devices. A bottom-gated top-contact transistor is used (fig. 2.2a) in this dissertation. A voltage from 0 to 100V was swept between the source/drain with a floating gate electrode and the current flowing into the drain was measured. A typical SCLC curves is plotted on a log-log scale and has more than two different slopes. The slope=1 part of the curve is called ohmic regime and the slope≥ 2 part is the trap-filling regime. As the electrical field across the two electrodes is small, the concentration of injected carriers from electrodes is smaller than the intrinsic free carrier concentration in the film. By this case, the conductivity in this region is limited by intrinsic free carrier concentration in the material. As seen in the curve (fig.4.7), the slope is 1 in ohmic regime because of the linear relationship between current and voltage. While, as the electrical field is increased to a certain level, the injected carriers concentration from the electrode overwhelm the intrinsic carrier concentration, thus starting to fill traps in the films. Depending on energy level of traps and their distribution in the bandgap, the slope can be much higher than 2, as only deep traps (they are close to Fermi level, thus be firmly localized) are filled, or be very close to 2, as all traps been filled. This trap-free regime, slope equal 2, is also called SCLC regime [8]. The cross-point of ohmic regime and trap-filling regime dictates intrinsic free carrier

concentration. Using this concentration, mobility can be calculated through the conductivity.

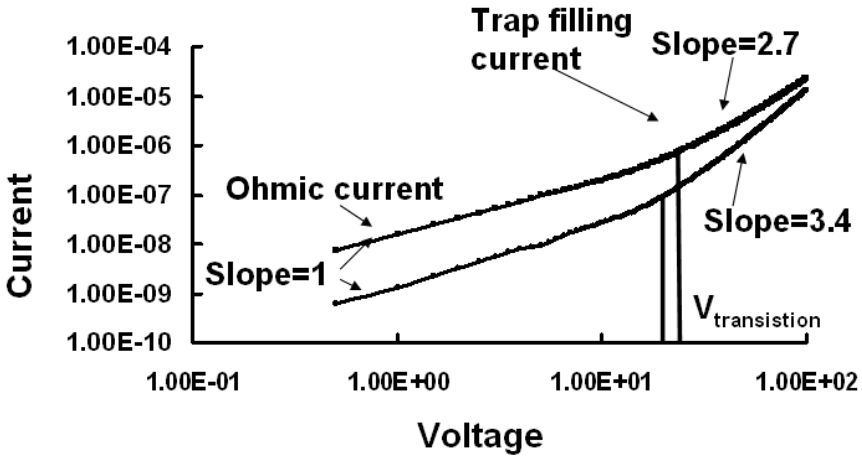

Figure 4.8, Representative SCLC curves of original pentacene-based transistors and DNA immobilized transistors

SCLC measurements before and after DNA immobilization were compared, illustrating clearly the doping mechanism of DNA molecules on the pentacene film. In the ohmic regime, the magnitude of current was increased because of immobilized DNA segments. This increase may is caused by free carrier concentration increase or mobility increase.. The change in the curves in the trap-filling regime is even more ellucidating. The slope change from 3.4 measured in the original pentacene transistor to 2.7 in the DNA immobilized pentacene transistors, indicating that deep traps have been filled by DNA molecules because of decreasing slope. Because the trap-filling action in hole-rich pentacene films is actually to increase hole concentration, it is most likely, that trapped electrons in the pentacene film was released by DNA segments, thus the pentacene film is doped.

4.2.3 Off-chip hybridization detection

As the next step, the responses of OTFTs to both ssDNA and dsDNA (off-chip hybridized) segments were measured to test the ability of pentacene OTFTs to detect DNA hybridization. The same recipe as before was followed. 250$\mu g/ml$ single and double-stranded Lambda blind III DNA molecules were immobilized on 20 different transistors each and saturation current ratio of each transistor was measured. A statistical t-test on those two groups of data was computed to evaluate the response difference between ssDNA and dsDNA (Figure 4.9).

The differentiation of these two distributions is evaluated graphically. Overlap lines of two diamonds, showing the distribution of estimated means of two populations, are clearly separated, thus concluding that there exists a significant difference between the means of the two populations (fig. 4.9). This differentiation, of course, can also be evaluated quantitatively using a t-test. Because the variance is unknown in both distributions, the global standard deviation of two distributions or two local standard deviations can be calculated separately, thus two kinds of t-test are done by assuming equal variance or unequal variance. Both calculations show the *type I error* (probability larger than the t-value) is less than 8×10^{-15}, much less than the 5% standard, such than we can confidently conclude the different means between those two populations, showing an identical conclusion as the graphic method.

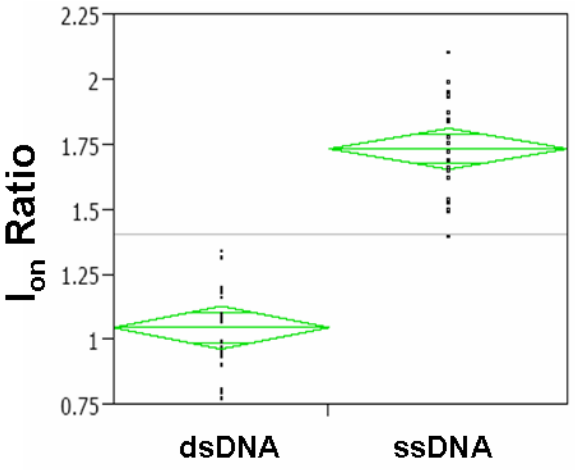

t Test

Assuming equal variances

	Difference	t Test	DF	Prob > |t|
Estimate	-0.68783	-12.218	38	9.87e-15
Std Error	0.05630			
Lower 95%	-0.80179			
Upper 95%	-0.57386			

UnEqual Variances

	Difference	t Test	DF	Prob > |t|
Estimate	-0.68783	-12.308	37.9352	8.1e-15
Std Error	0.05588			
Lower 95%	-0.80180			
Upper 95%	-0.57385			

Figure 4.9: Differential sensitivity of ssDNA and ds DNA, enabling the unambiguous detection of hybridization. Two response distributions of ssDNA and dsDNA are shown, and compared statistically to evaluate the difference between the two distributions. I_{on} ratio is the ratio of the post-DNA-exposure IDsat to original TFT IDsat and showed response of DNA molecules. Two diamonds are distribution of means of two response distributions and visually show their difference

As calculated, the 95% confidential interval of single and double stranded DNA response is between 0.57386 and 0.80179 respectively, and the mean of difference is 0.69, which will be the expected difference when we measure ssDNA and dsDNA with OTFTs in the future. Considering the variance of the measurement and the expected difference, only four transistors subjected to each sample are needed to ascertain a significance of

difference, which is substantially smaller than that needed in conventional fluorescence-based microarrays.

Although a small variance was observed in this experiment, larger variance was observed in following experiments; thus, experiments were typically performed using arrays of more than 10 transistors to ensure statistically accurate measurements. The ssDNA molecules cause a larger increase in the saturation current than the off-chip hybridized dsDNA molecules due to a higher efficiency of immobilization (fig. 4.3). The bases of DNA molecules are responsible for the hydrophobic interaction and the resulting immobilization of these molecules. While in a dsDNA the bases are enclosed inside the molecule because of the nature base-pairing principle, in a single stranded DNA these are exposed and thus result in a more effective immobilization compared to dsDNA molecules. Thus, in this experiment, we show for the first time that dramatically different saturation current shifts occur upon exposure to ssDNA and dsDNA using our OTFTs, enabling a reliable and unambiguous detection mechanism of DNA hybridization.

4.2.4 DNA expression level detection

A critical property required by cDNA-based DNA sensors is the detection of the expression level, namely quantification of the percentage of hybridization. To analyze the quantitative accuracy of the sensors developed herein, five different samples with expression percentages ranging from pure ssDNA solution to pure dsDNA solution were prepared and immobilized on four transistors each. A linear regression analysis was done

to estimate the relationship between saturation current ratios and percentage of dsDNA in ssDNA.

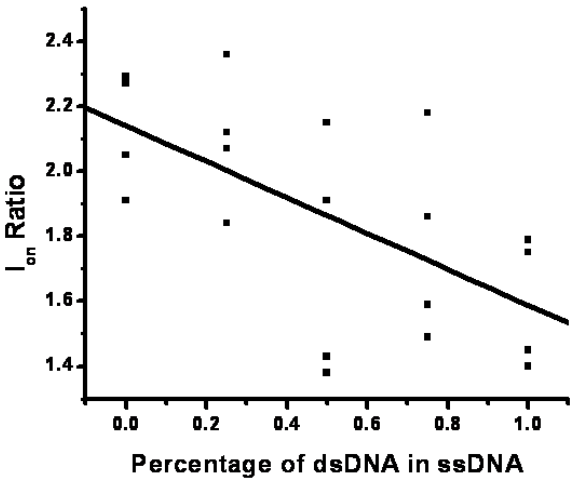

Lack Of Fit

Source	DF	Sum of Squares	Mean Square	F Ratio
Lack Of Fit	3	0.1347475	0.044916	0.6327
Pure Error	15	1.0648250	0.070988	Prob > F
Total Error	18	1.1995725		0.6053
				Max RSq
				0.4579

Analysis of Variance

Source	DF	Sum of Squares	Mean Square	F Ratio
Model	1	0.7645225	0.764522	11.4719
Error	18	1.1995725	0.066643	Prob > F
C. Total	19	1.9640950		0.0033

Figure 4.10, Variation in response of sensors with fractional concentration of hybridized DNA. Five concentrations used in the experiment are: 0%(pure ssDNA), 25%, 50%, 75% and 100%(pure dsDNA).Linearity of transduction was ascertained using a Analysis of Variance (ANOVA) calculation. The scatter is likely due to non-uniformity in immobilization caused by the manual immobilization-rinse-dry processes.

With experimental results and an analysis of variance (ANOVA) calculation, linearity of transduction is the only reasonable estimation (fig. 4.10). Under the null hypothesis that no relationship between DNA expression and sensor responses, the probability larger than F-ratio is much smaller than 5%, such that the null hypothesis is rejected, meaning a linear model is a good estimate of the relationship. It is important to note that because replications were measured for each DNA expression point, another important criterion worthy of doing is the “lack of fit” to test if the model is the best fit. It is usual that more

than one model can be fitted to a set of data. Therefore an evaluation of sufficiency of the model is necessary. Lack-of-fit test is a hypothesis test for this purpose. Its null hypothesis is no lack-of-fit existing in the model, meaning the model is the best one. Because in the lack-of-fit test the probability larger than F is much bigger than 5% (fig. 4.10 bottom left), the null hypothesis can not be rejected and thus a linear model is the best relationship between DNA expression and sensor responses.

Though the sensor responses DNA expression linearly, unfortunately, a large sample size must be used to compensate for big variance in the data, especially for the responses at 50% and 75% expression. Note that the variance in this experiment was found to be larger than the variance of the aforementioned experiments. Apparently, variance of OTFT responses to DNA is mainly from two sources: fabrication of transistors (non-uniformity of the film morphology makes performance vary between transistors) and variations in immobilization (this possibly results from non-uniform drying or non-uniform pipetting of DNA solution drops).

The fabrication-induced variance is caused by the nature of point-source thermal evaporation (used in this thesis to deposit pentacene), giving thickness variation across wafers. Thus the variance can be improved by carefully controlling the transistor fabrication processing. The second variance source, resulting from non-uniform drying or dipping can also be improved by patterning exposed reaction areas of pentacene TFTs with a Polyvinyl Aclohol (PVA) layer. All these techniques have been deployed with success and results detailing variance improvement will be discussed in section 4.5.

4.3. Oligonucleotide array application of OTFTs

Unlike cDNA microarrays that investigate genes on a function level; oligonucleotide microarrays measure mutated bases on molecular level [9]. It is believed that single base mutation is the major reason for the malfunction of genes. By finding the mutated base, ideally it is possible to cure the corresponding diseases by simply fixing the specific base. To reach this goal, in conventional commercially available microarrays, single-base-difference oligonucleotide groups are designed and synthesized in neighboring measurement sites (fig. 4.11). By comparing hybridization rate of unknown sequences with these designed oligonucleotides, the single mismatch can be identified. Because of the complexity of on-chip synthesis, less-than-25 bases oligonucleotides are always used in oligonucleotide microarrays.

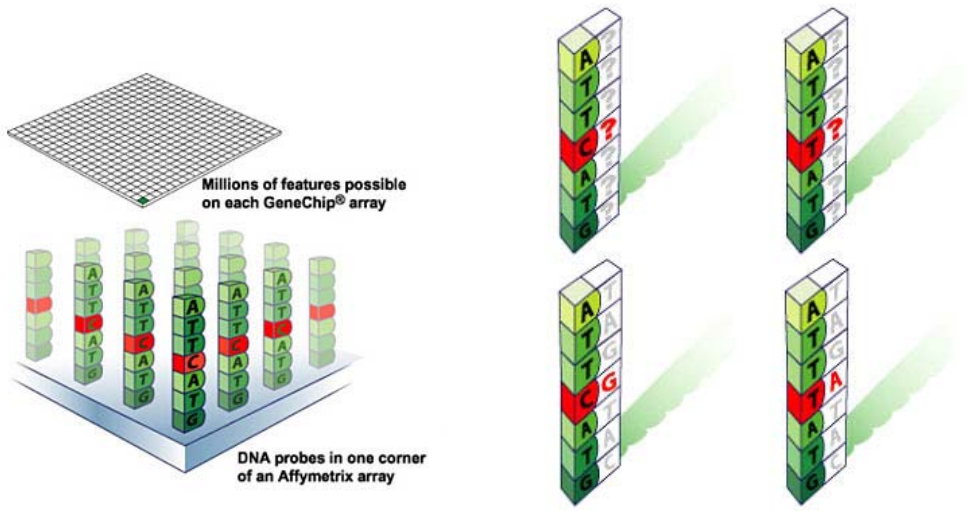

Figure 4.11: Scheme of oligonucleotide microarray used for single mutation detection. Oligonucleotides with single base difference in neighbor sites are designed and immobilized, thus the single base mismatch can be investigated by comparing hybridization rate on those sites.

OTFT-based short oligonucleotide hybridization detection is expected to be more difficult than corresponding long chain DNA hybridization detection because compared to long chain DNAs, there are fewer hydrophobic groups present in oligonucleotides, making their immobilization difficult. Normally, oligonucleotides longer than 50 bases are recommended for hydrophobic interaction immobilization. To investigate the applicability of OTFTs to oligonucleotide hybridization detection, four DNA samples were prepared and tested. Three of them are possible binary combinations between designed 20-bases oligonucleotides with sequences of 1) 5'-TGCAGTTTTCCAGCAATGAG, 2) 3'-ACGTCAAAAGGTCGTTACTC, and 3) 5'-ACTGTCAGTTCCAGTCGAAC. The fourth sample was created by hybridizing the first and second samples together to form dsDNA.

The same recipe and wafer fabrication conditions as Lambda DNA experiments were followed in oligonucleotide experiments. Twelve transistors for each sample were tested. Calculated t-value between responses for four samples suggested that sensory response for double-stranded oligonucleotides (sample 4) is dramatically different from that for all three single-stranded oligonucleotides mixtures. Furthermore, responses for all three ssDNA mixtures are essentially the same. Clearly, unambiguous detection of double-stranded oligonucleotide was achieved with pentacene OTFTs (fig. 4.12). Response for oligonucleotides showed a reverse trend from the aforementioned Lambda DNA experiments – this is likely caused by the reduced immobilization efficiency of the oligonucleotide strands.

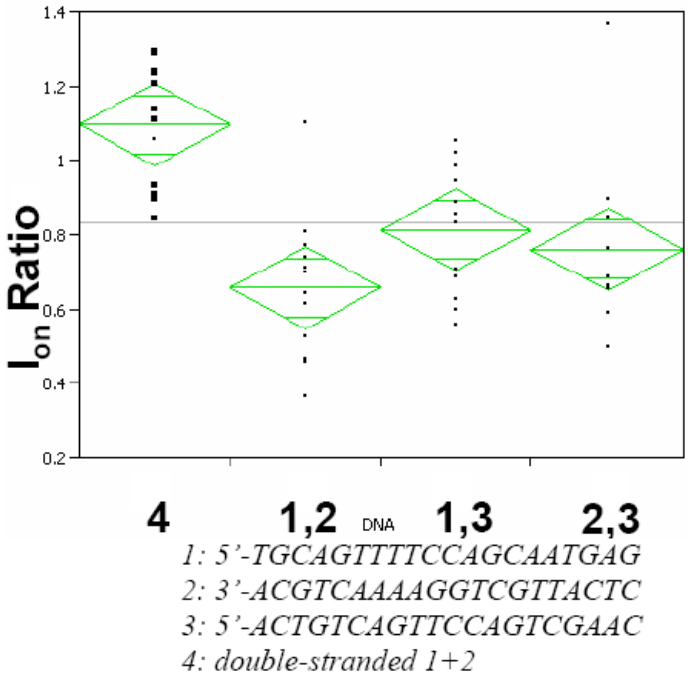

Figure 4.12: Differential sensitivity of double-stranded oligonucleotide (4), vs. various unhybridized single-stranded oligonucleotide mixtures (1,2; 1,3; 2,3) enabling the unambiguous detection of hybridization.. Sensor response distributions of four samples are shown and compared statistically to evaluate their difference. Diamonds show mean distributions of each response distribution and show response difference visually. The same recipes as long chain DNA experiments were followed.

4.3.1 Pulse-enhanced DNA on-chip hybridization

Previously studied DNA detection only measured off-chip hybridized DNA segments, meaning complementary single-stranded DNA segments were pre-hybridized and pipetted onto a sensor surface. This procedure is impractical because it not only requires significant amount of DNA copies but also is very time-consuming. Thus a fully on-chip procedure is necessary. The regular hybridization method, which includes a more than 2-hour baking step under designated temperature, can surely be done on chip after DNA solution is pipetted. But it unfortunately is also very time-consuming, though it can save

DNA usage. A better way to do ultra-fast hybridization is to use a pulse-enhanced method.

Rapid on-chip pulse-enhanced DNA hybridization [1] can improve hybridization speed dramatically from 2 hours to milliseconds or even nano-seconds. Electrical pulsing is believed to be able to release DNA molecules from their ionic surrounding and realign them to be parallel each other very quickly, thus facilitating hybridization. Those two actions make hybridization happen faster than conventional hybridization techniques. OTFTs are suitable for this technology because electrodes to supply electrical pluses already exist in a transistor setup. To that extent, pulse-enhanced hybridization was also deployed using the OTFT sensors.

In this experiment, measurements of three different kinds of DNA samples, namely synthesized dsDNA, unhybridized matched ssDNA and pulsed hybridized matched ssDNA, were performed. Eight transistors for each DNA samples were tested and resultant response distributions were again compared statistically. An electrical pulse with a transient time of 5ns, period of 0.5ms and voltage of 0.4V was applied between the OTFT source/drain electrodes after unhybridized matched ssDNA buffer solution was pipetted on transistors. The pulsed samples were air-dried and rinsed following the same recipe as the top short chain DNA experiment. The pulse width was found to be sufficient to achieve good hybridization (fig. 4.13), because, as suggested by the t-test, the response for the pulsed DNA samples was measured to be the same as that for the synthesized double stranded samples and both of them are, as expected, different from

the response for the single-stranded mixture. Taking advantage of this technology, the DNA hybridization detection with our TFTs can potentially be performed in 40 minutes.

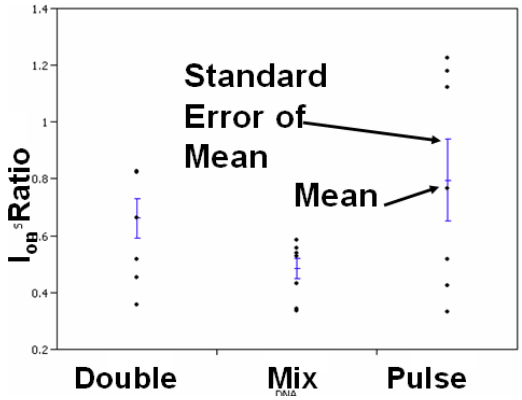

Figure 4.13, Rapid on-chip Pulse-enhanced hybridization demonstrated and tested with OTFTs. Three response distributions shown here from left to right are responses for synthesized double-stranded DNA ("double), unhybridized single-stranded oligonucletides mixture of No1 and 2 in figure 7("mix") and single- pulse-added mixture ("pulse").

4.4. Response Optimization

To understand the principle of DNA detection and maximize sensor response, various factors that influence transistor performance DNA detection were studied. In all optimization experiments, only the response for long chain DNA was considered and oligonucleotides may experience different optimization.

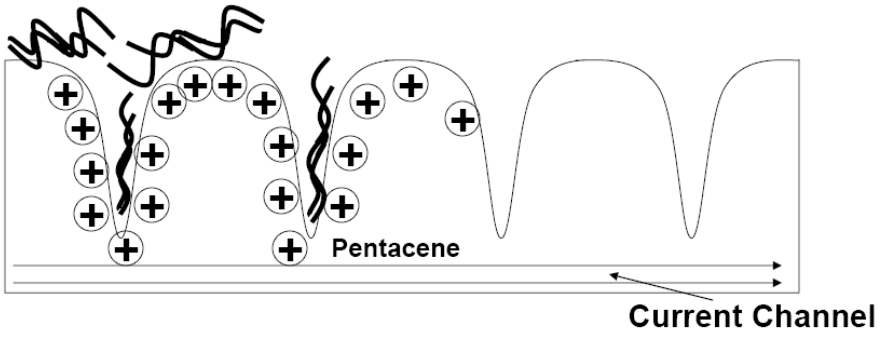

Figure 4.14: Scheme explaining influence factors for OTFT-based DNA sensitivity. Based on the proposed doping-based transduction mechanism, the concentration of

dopant, namely DNA concentration and surface roughness, and centroid of the dopant, namely, film thickness and exposed conductive layers, have significant effects on sensor sensitivity.

4.4.1 Optimization of transistor performance

High performance transistors are necessary for sensor operation to get high signal/noise ratio. As introduced in chapter 3, a screening experiment was done to figure out factors that influence transistor performance. It was found that four factors, namely pentacene thickness, surface hydrophobic coating The thickness effect on saturation current is expected because of the low hole concentration in pentacene, a thicker pentacene film can provide more accumulated holes than a thinner film, thus causing higher current, at least within the relatively thin range of channel thicknesses used in this work. The increased saturation current unfortunately is obtained at the cost of decreased I_{on}/I_{off} ratio, so the thickness of pentacene can't be increased freely. More specifically, the use of an HMDS coating, which changes the SiO_2 surface from hydrophilic to hydrophobic, improves the performance of transistors by increasing mobility and decreasing threshold voltage. The mobility shift is reasonable because as discussed in chapter 2, the HMDS coating on SiO2 surfaces changes surface energy and thus increases crystalline sizes, correspondingly increasing mobility. Simultaneously, the HMDS coating also shifts the threshold voltage for similar reasons, since the highly crystalline semiconductor thus has lower interfacial defects. Also importantly, the HMDS coating makes evaporated organic semiconductor films stable enough to survive subsequent rinse steps, etc. Therefore, in the dissertation, before the organic semiconductor deposition, a HMDS layer is always coated on the SiO_2 layer.

4.4.2 Optimization of sensor response

Given the proposed doping-based transduction mechanism, both doping concentration (i.e. DNA concentration) and doping position (i.e. sensitive film thickness) play very important roles in sensitivity of the sensor (fig. 4.14). A response surface experiment was designed to test both effects statistically. Three thickness of pentacene film, 100 Å, 200 Å and 300Å and two concentrations of DNA solution, 5*μg/ml* and 250*μg/ml*, were used. Standard least squares fit was used to find a relationship between single and double-stranded DNA response and pentacene thickness or DNA concentration, as the two curves in figure 4.15 show. As expected, higher concentration resulted in a larger sensor response. This response was also enhanced when using thinner pentacene layers, which is expected, based on the position of the doping charge centroid. The maximum response point was estimated to be at a DNA concentration of 250*μg/ml* and a pentacene thickness of 100 Å, as shown in figure 4.15. This optimum condition was used in all other experiments.

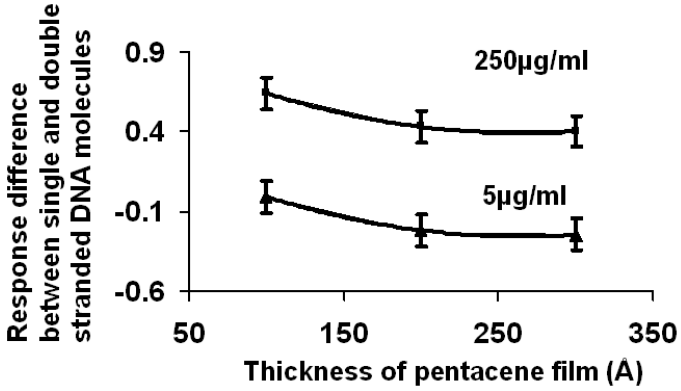

Figure 4.15, Effect of pentacene film thickness and DNA concentration on sensor sensitivity. The data is consistent with the expected doping model.

Another factor which may also change the doping concentration is the surface roughness of films (fig 4.15). AFM analysis confirms that DNA is trapped in grain boundaries and other troughs in the semiconductor surface (fig. 4.3), so a rougher surface can improve immobilization efficiency and further improve doping concentration and response of sensors. One experiment was done to prove the deduction. Pentacene grows on SiO_2 surface layer by layer and the factors that influence adsorption and growth speed of pentacene can change roughness. In the experiment, 250*μg/ml* DNA solution was used and both film thicknesses are 300Å. Two substrate temperatures, 27°C and 70°C, were used during evaporation of the pentacene films, resulting in the deposition of films of different roughness: low temperature gives rougher surfaces (rms (Root Mean Square) roughness =5.493nm VS rms roughness=4.448nm) because it allows faster adsorption of pentacene on the SiO_2 surface, forming pentacene islands on the surface faster than high temperature evaporation. Substantially rougher films as measured by AFM provide enhanced immobilization and sensitivity as expected: the response difference between ssDNA and dsDNA measured by the rougher pentacene TFTs is 0.3, compared to 0.19 of the response by the smoother TFTs (fig. 4.16).

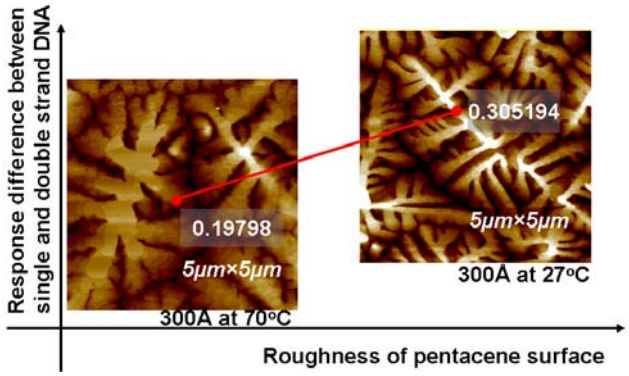

Figure 4.16, Effect of pentacene RMS roughness on sensor sensitivity. The increased sensitivity is caused by the enhanced immobilization efficiency in the rougher film.0.30 and 0.19 are the corresponding DNA response

In very thin pentacene films (<10nm) the roughness difference between wafers is unclear and shows insignificant impact on the immobilization efficiency of DNA molecules. Instead, an effect reverse to the top conclusion is shown: sensors with rougher surface have lower sensitivity than those with smoother surface. This reversion is also reasonable because the accumulation layer of the transistor only exists in the first several continuous monolayers of the film. In thin films, as more exposure of those layer occurs, , meaning smoother surface, immobilized DNA molecules are placed closer to the accumulation layer, further inducing higher sensitivity. Two wafers with clean time in acetone and IPA of 10 minutes and 20 minutes respectively, inducing different numbers of layers of continuous pentacene, were evaporated at the exactly same conditions, 100Å, 1Å/min and 70^{o}C to be immobilized with DNA molecules following the same recipe as above. The measured response difference exactly proved the deduction. Proven by AFM measurements, the wafer with smoother surface, thus more exposed continuous film area, clearly has higher sensitivity, the difference of response to ssDNA and dsDNA is as high as 0.7, than wafers with rougher surface, thus less exposed continuous film, the difference is only close to 0.5 (fig. 4.17).

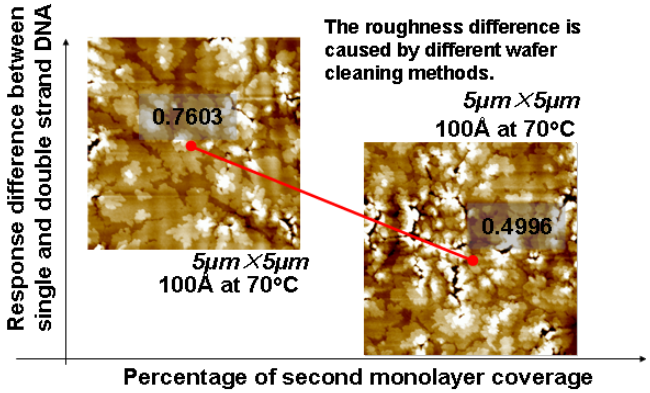

Figure 4.17, Effect of coverage of continuous layers on sensor sensitivity. Bigger coverage shows smaller sensitivity than the wafer with smaller coverage because of its

smaller distance between the conductive layers, the continuous layers and immobilized DNA

4.5. Variance shrinkage by optimizing evaporation process

Variations of organic transistors performance play a significant role in OTFT-based sensor design. The large variation of transistor performance causes large uncertainty of the measurements and thus requires large sample size to differentiate ssDNA from dsDNA. In order to minimize the variation, the variation sources were studied using statistical screening experiments. Four factors, including evaporated film thickness, deposition rate, substrate temperature and surface coating type on SiO_2 surface, were researched. A fractional factorial experiment design including eight experiments using eight wafers with different evaporation and coating conditions was done to investigate all four factors and some two factor interactions. On each wafer, five transistors were measured, covering four corner transistors and one middle transistor to provide reasonable variance range on a wafer. The corresponding variance is estimated by calculating range of the saturation current instead of calculate the standard deviation. This estimation gives better approximation of the true "variance" when sample size is smaller than ten. To make comparisons of variance on the same baseline, the range of saturation was unified to its average value. Again, ANOVA and the least square method were used to analyze measured data. Based on these statistic analyses, all four factors influence variance of transistor saturation (fig. 4.18). Therefore, the variance can be minimized using low deposition rate, thin semiconductor film and HMDS coating on

SiO_2 surface, which have already been used in above experiments. Low deposition rate were not used because, as discussed above, this degrades sensitivity.

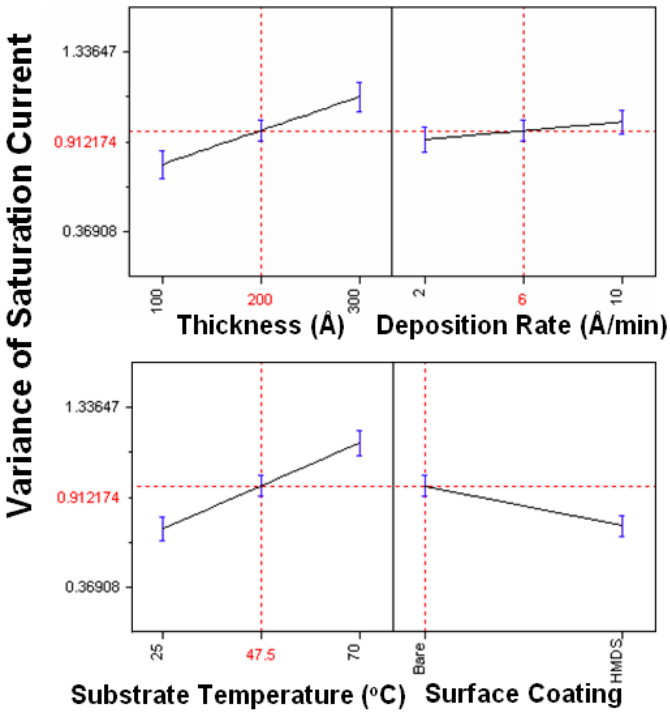

Figure 4.18: Factors influencing transistor saturation current variation. The y-axis is the normalized saturation current variance (Standard deviation/ average of saturation current). By carefully choosing evaporation conditions, the variance of transistor saturation current can be minimized.

The decreased variance can be partially explained by increased crystalline size. Both HMDS coating and lower deposition rate make crystalline size bigger, thus cutting down variance. While 70°C substrate temperature for deposition also increases crystalline size as proven in Chapter 2, the use of this high temperature also caused non-uniform temperature distribution within the evaporator due to poor temperature control within the equipment, causing large variance. Because a thick pentacene film always includes traps and defects in the semiconductor bulk, it explains the bigger variance than that observed

in thin films. The variance can be further reduced by patterning the DNA reaction area and will be discussed in detail in next chapter.

4.6 Conclusion

We have demonstrated the detection of DNA hybridization using organic TFTs that also are capable of on-chip electrically-enhanced sub-millisecond hybridization of oligonucleotides. Due to the doping effect of DNA on exposed organic semiconductor channels, it is possible to use the shift in transistor saturation current as a metric for DNA hybridization detection. Using this metric, a strong difference between hybridized an unhybridized DNA was observed, verifying the applicability of OTFTs to DNA hybridization detection. As a further step, the TFTs were also used as electrodes to achieve pulse-enhanced hybridization, which was also unambiguously detectable. The combination of these technologies, therefore, enables the realization of disposable, rapid-turnaround DNA analysis tools for field-deployable genomic diagnosis.

References

1. Fixe F., et al, Single base mismatch detection by microsecond voltage pulses, Biosensors and Bioelectronics, Vol. 21, pp 888, 2005
2. Kagan C.R., et al, Operational and environmental stability of pentacene thin-film transistors, Applied Physics Letters, pp 193505, 2005
3. Vander A. et al., Human physiology: the mechanism of body function, Eight Edition, McGraw-Hill, 2001
4. Ye R.B., et al, Effects of O_2 and H_2O on electrical characteristics of pentacene thin film transistors, Thin Solid Films, Vol, 464-465, pp 437, 2004
5. Fritz, J. *et al*, Electronic detection of DNA by its intrinsic molecular charge, PNAS, Vol. 99, pp 14142, 2002

6. Palermo, V., *et al*, Electronic Characterization of Organic Thin Films by Kelvin Probe Force Microscopy, Advanced Materials, Vol. 18, pp 145, 2006
7. Sinensky S. *et al*, Label-free and high-resolution proten/DNA nanoarray analysis using Kelvin Probe force microscopy, Nature Nanotechnology, Vol 2, pp. 653, 2007
8. Rose A., Space charge limited current in solids, Physical Review, pp 1538, 1955
9. Michael J. Heller, 2002, DNA MICROARRAY TECHNOLOGY: Devices, Systems, and Applications, Annu. Rev. Biomed. Eng. No.4, pp.129

Chapter 5

Integrating DNA sensors with Microfluidic channels --- Detecting on-chip hybridization

A microfluidic system to automatically deliver DNA solutions to detection sites is necessary for a self-supported DNA detection system. Unfortunately, the incompatibility of pentacene with organic solvents used in lithography process typically limits integration. In this chapter, 99% hydrolyzed PVA film is used as a pattern transfer layer to form microfluidic channels in conjunction with SU-8 because of its controllable etching rate using DI water as an etchant. The process doesn't change the morphology of pentacene film, and because the etchant is DI water, the process-induced performance shift is acceptable for successful DNA detection. Even better, the patterned microfluidic channels dramatically decrease data variance by precisely defining DNA reaction areas, thus this system is compatible with on-chip hybridization detection and can successfully differentiate hybridized DNA molecules from unhybridized ones

5.1 Current methods to make microfluidic channels on OTFTs

Because most organic semiconductors, such as pentacene, polythiophene, etc., can be easily damaged by lithography-related chemicals, such as acetone and photodevelopers, no photolithography methods are currently available to make microfluidic channels on

the top of OTFTs. This lack of precisely-shaped microfluidic systems limits the viability of biological applications of OTFTs. Instead, pre-patterned Polydimethylsiloxane (PDMS) concave structures are typically used to form sealed channels on the top of OTFTs (fig. 5.1) [1] [2]. Generally, a PDMS structure is made by pouring pre-mixed PDMS gel onto pre-patterned convex SiO_2 or SU-8 structures, followed by a room-temperature annealing or a heating process to cure PDMS gel. The cured PDMS therefore transfers structures on the substrate, such as making concave microfluidic channels. Because of its ease of use, the PDMS-based method has been broadly used to prototype microfluidic systems [3]. Unfortunately, the PDMS-based method is not suitable for microfluidic systems on OTFTs because a precise alignment with transistor channels is typically required, while normally pre-patterned PMDS channels have to be aligned mechanically with much lower layer-to-layer registration precision. Till now, the reported smallest microfluidic channel on OTFTs is 50μm wide aligned to a 150μm long organic transistor channel [2] with very low success and is not built on a system level. To make effective microfluidic system on OTFTs, a lithography procedure is thus needed.

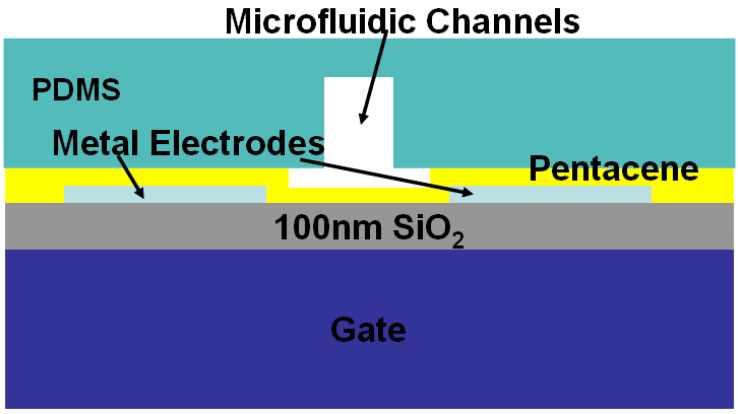

Figure 5.1: A current method to build microfluidic channels on the top of OTFTs. Pre-patterned PDMS channels are manually aligned onto fabricated OTFTs to form a sealed microfluidic channel. This manual alignment typically limits its integration level.

5.2 PVA as a photoresist

Poly Vinyl Alcohol (PVA) is the best candidate to make microfluidic channels, because of its solubility in DI water. Comparing with organic chemicals used in lithography, water is the safest chemicals with negligible effects on transistor performance degradation [4]. In recent years, the mixture of Poly Vinyl Alcohol (PVA) with ammonium dichromate (ADC), a photosensitizer, acting as a negative photoresisit has already been broadly used in isolating organic transistors [5], dramatically dropping transistor leakage current by breaking the off-current path around them. PVA is a water-soluble resin produced by the hydrolysis of polyvinylacetate which is made by the polymerization of vinyl acetate monomer [6]. Its dissolution-speed in water can be tuned by adding polar groups to the polymer (fig 5.2) in a process called hydrolysis.

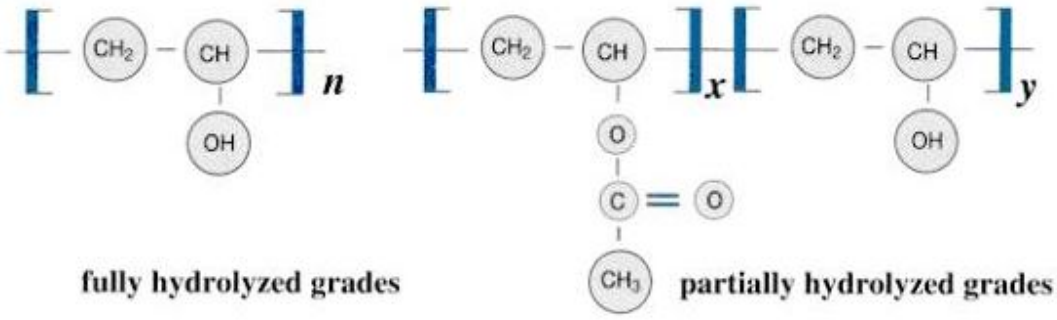

Figure 5.2: Chemical structures of both fully hydrolyzed and partially hydrolyzed PVA

It is clear that the more hydrolyzed PVA shows significantly slower dissolubility speed in water than the less hydrolyzed PVA (fig 5.3). As for the photoresist application, low hydrolysis PVA powder is typically used because of its high dissolubility speed. This low hydrolysis PVA can be dissolved completely in DI water readily after stirring for 30 to 60 minutes in 90^{o}C water. A typical recipe [7] of PVA photoresist lithography is to

dissolve PVA in water at the concentration of 4% by wt., with 0.05% by weight ADC added in the solution. The solution is then filtered with a 0.25μm Teflon filter to remove any particles that could create inconsistencies during the spin. The solution was poured onto the wafer at 0RPM, which was then spun at 4000RPM immediately for 45 seconds. The PVA was then exposed using a standard photomask in a contact printer. The exposure time varied widely, depending on the underlying surface. Effective patterning of PVA on top of SiO_2 film took significant short time than patterning PVA on top of pentacene. This is partially due to the lack of reflectivity of the pentacene surface, eliminating the double-exposure of PVA through reflection off of the underlying layer. Following exposure, the film was developed in a room-temperature water bath for two minutes. This recipe has been repeated successfully was slightly modified to test the applicability of microfluidic channels on OTFT-based DNA sensors.

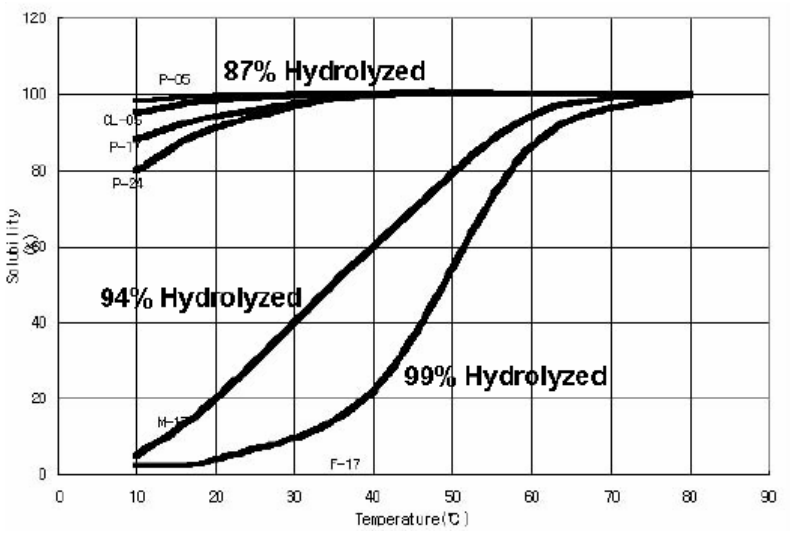

Figure 5.3: PVA solubility variation in different temperature water according to different hydrolysis ratio

5.3 99% hydrolyzed PVA-based microfluidic system

It is reasonable to consider using PVA photoresist directly to make microfluidic systems on the top of OTFTs, but, unfortunately, because its thickness is less than 100*nm*, it is not suitable for most of liquid delivery applications, which typically requires channel thickness around 50μm. Increasing viscosity of the photoresist by increasing the ratio of PVA in water is an alternative to possibly increase the spun film thickness. Unfortunately again, the increased spun thickness also causes partial development in water because of the low light penetration into the increased thickness of the photoresist. A 2-minute exposure at 90 *mW* on a contact printer was found to be unable to pattern the PVA photoresist with 6% PVA in water by wt% spun at the same recipe as above.

Instead of using PVA plus a photosensitizer as a photoresist, in this chapter, for the first time, a 99% hydrolyzed pure PVA is spun as a sacrificial layer to protect the organic semiconductor layer from following standard lithography steps. Taking advantage of the variability of PVA dissolubility speed in different water temperature, we dissolved 99% hydrolyzed PVA in 90^{o}C water. After cooling down the PVA solution, it is spun and then baked to remove most of water inside. This controlled baking processing successfully makes the film show slow dissolubility speed in room-temperature water and, more importantly, also in photolithography-related chemicals, such as acetone and photodevelopers. Thus, on the top of the PVA film, OCG-825, a positive photoresist, can be used to transfer designed patterns while the PVA film protects organic semiconductor

underneath. The transferred OCG-825 pattern then acts as the mask for the bottom PVA film that fortunately can be developed under warm water.

The slow dissolvability of baked PVA film is likely caused by the crystallization of the PVA polymer. To prove the deduction, herein, 99% hydrolyzed PVA dissolved in DI water with the weight concentration 4% was spun on a bare silicon wafer at 4000rpm for 30 seconds. After baking at 120^{o}C in a convection oven for 7 minutes in an oven, the AFM analysis showed that the PVA film has been clearly aggregated, illustrating apparent crystallization.

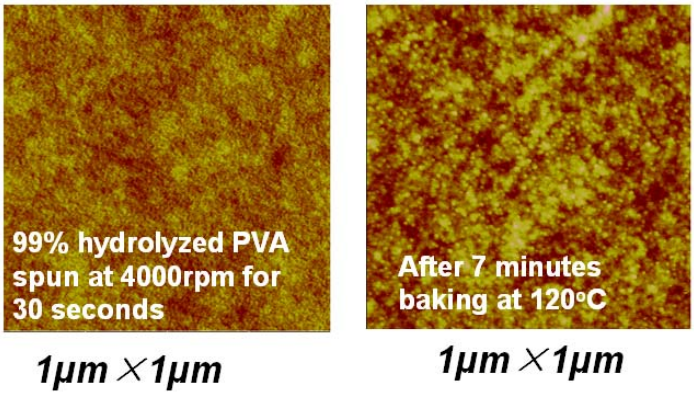

Figure 5.4: Crystallization of 99% hydrolyzed PVA by heating

To provide a big enough time window of PVA etching in warm water, the spin speed, baking temperature, baking time, developing temperature and developing time are optimized using a set of experiments (fig. 5.5). In all experiments, 4% PVA in DI water by wt% are always used as it is the largest allowed concentration. The dissolved PVA solution was then filtered using a 5*μm* Teflon filter to prevent any discontinuity during spin. A hot plate heated to 140^{o}C was used to bake spun PVA films because it gives controllable baking time that shifts PVA film from soluble to insoluble. While using 120

^{o}C, over 30 minutes is needed to make the shift occur, using 160 ^{o}C, even one minute bake causes extremely slow dissolubility of the film in warm water. Finally, baked samples were etched in a controlled-temperature water bath. The remained thickness of the etched PVA films was measured using AFM analyses and etching rate are correspondingly estimated by comparing with original thickness. As expected, the longer baking time results in lower etching rate and the thicker film, corresponding to the lower spin speed, leads to lower etching rate after baking. Clearly, the film spun at 3000rpm and baked for 8 minutes provide the slowest etching rate and, of course, gives the best control of etching (fig 3). Because using 50 ^{o}C or even 55 ^{o}C water as the etchant for the baked PVA film often causes visible residues on the pentacene film, making the sensor insensitive, the slowest etching rate using 60 ^{o}C water is chosen as the standard etching temperature in this dissertation, which will allow for a around 2 to 5 seconds etching time with around 90*nm* PVA thickness (fig. 5.5). A better control of etching rate is also validated by using a well-controlled oven, considering the vertical heating non-uniformity caused by the hot plate, but, of course, recalibration is needed before its usage.

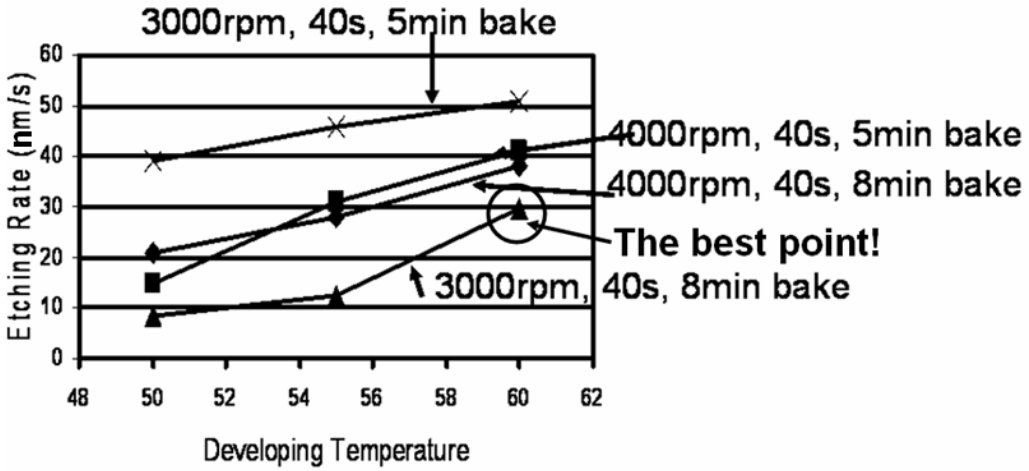

Figure 5.5: PVA etching speed variability according to the spin speed, baking time and baking temperature. The best point is chosen based on the most controllable etching speed

Based on the above knowledge, a detail processing (fig. 5.6) to make SU-8 microfluidic channels on the top OTFTs is proposed and demonstrated. A bottom-gated organic transistor with 100Å pentacene as the active layer was first fabricated (step 1), followed by spinning 99% hydrolyzed PVA solution with the concentration of 4% by wt. at 3000rpm for 40 seconds. The spun film was then baked on a 140^{o}C hot plate in UC Berkeley Microlab for 8 minutes. As the following step, the positive photoresist, OCG-825, was spun on it at 5000rpm for 30 seconds. Followed contact photolithography steps were used to pattern this positive photoresist layer. As the development of the positive photoresist, pentacene film was protected by the PVA film. This patterned photoresist correspondingly acts as the mask for PVA development using 60^{o}C water for 5 seconds (step 2). An SU-8, a negative photoresist, film was spun on it the patterned structure (step 3) at 3000rpm for 30 seconds. SU-8 is used here because it is a very stable material and broadly used in MEMS structures [8]. The spun SU-8 film was prebaked at 90^{o}C for 3 minutes and patterned using a contact printer with the exposure energy of 200mJ. Before the development step, the SU-8 film was hard baked at 90^{o}C for another 3 minutes. After developing the SU-8 film, the remained positive photoresist and PVA film was sequentially removed using acetone and 60^{o}C water for one minute and 10 seconds sequentially. 50μm wide SU-8 microfluidic channel aligned to 110μm transistor channels was fabricated using the proposed process.

Transfer curves of 7 transistors before and after the process were measured to watch resultant performance shift. By average, the saturation current only drops around 3 times and a representative transfers curves is shown (fig. 5.7). The small amount shift of

saturation current is believed to have negligible effects on DNA sensitivity of the pentacene film. More importantly, proven by AFM analyses, the process doesn't change the morphology of pentacene film, and thus the sustentation of DNA sensitivity is expected.

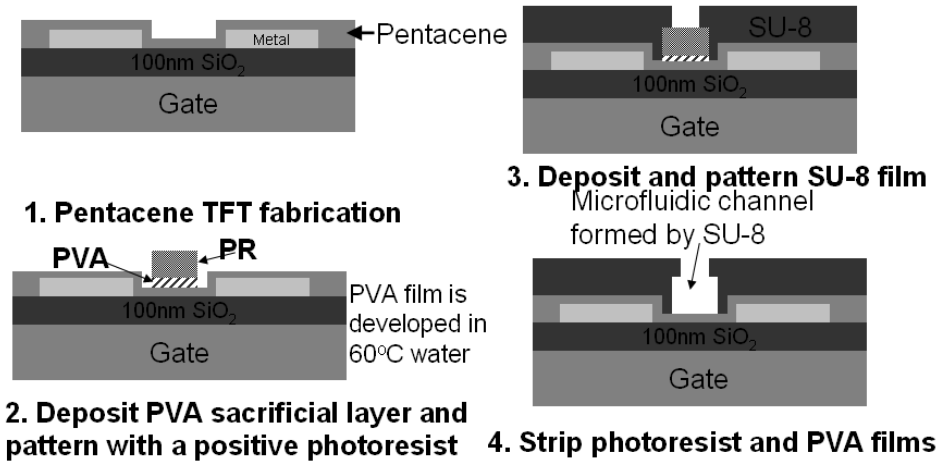

Figure 5.6: Scheme of Microfluidic channels manufacturing on the top of pentacene-based OTFT

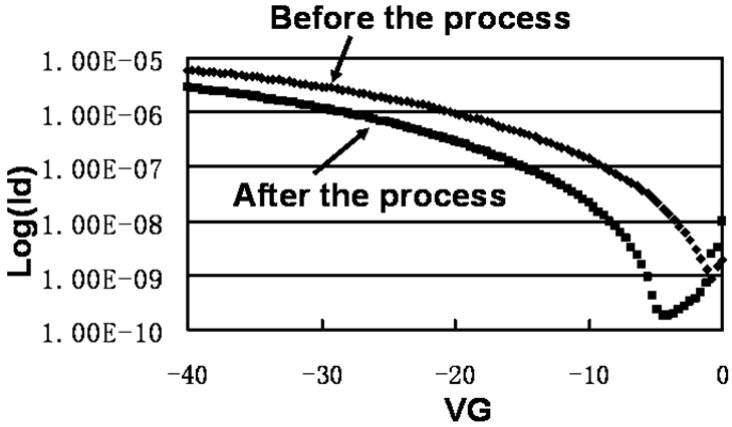

Figure 5.7: Typical transfer curves of transistors before and after PVA process, showing reasonable dropping of transistor performance

5.4 Microfluidic integration with OTFTs

Microfluidic channels on OTFTs not only deliver DNA solution but can also dramatically decrease variance caused by the non-uniformaity of pipetting. In the experiment, a PVA photoresist was used to cover source and drain electrodes to demonstrate the microfluidic channels discussed above for convenience. An 80μm (inset of fig 5.8) area was opened as the sensor active area by patterning PVA photoresist using a contact printer. In the area, double stranded lambda DNA molecules were immobilized. Because of the hydrophilicity of the PVA film, DNA won't survive on the surface after the rinse step. Experimentally, sixteen transistor for each kind of OTFT structures were measured and saturation current ratio before and after DNA immobilization was calculated. For each group of data, the standard deviation was calculated to represent their variance. Clearly, the microfluidic-pattered OTFTs were found to shrink variance close to three times (fig. 5.8). This decreased variance will certainly facilitate on-chip hybridization detection, which used to suffer from the big variance of measurement. One point worthy to notice in the results is that compared to response of bare OTFTs, the response was decreased and likely caused by the limited reaction area of PVA-patterned OTFTs. This point is even clearer on the on-chip hybridization detection discussed below.

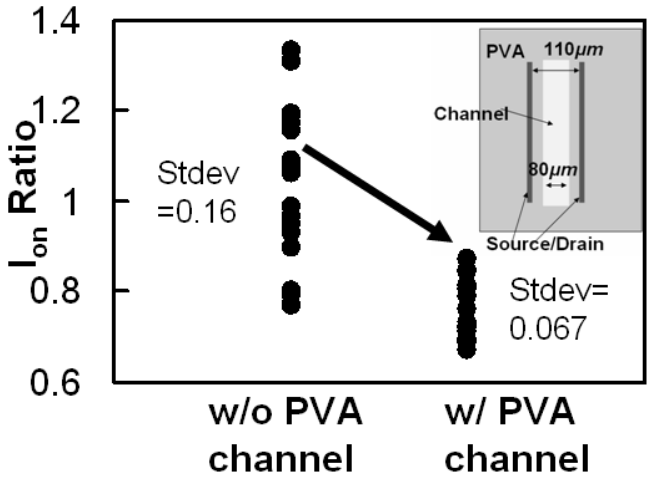

Figure 5.8, the variance shrinkage caused by patterned active area using PVA photoresist

5.5 On-chip hybridization using OTFTs integrated with microfluidic channels

Thus, by developing an OTFT-compatible microfluidic channel technology as discussed above, all the necessary components for a self-supported DNA microarray analysis system have been realized. To investigate the applicability of this system to on-chip hybridization, an experiment following the *Affymetrix* recipe was done. 50*μm* wide microfluidic channels on prepared pentacene-based OTFTs were made by PVA photoresist for convenience. PVA-based SU-8 channels are expected to show similar results. As-purchased unhybridized single-stranded oligonucleotides with the sequence of 1: 5'-TGCAGTTTTCCAGCAATGAG dissolved in 2×SSC to reach the concentration of 1*μg/ul* was first immobilized on the sensor array surface using the same recipe as used in our previous research (Chapter 4), except that 1×SSC was used in the rinse step. Two sequences of oligonucleotides were then pipetted onto the DNA-immobilized sensors surface, namely 2: 3'-ACGTCAAAAGGTCGTTACTC (i.e., matched) and 3: 5'-ACTGTCAGTTCCAGTCGAAC (i.e., unmatched) with also the concentration of 1*μg/ul*

in 2×SSC. The hybridization step was performed by leaving those mixtures in room temperature for two hours. The hybridization-finished wafer was then rinsed under flowing DI water for one minute and followed by storage in nitrogen overnight to be ready for characterization. Sixteen transistors for each group of combinations were then measured and t-test was used to test the equality of distributions of responses. As expected with the evidence of formed hybridized and unhybridized sensor groups, the significant difference between distributions of means of two response groups clearly illustrate the different sensor responses to these groups (fig 5), thus establishing that the sensor system presented here may be used for label-free readout of on-chip DNA hybridization.

The measured response was found to be smaller than the response difference obtained using unpatterned pentacene-based TFTs for off-chip hybridized DNA detection as discussed in previous chapters. This reduced response is likely caused by the small open areas defined by the microfluidic channels, 50μm out of 110μm here, thus the response can be further improved by optimizing the size and location of the open area. Of course, this optimization has to be balanced with simultaneously increased data variance.

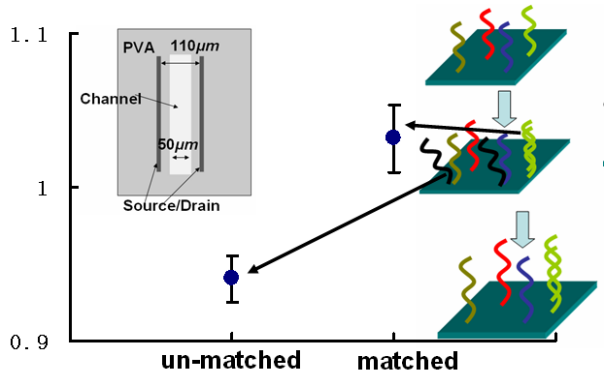

Figure 5.9: On-chip hybridization detection using OTFT sensors. The sensors clearly tell different responses to un-matched and matched sequences, showing capability of on-chip hybridization detection. Error bars in the figure show distribution of means of two populations.

5.6 Conclusion

For the first time, a novel method to lithographically make microfluidic channels on the top of OTFT was proposed and tested. Pure 99% hydrolyzed PAV film was used as the pattern-transfer layer to protect the OTFT transistor from damages by standard lithography steps. The resultant microfluidic channels not only can deliver DNA solutions but can also minimizing variance involved to close 3 times less than unpatterned structures. Those techniques together enable on-chip hybridization detection using OTFTs.

Reference:

1. George Maltezos, et al, Tunable organic transistors that use microfluidic source and drain electrodes, Applied Physics Letters, Vol. 83, pp 2067, 2003
2. Jeffrey T. Mabeck, et al, Chemical and biological sensors based on organic thin film transistors, Anal. Bioanal Chem, Vol. 384, pp 343, 2006
3. Abbasi F., et al, Modification of polysiloxane polymers for biomedical applications: a review, Polymer International, Vol. 50, pp 1279, 2001
4. Kagan C.R., Afzali A., Graham T.O., Operational and environmental stability of pentacene thin-film transistors, Applied Physics Letters, Vol. 86, pp 193505, 2005
5. Marcus Halik, et al, Fully patterned all-organic thin film transistors, Applied Physics Letters, Vol. 81, pp 289, 2002
6. DC Chemical Company, Ltd., http://www.dcchem.co.kr/english/product/p_petr/p_petr8.htm
7. Brian Mattis Doctoral dissertation, the Department of EECS, UC Berkeley
8. http://www.microchem.com/products/su_eight.htm

Chapter 6

Conclusions and Future Work

Based on the achievements discussed in previous chapters, it is concluded that OTFTs are capable of deploying fast and ultra-low-cost DNA detection, thus achieve widely-accessible gene analysis toolkits for early-stage disease diagnosis and personalized medicine. The power of our sensor system is made even apparent by comparing the protocols used herein with conventional protocols. Three critical steps exist in both protocols, namely immobilization, hybridization and signal readout. In conventional protocols, both immobilization and hybridization are time-consuming steps because they require multi-step complex chemical reactions. Meanwhile, using this new technology, the most time-consuming portion is the immobilization step. Because physical adsorptive immobilization was used, this step only needed around 30 minutes. On-chip pulse enhanced hybridization will further accelerate the detection for oligonucleotide array. Through the combination of electrical readout and on-chip hybridization, it is possible to dramatically reduce turnaround time (less than 40min vs. larger than 24hr) while simultaneously eliminating the need for specialized optical readout equipment. Indeed, the electrical readout achieved herein makes the possibility of handheld analysis with a disposable plastic sensor "strip" intriguingly near. Furthermore, integrating OTFT-based DNA sensors with microfluidic channels makes the current system a step closer to being a self-supported DNA detection system. With the successful microfluidic fabrication, DNA solution can be automatically delivered to detection sites. Thus with our system,

ideally, the gene test in future hospitals could be as easy as urine or standard blood test. This deduction is further supported by the evidence that the dramatically decreased data variance brought simultaneously by built-in microfluidic systems directly facilitates the viability of the on-chip hybridization capability of our system.

Although we have demonstrated all necessary techniques for a self-supported ultra-low-cost and fast DNA analysis tool, several more steps are still needed before we can finally ship out products. First, with current sensory sensitivity, a Polymerase Chain Reaction (PCR) process is still required. This step unfortunately is also a time-consuming step using current technologies. Therefore, either a PCR chip has to be integrated with the sensor system or the sensitivity has to be improved dramatically to skip the PCR process. Second, current DNA detection is still measured one by one using a probe station, which unfortunately make it slower than integrated DNA sensors, such as silicon-transistor-based DNA sensors. This problem can be readily solved by make a memory-like array alignment of organic transistors and thus addressing circuitry can be used to automatically select measured sites. In this chapter, methods and possible research to solve those problems are suggested.

6.1 Optimization of DNA immobilization using fluorescence experiments

Most experiments in this dissertation use 250$\mu g/ml$ DNA solution for both hybridization process and immobilization process as the optimum condition confirmed by experiments discussed in Chapter 3 and 4. This concentration is also typically used for both cDNA

and oligonucleotide assays recommended by companies like “Affymetrix” [1]. Such a high concentration cannot be directly extracted from a limited number of cells but has to go through a DNA replication step, namely Polymerase Chain Reaction (PCR). This added step is unfortunately time-consuming because it normally requires multi temperature cycling steps and several more purification steps to remove salt ions and irrelevant DNA fragments involved in PCR [1] [2], thus limiting the whole process speed. In order to realize a PCR-free DNA microarray detection, an ultra-sensitive DNA sensor has to be implemented. Lots of efforts have been made to improve sensor sensitivity using different sensory mechanisms. For example, silicon nanowires have been used to improve the sensitivity to below tens of femtomolar range, taking advantages of the high surface/volume ratio of nanowires [3]. Our sensors, of course, have the same potential to reach much higher sensitivity than our current system.

The sensitivity of our OTFT-based DNA sensors can be further improved by optimizing the immobilization efficiency. For all experiments, an air-dry process is simply used to immobilize detectable DNA molecules. This air-dry process can be influenced by many factors. As proved in chapter 2 and 5, the morphology, including thickness and roughness, of evaporated pentacene film has significant effects on sensor sensitivity, which is believed to be caused by their resultant immobilization efficiency. Besides these two factors, the air-drying time and solution used for rinse also will influence immobilization efficiency. A longer air-drying time by controlling environmental humidity certainly will help to increase numbers of immobilized DNA molecules because of the increased DNA diffusion time. Of course, this time increasing has to be compromised with possible

damages or doping caused by salt ions in buffer solution. The rinse solution also probably influences immobilization efficiency because of the instability of DNA molecules in DI water. A full factorial experiment is helpful to understand the significance of all five factors listed in table one. The goal of these experiments is of course to minimize required DNA concentration for certain high level sensory sensitivity. Exploiting fluorescence signals labeled DNA segments; experimental results will certainly assist higher immobilization efficiency, as a result higher sensitivity.

6.2 New organic materials for covalent bonding DNA immobilization

The ultimate way to improve sensitivity is to switch the immobilization methods to covalent-bonding-based DNA immobilization. Hydrophobic interaction based DNA immobilization is an easy and stable technology broadly used in the early-stage of DNA-related research [4] [5]. Unfortunately, because of its inherently non-directional immobilization, hydrophobic interaction immobilization actually reduces hybridization efficiency significantly [6], and is thus not popular in current DNA microarray applications. Instead, a covalent bonding based DNA immobilization is more attractive. Because pentacene molecules don't have any side functional groups, it essentially can't provide covalent bonding with DNA molecules. Therefore, novel organic materials have to be considered.

Typically, to immobilize DNA molecules chemically, sensor surfaces have to be modified to have hydroxyl or amino groups to bond with DNA molecules with

correspondingly modified ends [7]. Oligothiophene is a good candidate for this mission because of its readily modified structures and high performance [8] and has already been used as both vapor and biological sensors [9] [10]. More importantly, the monolayer structure of oligothiophene will definitely induce ultra high sensitivity compared to current bulk structures of pentacene-based DNA sensors.

6.4 Organic Transistor configuration optimization

For all experiments done in the dissertation, constant and fairly big channel length/width transistors (1.1mm/110μm) were used. The dimension apparently is not compatible with high density DNA detection, thus efforts to investigate effects of shrunk channel length has to be made. As expected, the scaling of organic TFTs approximately follows principle of silicon scaling, showing increased saturation current, decreased I_{on}/I_{off} ratio, V_T roll-off and Drain Induced Barrier Lower (DIBL) [13]. As a result, the shrunk transistors are expected to improve sensor sensitivity because of increased saturation current and increased surface effect [14]. Of course, transistor channels can't be shrunk to less than crystalline size because of the crystalline boundary induced immobilization nature of our sensor mechanism. Therefore, an optimization analysis becomes necessary. Because of almost constant contact resistance during shrinking, it will reasonably play more important role in the sensor sensitivity, which also has to be paid attention to.

6.4 Memory-like DNA microarray setup for automatic reading

For all experiments in the dissertation, transistors were measured one-by-one in a probe station. This clearly makes whole analysis extremely slow. An integration of addressing circuits and memory-like construction of DNA sensor is particularly interesting to dramatically accelerate DNA analysis. Because of the un-mature status of organic electronics, silicon-based circuits are recommended with core sensory parts built by organic transistors. A fully addressable electrically-readable DNA sensor will make intriguing improvement for current DNA microarray system.

6.5 Moving from evaporated organic materials to printed organic materials

The most attractive advantage of organic electronics is its printability, making functional circuits ultra-low-cost and mechanically flexible. Clearly, the evaporated pentacene used in the dissertation is not compatible with this criterion. Moving into printable OTFT-based biosensors definitely is the trend in the near future. Pentacene molecules can be made soluble by adding side groups [15]. Because of typical rougher surface compared to evaporated pentacene films, printed pentacene based OTFTs are expected to give higher sensitivity caused by improved immobilization efficiency. But the lower performance of printed transistors, normally caused by increased trap concentration and amorphous-like morphology, will set barriers for high sensitivity.

6.6 Conclusion

As the first time, this dissertation studied an OTFT-based DNA analysis tool, integrating OTFT-based DNA sensors and microfluidic systems. Because of their ultra-low-cost manufacturing and high chemical and biological sensitivity, OTFTs enable disposable, fast, self-supported and widely-accessible DNA analysis toolkits, facilitating early-stage disease diagnosis and personalized medicine. To finally reach the proposed goal, several other steps, like optimizing immobilization, understanding physics of DNA-induced doping, designing addressing circuit and so on, are recommended in this chapter.

Reference:

1. http://www.affymetrix.com/Auth/support/downloads/manuals/expression_print_manual.zip
2. http://en.wikipedia.org/wiki/PCR
3. Jong-in Hahm, et al, Direct untrasensitive electrical detection of DNA and DNA sequence variations using nanowire nanosensors, Nano Letters, Vol. 4, pp 51-54, 2004
4. Gillespie D. et al, A quantitative assay for DNA-RNA hybrids with DNA immobilized on a membrane, Journal of molecular biology, Vol. 12, pp 829, 1965
5. Allemand J.F. et al, pH-dependent specific binding and combing of DNA, Biophysical Journal, Vol. 73, 1997
6. Dugas, V., et al, Immobilization of single-stranded DNA fragments to solid surfaces and their repeatable specific hybridization: Covalent binding or adsorption?, Sensors and Actuators B, Vol. 101. pp 112, 2004
7. P.E. Lobert, et al, Immobilization of DNA on CMOS compatible materials, Sensors and Actuators B, Vol. 92, pp. 90, 2003
8. Paul Chang, UC Berkeley EECS dissertation
9. mabeck, J.T., et al, Chemical and biological sensors based on organic thin-film transistors, Analytical and Bioanalytical Chemistry, Vol. 384, pp 343, 2005
10. Torsi L., et al, Correlation between oligothiophene thin film transistor morphology and vapor responses, J. Phys. Chem. B, Vol. 106, pp 12563, 2002
11. Minakata, T., et al, Highly ordered and conducting thin film of pentacene doped with iodine vapor, Journal of Applied Physics, Vol. 69, pp 7354, 1991
12. Brinkmann M., et al, Electronic and Structural Evidence for Charge Transfer and Localization in Iodine doped pentacene, J. Phys. Chem. A, Vol. 108, pp 8170, 2004

13. Lee J., et al, 10-nm Channel Length Pentacene Transistors, IEEE Transactions on Electron Devices, Vol. 52, pp 1874, 2005
14. Torsi L. Organic thin film transistors as analytical and bioanalytical sensors, Anal Bioanal Chem, Vol. 384, pp 309, 2006
15. Volkman S. et al, Inkjetted organic transistors using a novel pentacene precursor, Proceedings of the Materials Research Society Spring 2003 meeting, Volume 769, H11.7, 2003